Risk analysis of earthquake-induced submarine landslides in deepwater sites

Thesis presented for the degree of Philosophiae Doctor (PhD)

UiO : University of Oslo

Rafael Rodríguez Ochoa

Department of Geosciences

Faculty of Mathematics and Natural Sciences

University of Oslo

Oslo Norway, June 2015

Series of dissertations submitted to the
Faculty of Mathematics and Natural Sciences, University of Oslo
No. 1673

ISSN 1501-7710

Cover: Hanne Baadsgaard Utigard.
Print production: John Grieg AS, Bergen.

Produced in co-operation with Akademika Publishing.
The thesis is produced by Akademika Publishing merely in connection with the thesis defence. Kindly direct all inquiries regarding the thesis to the copyright holder or the unit which grants the doctorate.

Para papá

Acknowledgments

I want to thank the Consejo Nacional de Ciencia y Tecnología (CONACYT) and the International Centre for Geohazards (ICG) for providing funding to carry out this PhD programme.

I also want to thank the Instituto Mexicano del Petróleo (IMP) for encouraging me to get involved in this adventure and for providing the data to do the analyses, special thanks to Oscar Valle and Jaime Nuñez.

Special thanks to my main supervisor Farrokh Nadim for his guidance, motivation and patience through the PhD studies, also to supervisors Kaare Høeg and Hans Petter Jostad. I want to thank the International Centre for Geohazards (ICG) and the Norwegian Geotechnical Institute (NGI) for providing the resources and perfect environment to develop this research. I also thank NGI employees, postdoctoral researches and visitors for sharing their knowledge and making my stay in Oslo a very pleasant one. Special thanks to Anders Solheim, Bjørn Kalsnes, Amir Kaynia, Tore Jan Kvalstad, Limin Zhan, Zhongqiang Liu, Victor Taboada, Dieter Issler, Khoa Huynh, and Maarten Vanneste. I am indebted to José Cepeda for his help during the challenging times of this adventure in the technical, practical and personal matters.

I want to express my gratitude to the University of Oslo (UiO), Delft University Technology (TU Delft), and the Center for Marine Environmental Sciences (marum) at University of Bremen, for providing the sources to build up my PhD studies. Special thanks to Michael Hicks and Patrick Arnold for their technical and practical assistance during my stay at the Geo-Engineering Section at TU Delft as visiting PhD student.

I want to thank James Hance for sharing his seafloor slope failure database, and Robert Gilbert for his assistance to obtain the database that was used to carry out runout back analyses, and for sharing interesting chats at lunch time during his sabbatical year at NGI.

My loving thanks to my father, Rafael Rodríguez Lozano (†), and my mother, Teresa Ochoa Vazquez, for their love and endless support.

Special and loving thanks to my wife and non-official "platinum sponsor" Carmen, for her continuous love and support in my life; also to the new king at home, who makes our life full of joy and happiness with his laughs and screams, our son Aksel Rafael.

Summary

Despite the recent trends to look for alternative sources of energy as substitutes to the traditional hydrocarbon fuels, still vast amount of oil and gas sources are coming from offshore reservoirs to feed the increasing need of energy in the world. The energy sector is still actively developing offshore fields to develop hydrocarbon reservoirs that are located beneath the seafloor, and there is an increasing interest in the quest for hydrocarbons in deepwater sites. These sites are exposed to risks from various types of geohazards, the most important of which is the risk posed by potential instability of submarine slopes located along the continental slope.

The research presented in this PhD thesis explored the stability of submarine slopes in deepwater sites from the geotechnical point of view. Since one of the main causes of the failure of submarine slopes is seismic activity, special consideration was given to the analysis of the dynamic response of submarine slopes under earthquake loading. The dynamic response of clay slopes is a function of the undrained shear strength, mass density and stiffness of the sediments. Much of the work presented in this thesis focused on the characterization of the undrained soil shear strength before, during and after the earthquake event. Understanding the evolution of the soil shear strength subjected to severe ground shaking is the key to understanding the evolution of the slope stability in time and space. Additionally, the combination of seismic loading and soil interfaces (preconditioning factor) in the soil profile, were analysed to explore the initiation process of slope failure. Several recent studies imply that soil interfaces such as weak layers played a key role in the failure initiation process of well-known cases such as the Storegga and Grand Banks submarine slides, among others.

The classical deterministic approach to slope stability assessment was complemented with a probabilistic approach to estimate the hazard and risk associated to the failure of submarine slopes. Special emphasis was given to the slope failure frequency model by developing a procedure to account for the uncertainties in earthquake characteristics and slope dynamic response. Furthermore, the transformation of the failed mass from slump to mass gravity flow, with special attention to the estimation of the runout distance, mudflow front velocity, and thickness of the failed mass on its way down along the continental slope was explored by means of numerical simulations. The numerical simulations that modelled the mechanics of the debris flow were complemented with the Monte Carlo simulation method to account for the uncertainties in the input parameters of the model, and estimating the probability of mudflow impacting the critical seabed facilities. This calculated probability of mudflow reaching the facility, together with the development of the slope failure frequency model, provided the basis for the earthquake-induced slope failure hazard analysis.

The risk analysis was done by assessing the direct consequences of slope failure. The direct consequences were quantified by developing vulnerability curves for the offshore installations at risk, the expected mudflow front velocity and thickness when impacting offshore structures, and the estimated impact forces versus lateral capacity of foundations.

The PhD research utilized information from the Lakach project, which is the first deepwater site to be developed in Mexico. This site is located in the Gulf of Mexico, close to the Veracruz state, on the continental slope with a water depth of 1,200 m. This deepwater site project is facing the threat of potential submarine slope failures at the border of the continental shelf and the continental slope, in water depth of about 500 m. These slope failure treats were investigated during this PhD programme.

The PhD research generated in total 9 research products: 3 peer-reviewed journal papers, 1 conference paper, 3 symposium papers, 1 AGU (American Geophysical Union) abstract, and 1 technical report. The 3 peer-reviewed journal papers are listed in the List of Journal Papers section, and the remaining research products are listed in the Appendices section.

In general, 3 papers and the technical report deal with the mechanics of the slope stability and debris flow dynamics from a deterministic point of view; 1 paper and the AGU abstract complement the deterministic approach with the frequency model to perform slope failure hazard analysis; 3 papers complement the slope failure hazard analysis with their corresponding consequences to assess the risk associated with slope failure.

List of Journal Papers

Rodríguez-Ochoa R, Nadim F, Cepeda JM *Offshore risk: Earthquake-induced slope failure in the Gulf of Mexico*. Canadian Geotechnical Journal (submitted for publication).

Rodríguez-Ochoa R, Nadim F, Cepeda JM, Hicks MA, Liu Z (2015) *Hazard analysis of seismic submarine slope instability*. Georisk: Assessment and Management of Risk for Engineered Systems and Geohazards:1-20. doi:10.1080/17499518.2015.1051546

Rodríguez-Ochoa R, Nadim F, Hicks MA (2015) *Influence of weak layers on seismic stability of submarine slopes.* Mar Pet Geol 65 (0):247-268. doi:http://dx.doi.org/10.1016/j.marpetgeo.2015.04.007

Table of Contents

Chapter 1

1. INTRODUCTION

1.1 Motivation

Among the variety of geohazards in deepwater sites, the failure of submarine slopes on the continental shelf and continental slope is one of the most significant hazards (Parker et al. 2008) that may impact the marine environment, the economic sector, and threaten human lives in coastal areas. The most frequent trigger of submarine slope failures is linked to seismic activity by itself (Hance 2003), or in combination with preconditioning factors, also known as slow triggers, such as soil boundary interfaces (e.g. weak layers) (Locat et al. 2013; L'Heureux et al. 2012; Solheim et al. 2005b).

The oil and gas industry in Mexico has decided to start exploiting hydrocarbons in deepwater environments. It is expected that risk assessment for submarine slides will assist the Mexican oil industry in the decision making process concerning the development of oil and gas offshore fields in deepwater sites in the Mexican part of the Gulf of Mexico. On the Mexican part of the Gulf of Mexico, the seismic activity is an important trigger for submarine slides that needs to be evaluated (Geomatrix 2006).

After intense geophysical explorations for potential hydrocarbon reservoirs in the Gulf of Mexico, a natural gas reservoir near the Veracruz state was identified that the national oil company PEMEX decided to develop. Therefore, important resources were designated to initiate the development of the first deepwater project in Mexico, and PEMEX together with the Mexican Petroleum Institute (IMP), and the Mexican National Council for Science and Technology (CONACYT) initiated research and training programs to face the new challenge of developing hydrocarbon fields in deepwater sites.

The first deepwater natural gas field to be developed is named Lakach, and has a water depth of about 1,200 m. PEMEX designated Fugro to perform the geological, geophysical and geotechnical exploration with the aim to characterize the site for future development. The reports generated by Fugro, together with previous seismic hazard studies in the region performed by Geomatrix (2006), formed the basis for carrying out risk analysis of submarine landslides triggered by earthquakes in the Gulf of Mexico.

The work described in this doctoral thesis is part of the research initiated by the Mexican Petroleum Institute (IMP), together with the Mexican National Council for Science and Technology (CONACYT) to address the challenges mentioned above. The research was carried out at the Department of Geosciences of University of Oslo (UiO), and the Norwegian Geotechnical Institute (NGI).

1.2 Objectives

The general objective of the research was to quantify the risk associated with earthquake-triggered submarine slides at the Lakach deepwater site using the available geological, geophysical, geotechnical and seismic data.

This required studying the response of clay slopes under earthquake loading, as well as the initiation process of submarine slope failures. Moreover, a frequency model of submarine slope failures in the region had to be established to assess the hazard and perform a risk analysis.

The quantification of the consequences related to the earthquake-induced landslide in the Lakach field is part of the risk assessment. Therefore, another objective of the research was the estimation of runout distances, front velocities and impact forces of debris flows against seabed structures. The above project-oriented objectives were combined with research-oriented objectives to fill the gaps in the current state of knowledge, by accomplishing the following goals.

- Identify the state-of-the-art in the earthquake-induced submarine slide risk analysis by carrying out literature review from relevant information sources.
- Detect areas to improve and develop the body of research in existence. The areas that were identified with potential to improve the state of knowledge are listed below:
    1. Quantify the influence of contrasting soil boundaries in the soil profile to induce slope failure.
    2. Study the evolution of the slope stability before, during and after an earthquake event.
    3. Develop alternative procedures to quantify the reduction of the undrained shear strength due to cyclic degradation and undrained creep.
    4. Suggest a new approach to quantify the seismic slope failure frequency, with special emphasis in the estimation of the annual failure probability (AFP).
    5. Develop vulnerability curves for offshore structures exposed to debris flow impact, aiming to quantify the consequences during the risk analysis.

1.3 Thesis Structure

Chapter 2 presents the central features of the seismic slope stability assessment in this research. It provides the geological, geotechnical and seismic description of the Lakach site, with special attention in the characterization of the continental shelf and continental slope. It also stresses the influence of soil boundary interfaces (preconditioning factor), together with the seismic activity, in the slope failure initiation process. Finally, chapter 2 highlights the importance of assessing the stability evolution of submarine slopes subjected to seismic loading with the aim to improve the current slope failure prediction capacity. This assessment involves the estimation of the undrained shear strength s_u, before (pre-seismic), during (co-seismic), and after (post-seismic) the earthquake event.

Journal paper no. 1 explores in detail the topics presented in chapter 2. Moreover, conference paper no. 1, enclosed in Appendix 1, studies the influence of the thickness of soil columns and the stiffness of half-spaces in the dynamic response of clay slopes. Report no. 1, enclosed in Appendix 6, examines the basic elements of seismic stability assessment of submarine slopes.

Chapter 3 presents the probabilistic approach adopted in this study for earthquake-induced slope failure, with special emphasis in the slope failure frequency model, mudflow runout distance, and the consequences of mudflow impact on offshore structures.

In section 3.1 the probability of earthquake-induced slope failure is analysed from an analytical point of view. It displays the key elements of the probabilistic approach that were applied in this research to estimate the annual failure probability (AFP): (1) Probabilistic Seismic Hazard Analysis (PSHA); (2) Ground Response Analysis; (3) Advanced Laboratory Tests; and (4) Fragility Curve Approach. The Fragility Curve Approach that was developed during this PhD programme provides an alternative method to estimate the AFP parameter. Further information about this approach is presented in journal paper no. 2. American Geophysical Union (AGU) conference abstract, enclosed in Appendix 5, explores the interpretation of the Fragility Curve Approach results.

Section 3.2 considers the probability of debris flow impact on seabed structures, assuming that the slope failure will evolve into a mass gravity flow. The presented methodology relies on numerical simulations of debris flows to predict runout distances, front velocities, and thickness of the debris flow in the time and space domains. It also shows the implementation of the Monte Carlo simulation method in the numerical simulations to account for the uncertainties in the input parameters of the numerical model. The application of the Monte Carlo method in the numerical simulations allows the generation of probability distribution functions of runout distance, mudflow front velocity, and mudflow thickness with the aim to estimate the probability of debris flow impact on seabed structures and their consequences. Symposium paper no. 3, enclosed in Appendix 4, explores the model uncertainty of the computer code BING used in the numerical analyses.

Section 3.3 presents the estimation of the direct consequences of slope failure in the Lakach project, by developing vulnerability curves of the elements at risk (Manifold South and

Manifold North). Section 3.4 makes the integration of results from section 3.1 to section 3.3 to quantify the risk in the Lakach project by using the classical definition of risk (i.e. Risk = Hazard × Consequences). Journal paper no. 3 examines the risk analysis procedure for Lakach site in detail. Symposium papers no. 1 and 2, enclosed respectively in Appendix 2 and Appendix 3, also explore the seismic slope failure risk analysis procedures.

Chapter 4 presents the main findings of this research programme, and chapter 5 the conclusions and recommendations for future work.

Chapter 2

2. SEISMIC SLOPE STABILITY ASSESSMENT

2.1 Site Characterization

2.1.1 Geological Setting

The area under investigation extends on both sides of the continental shelf break on the southern margin of the Gulf of Mexico (Fig. 1). A relatively wide continental shelf with gentle slope extending into deepwater characterizes the continental margin. The sediments form a mixture of siliciclastic and carbonate components. The dominant regional geological processes include normal deposition of sediments, slope failures and depositional processes associated to mass transportation, faulting, and oceanographic processes such as waves and currents. Secondary geological processes may include low frequency volcanism and earthquake events (Fugro GeoConsulting 2009).

Water depth increases from 76 m on the continental shelf, in the southern part of the study area, to about 1,490 m in the northern portion of deepwater. Seafloor gradients are about 1 degree or less on the continental shelf, about 3 degrees on the continental slope, and may locally exceed 24 degrees in geological features with steep sides on the seabed. The morphological features of the seabed include low relief faulting and fault scarps, and a seafloor from "hummocky" to wavy type related to buried mass transport deposits in Pleistocene period (Fugro GeoConsulting 2009).

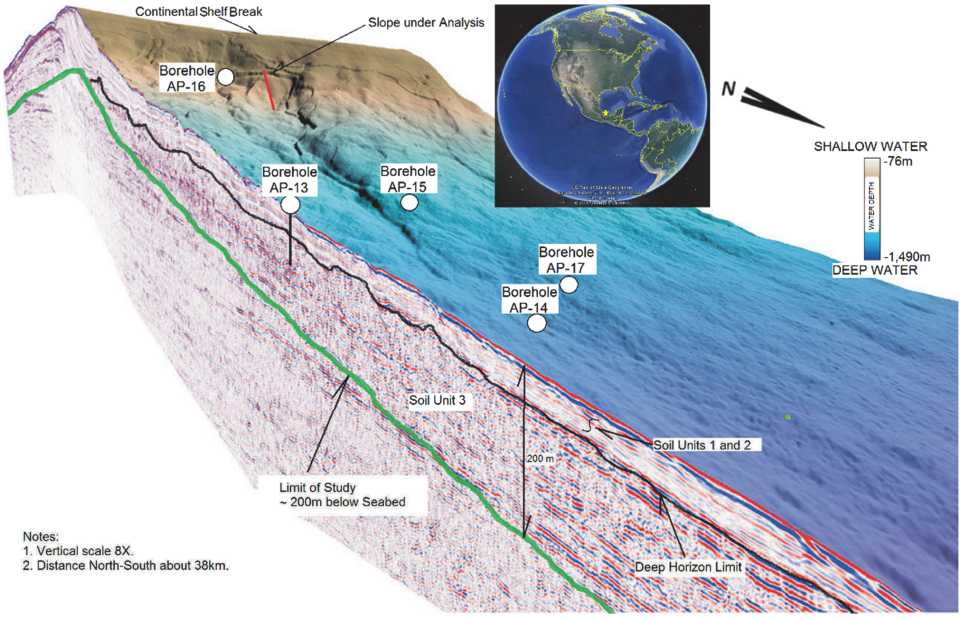

Figure 1. Geological model of Site 1, and slope under investigation in the Gulf of Mexico (modified after Fugro GeoConsulting 2009).

2.1.2 Geotechnical Setting

The seabed soils on the continental slope consist of calcareous clays ranging in consistence from very soft to hard with depth. Most of these soils are stratified and interbedded with debris flow deposits overlaying mass transport sediments. In the continental shelf, the seabed and shallow soils consist of very soft clays, and in the overconsolidated soil outcrop area the soils are mainly calcareous sands with carbonate skeletal materials and cemented carbonate aggregates (Fugro GeoConsulting 2009).

In general, the soils in the area can be characterised in three soil units. The soils from Unit 1 consist of shallow soils, mostly stratified unconsolidated, which are younger than the erosive surface identified in the CPT data (the shallow horizon). The variability in the thickness of this unit near the prominent sediment evacuation route is attributed in part to the loss of sediments by evacuation events due to slope failures during the Pleistocene and Holocene. The soils from Unit 2 consist of stratified soils containing debris flow deposits, and are located from the shallow horizon to the top regional mass transport deposits (the deep horizon). Unit 3 soils consist mostly of mass transport deposits, and are located from the deep horizon to 200 m below the seabed (Fugro GeoConsulting 2009).

In situ and laboratory tests of sediments from the site identify them as cohesive materials classified as high plasticity clays, calcareous soils with carbonate content between 11 to 23%. The predominant clay mineral is montmorillonite followed by illite, and the total of clay component is about 60 percent of the fines (Fugro Chance de México 2009).

Laboratory soil sensitivity varies from 3 to 5 up to 20 m below seafloor, and from 1.5 to 3 beneath 20 m. The estimated OCR's indicate that the cohesive soils in general fluctuate from normally consolidated to slightly overconsolidate (Fugro Chance de México 2009).

2.1.3 Seismic Setting

The Bay of Campeche is located in a region of moderate to high seismic activity. It is a relatively passive tectonic area, but it is located a few hundred kilometres north of the active triple junction among plate boundaries of North America plate, Caribbean plate and Cocos plate. Most seismic activity in the region is related to subduction margins along convergent Cocos plate (subducted) and North America plate, as well as the sliding process in the transform plate boundaries between the North America plate and the Caribbean plate (Fig. 2) (Geomatrix 2006).

The Trans-Mexican Volcanic Belt is related to the northern section of the subduction zone where the North American plate is subducting the Cocos plate along the Mesoamerican trench. This mostly calcareous-alkaline active volcanic arc has an East-West direction along central Mexico, from the Pacific Ocean to the Gulf of Mexico (Suarez and Singh 1986; Nixon 1982). The south-eastern end of this volcanic region that is close to the Bay of Campeche, is Tuxtla Volcanic Complex, which has had volcanic eruptions. The Trans-Mexican Volcanic Belt is characterized by normal faults, on the Quaternary period, with west-east direction and the development of horst and graben geological structures (Geomatrix 2006).

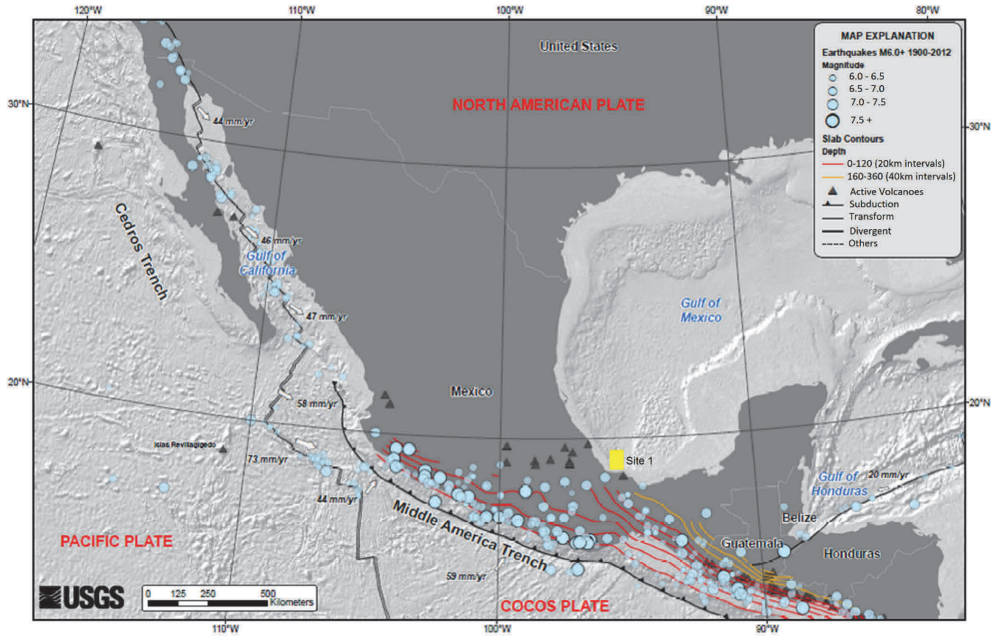

Figure 2. Historic seismicity in Mexico (modified after United States Geological Survey 2014). The map shows the epicentres of earthquake events of magnitude equal to or larger than M 6 from 1900 to 2012. The subduction zone from the Pacific Ocean, active volcanoes, and the transform zone from the Caribbean Sea are important sources of seismic activity near the Site 1.

2.2 Contrasts in Geotechnical Soil Properties

The initiation process of submarine slope failures in active margins is often associated with the combination of seismic activity and preconditioning factors like the formation of soil layer interfaces between contrasting soil geotechnical properties that form potential sliding failure surfaces (L'Heureux et al. 2012; Locat and Lee 2009; Bryn et al. 2005a; Bryn et al. 2005b; Solheim et al. 2005a; Norwegian Geotechnical Institute 1997). These soil layer interfaces can be found in the soil profile forming one, two or more soil boundaries in the soil mass.

2.2.1 One Soil Boundary

The journal papers no. 2 and no. 3 proposed respectively a hazard analysis and a risk analysis, related to the stability of a submarine slope dealing with one boundary between two soil units with contrasting geotechnical properties. The soil boundary, which may induce a shallow slide, is located about 8 m depth from the seafloor.

This type of soil interface is common in the marine environment, and it is formed due to the interaction of normally consolidated soils (NC) overlying overconsolidated soils (OC), resembling a "young" soft clay drape covering aging soils. This type of slide surface can be

modelled using an infinite slope model (Nadim et al. 2003). These boundaries between "old" and "young" soil layers are formed due to the deposition of soil sediments over slide surfaces leading to the formation of overconsolidated soils beneath them.

2.2.2 Two Soil Boundaries

A soil layer with contrasting geotechnical properties compared to the neighbouring soil layers, usually with lower shear strength and stiffness, located into the soil profile can be identified as a weak layer (Locat et al. 2013). Weak layers are getting more attention in the geo-sciences and geo-engineering communities due to their contribution in the initiation process of slope failures on land and offshore environments (Locat et al. 2013; L'Heureux et al. 2012; Picarelli et al. 2012; Urgeles et al. 2007; Camerlenghi et al. 2007). However, despite their intuitively relevant role in the initiation process of slope failures, the first attempt to set a definition of "weak layer" from a geotechnical point of view was done recently by Locat et al. (2013).

The journal paper no. 1 quantifies the effect of a weak layer, located at 25 m depth from the seafloor, in the stability of a submarine slope. Paper no. 1 shows through numerical analyses the negative effect of weak layers on the stability of submarine slopes before, during, and after an earthquake event.

2.3 Evolution of Seismic Slope Stability

When dealing with the stability of submarine slopes, it is important to assess the spatial and temporal stability, especially when one wants to go further in the stability analysis accounting for the hazard and risk associated to the slope failure. Journal papers no. 1, 2 and 3 account for the slope stability in the space and time dimensions by analysing the slope stability before (pre-seismic), during (co-seismic), an after (post-seismic) an earthquake event (Fig. 3). In general, the slope stability approach that was applied is a combination of numerical modelling and advance laboratory testing. This approach has shown to be an efficient technique to overcome the current limitations in the numerical models to predict the degradation of undrained shear strength due to the generation of excess pore pressure and strain softening during cyclic loading (Nadim et al. 2014; Andersen et al. 2012).

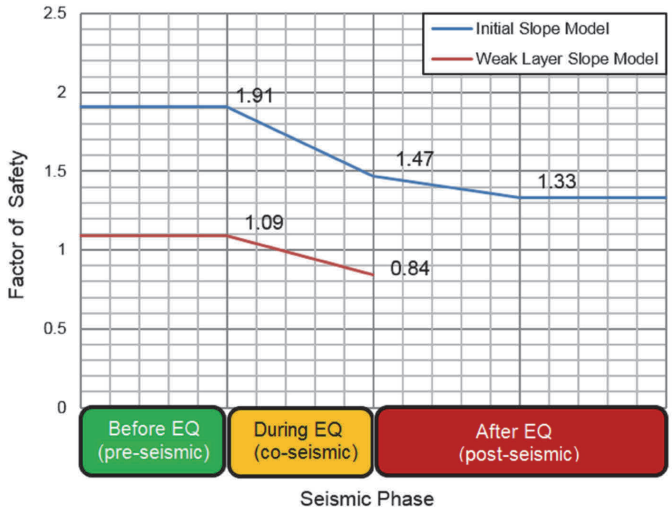

Figure 3. Evolution of seismic slope stability. The curves show the quantification of different states of stability of a submarine slope in the Gulf of Mexico throughout the different seismic phases: Before EQ (pre-seismic), During EQ (co-seismic), After EQ (post-seismic); and assess the influence of a weak layer on its stability.

2.3.1 Pre-Seismic Stability

The stability of submarine slopes is analysed before an earthquake event based on traditional numerical methods like the limit equilibrium method (LEM) or the finite element method (FEM) and using the soil properties under monotonic loading such as the undrained shear strength s_u. The stability status of the slope is typically quantified based on the factor of safety (FS), which is the ratio between the resistance forces and the driving forces. The pre-seismic factor of safety is considered a reference measure of the initial stability of the slope.

2.3.2 Co-Seismic Stability

At this stage the stability of the submarine slope is analysed just after the earthquake event has finished, and accounts for the degradation of the soil undrained shear strength due to the disturbance of the soil structure, excess pore pressure generation and strain softening effects. The degradation of the undrained shear strength was quantified based on 1-D and 2-D response analyses in combination with laboratory tests. The numerical codes AMPLE (Nadim 1985) and PLAXIS 2D (Brinkgreve 2011) were used to perform ground response analyses in one and two dimensions respectively. In journal paper no. 2, the Andersen et al. (2012) approach was used in conjunction with available monotonic simple direct shear test results, from sampled soils at the site, to estimate the soil shear strength degradation after earthquake loading. Alternatively, in journal paper no. 1 Failure Interaction Diagrams (FID's) were proposed to quantify the shear strength degradation (Fig.

4). This approach was proposed when the computed permanent earthquake-induced shear strains are smaller than the shear strain at the peak stress in the stress-strain curves. The stress-strain curves can be obtained from simple direct shear tests or equivalent soil resistance tests (Fugro Chance de México 2009).

The dynamic response analyses showed a concentration of larger displacements in the soft side of the soil interfaces than in the rest of the soil column. This is congruent with the propagation of shear waves theory. When incident waves traveling from the bedrock (half space) to the seafloor find in their way relevant soil interfaces [i.e. change from material 1 (hard soil) to material 2 (soft soil)] the displacement amplitude of the transmitted wave will be larger than the incident wave. The difference in displacement amplitude is a function of the contrast in stiffness (G_{max}) and density (ρ) of the two soil layers, and can be quantified based on the impedance ratio coefficient (α_z), where the smaller the coefficient the larger the contrast (Kramer 1996).

If the clay layers in the submarine slope exhibit significant strain-softening behaviour during the earthquake loading, it may be possible that slope failure occurs during the earthquake event. This type of slope failure was described by Biscontin et al. (2004) in *Scenario 1*, which is one of the three proposed slope failure scenarios based on ground response analyses using effective analysis SIMPLE DSS constitutive model.

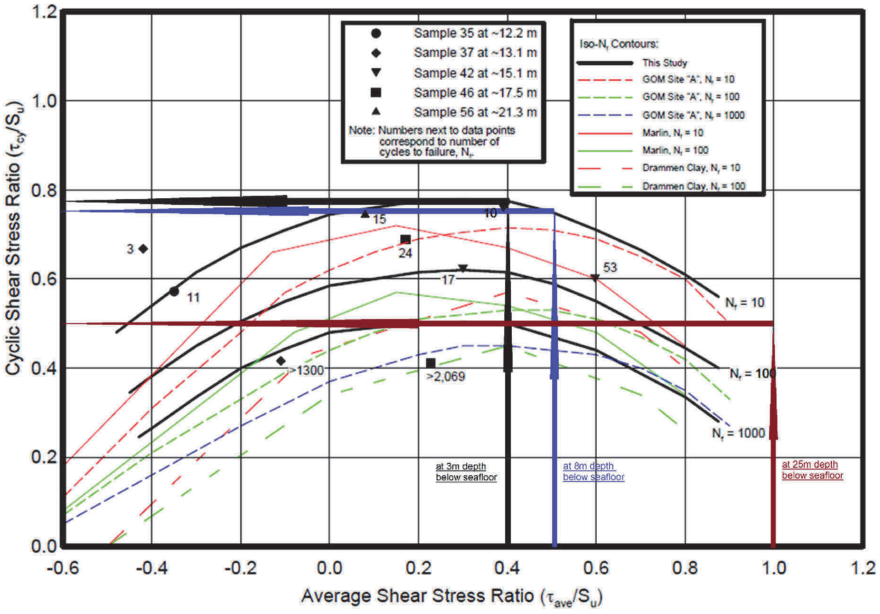

Figure 4. Failure Interaction Diagrams (FID's), based on cyclic triaxial tests were proposed to quantify the shear strength degradation. This approach was suggested when the permanent earthquake-induced shear strains are smaller than the shear strain at the peak stress in the stress-strain curves (modified after Fugro Chance de México 2009).

2.3.3 Post-Seismic Stability

The post-seismic slope stability accounts for the additional reduction of shear strength in the soil layers that were subjected to large deformations (i.e. earthquake-induced shear strain larger than shear strain at the peak stress of stress-strain curves). This additional soil strength reduction is based on undrained creep (i.e. ongoing deformation before excess pore pressure dissipation under constant load) and affects mainly the soil layers with remaining shear strength value close enough to the acting gravity forces on the clay slope. Moreover, Andersen et al. (2012) showed experimentally that the cyclic effect before undrained creep could lead to failure at the same load level where soil samples that were not subjected to cyclic loading before performing the undrained creep test did not fail.

Currently, the shear strength reduction due to undrained creep can be estimated based on Andersen et al. (2012) approach, who proposed an additional reduction of 15-25% of the co-seismic shear strength to account for the fitting between the monotonic and cyclic curves, as well as the (negative) shear rate effect due to undrained creep.

According to Havel (2004), failure could happen under distortion creep if the soil reaches the secondary creep phase. The limit between the primary and secondary phases of creep can be estimated using the shear stress ratio τ/τ_f proposed by Meschyan (1995) based on deviatoric creep results in clay. According to Meschyan test results, the limit between the development of the primary and secondary phases of creep is between 0.4 and 0.55 of the shear stress ratio τ/τ_f, where τ is the mobilised shear stress and τ_f is the clay shear strength.

In journal paper no. 1, a new interpretation of creep tests performed on Direct Simple Shear Apparatus was proposed to quantify the additional degradation of shear strength due to undrained creep, when strain softening is not expected in the clay layers. The proposed interpretation, open to discussion, exploits the apparently decreasing tendency of the shear stress with creep time to forecast undrained shear strength as a function of the creep time, by following the failure curve (i.e., red curve $\gamma = 15\%$) (Fugro Chance de México 2009).

Journal paper no. 2 showed that, the shorter the return period of the earthquake, the greater the difference between the co-seismic and the post-seismic conditional failure probabilities (Table 1). This implies that the relative probability of slope failure based on undrained creep increases in low magnitude earthquakes (frequent motions), which is consistent with the hypothesis of some researchers who suggest that undrained creep is the main reason for underwater slope failures. This type of slope failure was described by Biscontin et al. (2004) in *Scenario 3*, which is one of the three proposed slope failure scenarios based on ground response analyses using effective analysis SIMPLE DSS constitutive model.

It is believed that the failure of submarine slopes due to undrained creep may take days, weeks, months or even several years after the strike of an earthquake.

Table 1. Conditional probability of slope failure.

Return Period Earthquake (years)	Peak Ground Acceleration (g)	Co-Seismic Conditional Failure Probability	Post-Seismic Conditional Failure Probability	Conditional Relative Increase in Failure Probability Due to Undrained Creep (times)
1,000	0.155	0.01	0.08	8.00
5,000	0.280	0.11	0.23	2.09
10,000	0.355	0.22	0.32	1.45
100,000	0.730	0.48	0.53	1.10

Chapter 3

3. HAZARD AND RISK ANALYSIS OF EARTHQUAKE-INDUCED SLOPE FAILURE

3.1 Probability of Earthquake-Induced Slope Failure (Analytical Approach)

To estimate the risk associated with the failure of submarine slopes, it is imperative to quantify the hazard and the consequences. Hazard analysis concerning earthquake–triggered submarine slope failure is not a trivial problem due to the lack of information to establish the frequency model. This section presents the key elements of the proposed slope failure Fragility Curve procedure developed in journal paper no. 2, to perform hazard analyses related to the failure of submarine slopes induced by seismic activity.

3.1.1 Probabilistic Seismic Hazard Analysis (PSHA)

Among the diverse causes of slope failures in offshore environments, earthquakes are recognized as one of the main triggers of submarine slope failures in active margins (Urlaub 2013; Hance 2003; Locat and Lee 2002; Morgenstern 1967). Therefore, it is imperative to study the frequency of these natural events in relevant areas for the human interests. Seismic activity is linked to plate tectonics and volcano processes, as well as intraplate deformations. One of the major uncertainties in assessing earthquake-induced submarine slope failures is related to the probability of an earthquake event by itself.

Prediction of earthquakes is only possible in a statistical sense, although there are several lines of research attempting to make earthquake predictions. An analysis procedure that is widely used to deal with the earthquake uncertainty is the Probabilistic Seismic Hazard Analysis (PSHA) originally proposed by Cornell (1968). This type of probabilistic analysis accounts for all the seismic sources relevant for the site of interest, as well as the attenuation of the ground movements from the seismic source to the site. The basic formulation is meant to quantify the probability of a given ground motion parameter, usually the peak ground acceleration (PGA), exceeding a specified value at the site of interest. Usually, outcomes from a PSHA can be represented in a plot identified as seismic hazard curve (Fig. 7). Additionally, seismic response spectra are developed with equal probability of exceedance at all frequencies (so-called uniform hazard spectra), as well as representative acceleration time histories of the expected ground motions for several return periods (Geomatrix 2006).

3.1.2 Ground Response Analysis

Ground response analyses are used to predict the response of soil sediments under cyclic loading to forecast adverse effects such as slope failures, soil liquefaction and structural damage leading to fatalities or loss of property. Because of the complex nature of the mechanism of fault break, as well as the complex mechanism of energy transmission between the source and the site, ground response analyses are mainly focused on determining the response of the soil deposit to the motion of the bedrock immediately beneath it. With time, a number of techniques have been developed for ground response

analysis. These techniques are often grouped according to the dimensionality of the problems they can address (Kramer 1996).

Ground response analyses require soil constitutive models that imitate key features of the cyclic soil behaviour in order to simulate the response of sediments under earthquake loading. In general, there are three broad classes of soil models: Equivalent Linear Models, Cyclic Nonlinear Models and Advanced Constitutive Models. Equivalent linear models are the simplest and most commonly used but have a limited ability to represent many aspects of soil behaviour under cyclic loading conditions. At the other end of the spectrum, advanced constitutive models can represent many details of dynamic soil behaviour, but their complexity and difficulty of calibration currently make them impractical for many common geotechnical earthquake engineering problems (Kramer 1996).

Based on the probabilistic seismic hazard analysis (PSHA) carried out by Geomatrix (2006) near the slope under investigation (Fig. 5), Geomatrix recommended four representative acceleration time histories for site effect analyses (Table 2). According to the target response spectrum recommended by Geomatrix (Fig. 6), the motions were scaled in the frequency using equivalent linear dynamic software SHAKE-N (Selnes 1987). The digital acceleration records of Motions 1, 2 and 4 were downloaded from PEER (Pacific Earthquake Engineering Research Center) website, (University of California 2010) having two components each motion. The motion 3 with its two horizontal components was downloaded from COSMOS (Consortium of Organizations for Strong Motion Observation Systems) website, (COSMOS 1999). The four motions, each with 2 horizontal components (in total 8 digital records), were baseline corrected using the software SeismoSignal v. 5.1.0 (Seismosoft_Ltd 2013).

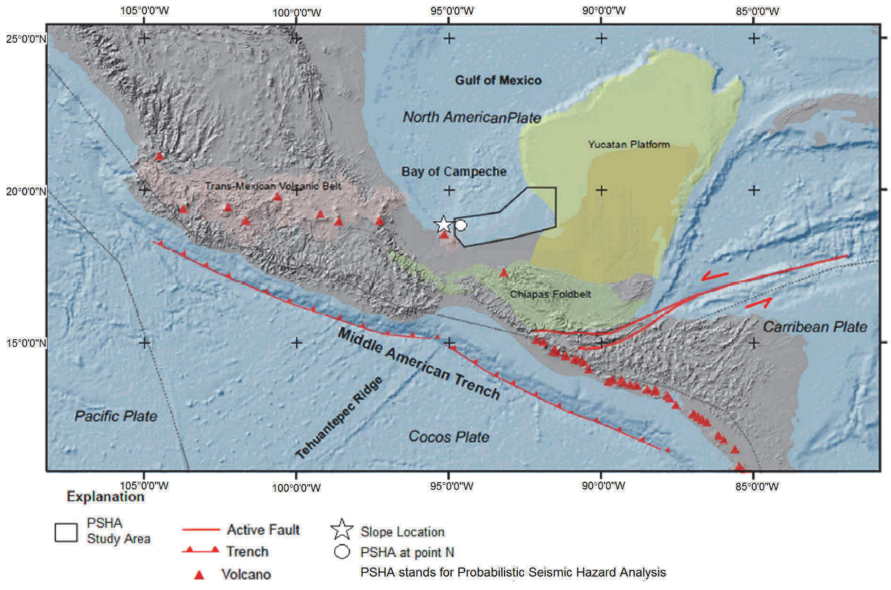

Figure 5. Tectonic structure, Campeche Bay, Mexico (modified after Geomatrix 2006).

Table 2. Recommended motions by Geomatrix for site effect analyses.

Motion	EQ/Station	Date	Component	Magnitude	Focal Distance (km)
1	Mammoth Lakes, California/Bishop-Paradise Lodge	May 27th, 1980	N70E S20W	6.0	44
2	Imperial Valley, California/Superstition Mountain	Oct 15th, 1979	N45E S45E	6.5	25
3	Nisqually, Washington/Mt. Erie, UW.ERW Station	February 28th, 2001	N0E N90E	6.8	150
4	Denali, Alaska/UA Station K2-06	November 3er, 2002	N0E N90E	7.9	270

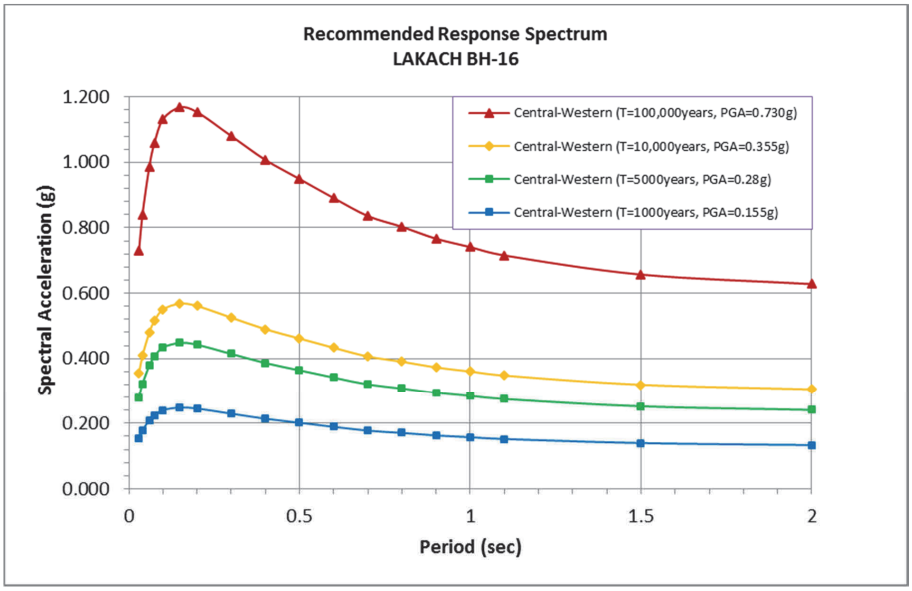

Figure 6. Recommended response spectra for the site.

Based on the historical seismicity of the site, it was estimated that the relevant return periods for these analyses may correspond to earthquake events of 1,000, 5,000 and 10,000 years return period. However, an additional 100,000 years earthquake event was also analysed to explore the slope response under large magnitude earthquakes (Figs. 6 and 7).

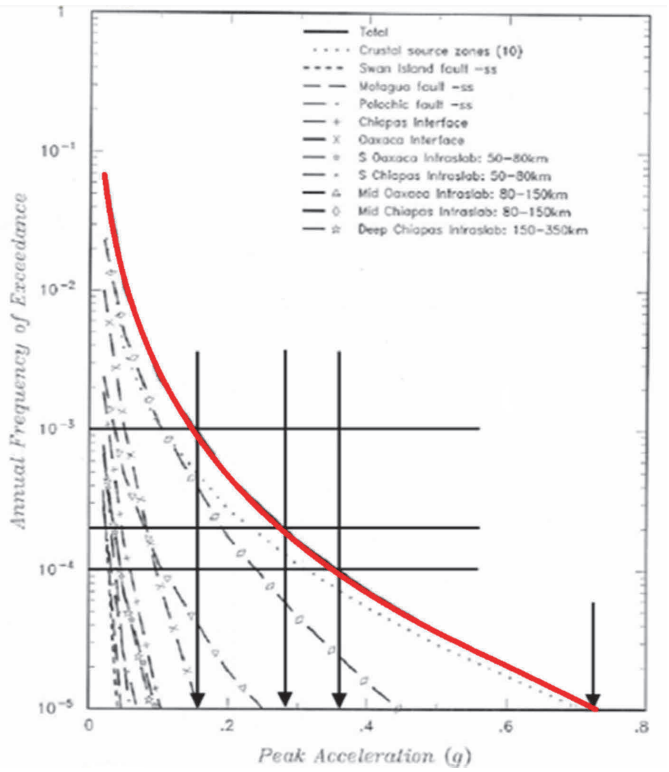

Figure 7. Seismic hazard curve for site N, closer point to the slope under investigation, with relevant return periods 1000, 5000, 10,000 and 100,000 years.

The dynamic analyses were carried out using the software AMPLE, code developed by Nadim (1985). The AMPLE slope model assumes an infinite slope with the propagation of shear waves perpendicular to the slope. The constitutive model that was used to run the analyses was the Hyperbolic (non-linear, failure-seeking model), which needs as input the soil shear strength $\tau_{strength}$ and the maximum shear stiffness G_{max}. The main output from the dynamic analyses is the accumulation of shear strains in the downslope direction of the slope to assess the shear strength reduction. To account for the uncertainties in the dynamic response of the submarine slope, dynamic response analyses for various combinations of representative earthquake ground motions and dynamic soil properties were carried out using the Monte Carlo simulation method.

The shear strength of soil, $\tau_{strength}$, is not an invariant parameter and depends on several factors. Determination of the appropriate value of $\tau_{strength}$ is complex because the different conditions of loading during an earthquake event induce outcomes in opposite directions (rapid rate of loading increases the shear strength, while excess pore pressures generated by cyclic loading decrease the soil strength) and their combined effect on the soil strength occasionally gives surprising results.

After analysing the random variables involved in the dynamic analysis using AMPLE, the variables presented in Table 3 were identified as the most relevant for this analysis. The probability distribution functions and assumed range of variation for each random variable were established after an exploratory analysis.

The variables taking into account in this analysis are meant to quantify the uncertainties in the response of the soil column.

Table 3. Random variables for the dynamic response analysis.

No.	Variable	Assumed Range	P. Distribution Function
1	$s_{u\ static}$ Factor	0.85-1.25	Lognormal (mean=1.05; mu=0.0246)
2	Peak ground acceleration, PGA	For 1,000 years return period: Range: 0.140-0.171g (10% upper and lower from the mean)	Normal (mean=0.155g)
		For 5,000 years return period: Range: 0.238-0.322g (15% upper and lower from the mean)	Normal (mean=0.280g)
		For 10,000 years return period: Range: 0.266-0.444g (25% upper and lower from the mean)	Normal (mean=0.355g)
		For 100,000 years return period: (30% upper and lower the mean) Range: 0.511-0.949g	Normal (mean=0.730g)
3	Control Motion	4 motions, 2 components each from 1 to 8 (Mammoth Lakes, M6.0; Imperial Valley, M6.5; Nisqually, M6.8; Denali, Alaska, M7.9)	Discrete Uniform Distribution
4	Strain Rate Factor f(ground response) $s_{u,h\text{-}sr}/s_{u,static}$	Range of predominant frequencies of original control motions: 0.35-13 Hz. Recommended target response spectra have max spectral acceleration at T=0.15sec, f=6.7 Hz. Fundamental frequency of the 200m soil profile: 0.35 Hz, T=2.9 sec. Range of shear strain rate at large strains in the first 20m below seafloor after analysing the response of the soil profile with two relevant motions: 500-2500 %/hr Equivalent strain rate factors according to Andersen et al. (2012): 1.2-1.5	Continuous Uniform Distribution (mean=1.35)

For the 10,000 and 100,000 earthquake events, 100 realizations were selected for each random variable using the Latin Hyper Cube stratified sampling technique (McKay et al. 2000) to guarantee a good representation of the distribution function with just 100 realizations. For the 1,000 and 5,000 earthquake events, up to 500 realizations for each random variable were generated due to the low conditional probability of failure for these return periods. The combination of random variables were set up based on the order given by the calculated realizations for each random variable using MATLAB (MathWorks 2012) version 8.

3.1.3 Advanced Laboratory Tests

Based on laboratory tests, Nadim et al. (2007) made a compilation of the main aspects of a typical soil element within a submarine slope to address the strength behaviour of clays in submarine slopes under earthquake loading. The following factors were investigated:

- Rapid Rate of Loading. It was confirmed that the undrained shear strength increases as the rate of loading increases.
- Permanent (static) Shear Stress. It was observed that the effect of a consolidation shear stress τ_c (i.e., gravity forces in slope) increases the strength of the soil when shearing downhill, but reduces the available shear strength for the slope by decreasing the difference between the permanent shear stress τ_c and the soil shear strength s_u.
- Post-earthquake static shear strength and creep deformations after the earthquake. It was shown that the cyclic shear strains induced by the earthquake tend to reduce the shear strength. If the earthquake-induced cyclic shear strains are large, the slope could undergo further creep displacements after the earthquake and experience a significant reduction of static shear strength.

The reduction in the post-earthquake undrained shear strength was specified partly based on the approach suggested by Andersen et al. (2012), using the results of laboratory testing carried out by Fugro Chance de México (2009) in soil samples obtained from the site, near the location of the slope under investigation.

Andersen's approach specifies that the stability of a slope subjected to earthquake loading may be analysed by first running a dynamic analysis, to determine the permanent shear strain due to earthquake. Then, the post-cyclic shear strength may be estimated as the shear stress on the monotonic stress-strain curve, corresponding to the calculated permanent shear strain (Fig. 8). This shear strength should be reduced by 15-25% to account for the following two effects:

- Undrained creep occurring before significant dissipation of the earthquake-induced excess pore water pressure. Considering the effect time to failure on the shear strength during undrained creep.
- The post-cyclic stress-strain curve stands somewhat below the virgin monotonic stress-strain curve.

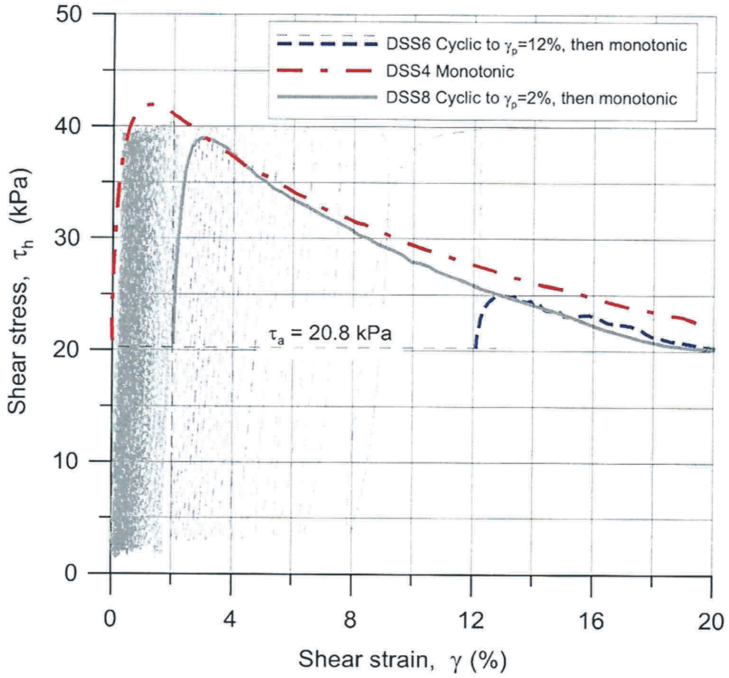

Figure 8. Stress-strain behaviour in monotonic, cyclic and post-cyclic monotonic direct simple shear tests (DSS) with $\tau_{ave}=\tau_c=20.8$ kPa$=0.16\ \sigma_{vc}'$ (after Andersen et al. 2012).

In this research, the effect of undrained creep in the clay layers is considered using available creep tests performed on soil samples from the site.

3.1.4 Fragility Curve Approach

This approach is a modification of the methodology developed by Nadim (2012), during projects linked to risk analyses in several offshore geohazards studies for the oil and gas industry.

This procedure has 10 steps and makes use of several mathematical techniques like Monte Carlo simulation, FORM and Bayesian Updating, in order to estimate the unconditional annual failure probability (UAFP). The Fragility Curve procedure attempts to deal with key uncertainties associated with the estimation of the UAFP parameter. It also allows to estimate the UAFP during the seismic activity (co-seismic) and after the seismic activity (post-seismic), providing additional information to decision makers, in order to mitigate the risk associated with earthquake-induced submarine landslides.

3.1.4.1 Co-seismic and Post-Seismic Fragility Curves of Slope Failure

The co-seismic and post-seismic fragility curves of slope failure were developed by fitting cumulative distribution functions (CDF's) to the estimated conditional probabilities of slope failure, during and after the earthquake event respectively. The term "fragility curve" was borrowed from the earthquake engineering field, where it is widely use to assess the probability of structural failure based on the amplitude of a given motion parameter (e.g. peak ground acceleration, PGA).

For the slope under analysis, lognormal probability distributions were proposed to match the conditional failure probabilities, which led to the creation of the slope failure fragility curves. The moments of the lognormal function representing the co-seismic hazard condition are M= 0.8737g and Std= 0.6948g, and the moments of the lognormal function representing the post-seismic condition are M= 0.8280g and Std= 0.8523g (Fig. 9).

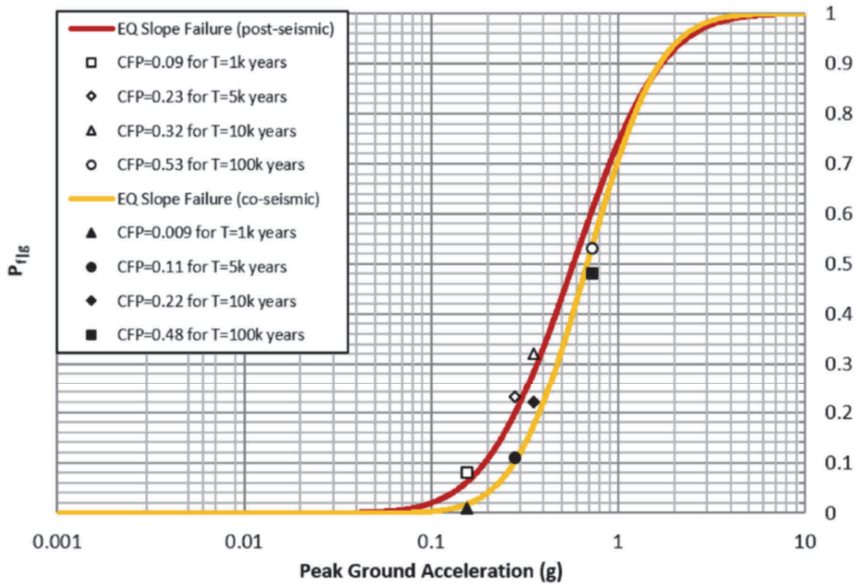

Figure 9. Lognormal cumulative distribution functions proposed to match the calculated conditional failure probability points for co-seismic and post-seismic sceneries, leading to the creation of the co-seismic and post-seismic fragility curves.

3.1.4.2 Expected Value Mathematical Operator

A key element to carry out hazard analyses using the Fragility Curve approach involves the use of the expected value mathematical operator. The unconditional annual failure probability (UAFP) can be estimated by applying the expected value operator to the annual failure probability (AFP) random variable. The expected value of a random variable is the integral of the random variable with respect to its probability measure. The following probability functions were used to estimate the expected value of the AFP:

a) Slope failure fragility function, normalized with respect to the return period, which evaluates the possible value the random variable can assume;

b) Derivative of the seismic hazard function, which evaluates the probability of occurrence of that value.

Thus, the UAFP is the probability-weighted average of the AFP random variable. Eq. (1) shows the mathematical formulation.

$UAFP = f(Seismic\ Hazard\ Function, Fragility\ Function)$=

$$UAFP = E[AFP] = \int_0^{\infty} f_X(x) \cdot (P_{f|x}/Tx) \cdot dX = \int_0^{\infty} f_X(x) \cdot AFP_{f|x} \cdot dX \quad (1)$$

where:

$UAFP$ = Unconditional annual failure probability

AFP = Annual failure probability random variable

$E\ [AFP]$ = Expected value of the AFP (probability weighted average of the annual failure)

$f_X\ (x)$ = Probability density function fitting the seismic hazard curve

$P_{f|x}$ = Slope failure fragility function

T_x = Return period corresponding to the peak ground acceleration x in $f_X\ (x)$

$AFP_{f|x}$ = Annual failure probability corresponding to the peak ground acceleration x ($P_{f|x}$ normalized with respect to T_x)

X = Random variable representing the peak ground acceleration (PGA) in the bedrock

x = Values that take the random variable X

In this study, a generalized pareto (GP) probability function was proposed to fit the seismic hazard curve recommended for the site (Fig. 10). The GP probability function that best fits the seismic hazard curve has parameters $k = 0.345$, $\sigma = 0.0049$, $\theta = 0$.

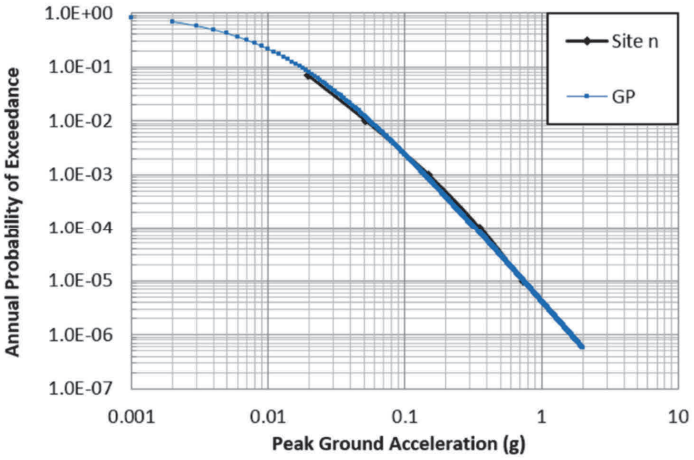

Figure 10. Generalized pareto distribution function used to fit the recommended seismic hazard curve located near the slope under investigation, identified as site n.

3.1.4.3 Annual Failure Probability (AFP)

Fig. 11 shows the integration of the previous probability functions from 0 to 1g, according to Eq. (1), to estimate the co-seismic and post-seismic unconditional annual probability of slope failure; that range was analysed due to its large contribution to the UAFP. Table 4 shows the results of the integration.

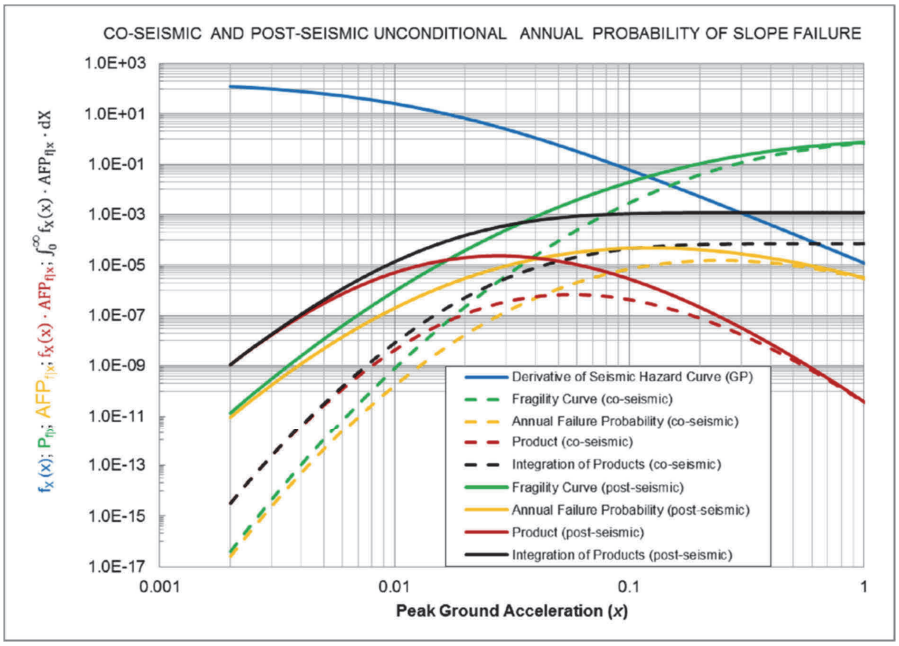

Figure 11. Integration of the slope failure fragility functions and the seismic hazard function, according to Eq. (1), to estimate the co-seismic and post-seismic unconditional annual failure probabilities. Dotted lines corresponds to co-seismic conditions and continuous lines corresponds to post-seismic conditions.

From Fig. 11, the annual failure probability curves (yellow curves) show that, the largest contribution to the co-seismic UAFP (dotted yellow curve) is between 0.2g and 0.3g. According to the seismic hazard curve (Fig. 10), it corresponds to earthquakes with return periods between 2,500 and 6,666 years. On the other hand, the largest contribution to the post-seismic UAFP (continuous yellow curve) is between 0.1g and 0.15g, it corresponds to earthquakes with return periods between 500 and 1000 years. However, the product of the functions (red curves) shifts the peak contributions to the left corresponding to earthquakes with lower return periods, since earthquakes with lower return periods have larger probability of occurrence than earthquakes with larger return periods.

Table 4. Unconditional annual probability of slope failure for the site in the Gulf of Mexico.

Probability distribution fitting the seismic hazard function	**Probability distribution fitting co-seismic fragility function**	**Co-Seismic Unconditional Annual Failure Probability ($UAFP_{co}$)**	**Probability distribution fitting post-seismic fragility function**	**Post-Seismic Unconditional Annual Failure Probability ($UAFP_{post}$)**
Generalized Pareto	Lognormal	$7 \cdot 10^{-5}$	Lognormal	$1.2 \cdot 10^{-3}$

The results show that the $UAFP_{post}$ increases by 17 times with respect to the $UAFP_{co}$. This suggests that, undrained creep developed in the clay layers of the slope after the earthquake event plays an important role in the slope stability. However, this information must be complemented with geological evidence from the site to decrease uncertainties (Gilbert et al. 2014). In the next section, geological information from the site is analysed to crosscheck with the numerical simulations.

3.1.4.4 Comparison with Geological Evidence

To obtain a sound estimate of the UAFP, analytical simulations must be compared with the geological evidence. The geological evidence of submarine slope failures at the site is based on the work carried out by Fugro GeoConsulting (2009) during the geological and geotechnical investigation in the area. Some relevant conclusions are pointed out below:

- Sediment Accumulation Rates

In the area where the submarine slope is located in the Gulf of Mexico, the continental shelf is narrower comparatively, and this factor may facilitate the transport of inner shelf sediments to the continental slope. The rate of accumulation of Holocene soils shows a decrease with increasing water depth and distance from the edge of the continental platform. The rate of sediment accumulation also shows local variations related to soil loss due to slope failure and slope mass transport processes.

This trend in the layer thicknesses is also observed in the underlying sediments of Pleistocene and older sediments, and is directly related to the trend in which the rate of clastic sedimentation decreases as the distance from on land geo-sources, such as river outlets, increases. Therefore, the more distal portions of the area receive less sediment than the more proximal areas.

Based on the dating results, the Upper Holocene depositional rates decrease from 136 cm / ky (DC -15) in the upper part of the continental slope to 57.7 cm / ky (DC- 09) on the lower part of the continental slope (Fugro GeoConsulting 2009).

- History of Slope Failure in the Continental Slope

The results of the sedimentological, biostratigraphy and radiocarbon analyses on selected samples extracted by piston cores showed that slope failures and mass transport processes in the Late Pleistocene [i.e., 2.588 my B.P. (million years before present) to 11,700 yrs B.P.] were much greater in extent than any recent activity. Evidence of slope failure from the Early to Middle Holocene (approximately over 4,000 years ago) has been documented by the existence of a hiatus in sediment dating profiles within several piston cores taken from deepwater. However, this most recent activity does not involve an area as large as the continental slope, compared to slope failures and mass transport episodes that occurred during the Pleistocene period.

According to Fugro GeoConsulting (2009), one has not found evidence of most recent slope failures and erosive flows of mass transport at large scale. However, the existence of shallow water foraminifera and muddy turbidites in three soil cores within the transitional slope, below the continental shelf border, indicates that local slope failures may have occurred in relatively restricted extent in the areas of greater slope gradient about 1,370 years ago.

That estimation corresponds approximately to an annual probability of slope failure of 1/1,370 years $\approx 7.3 \cdot 10^{-4}$. This value is close to the estimated $UAFP_{post}$ of $1.2 \cdot 10^{-3}$, calculated by numerical simulations for the slope under investigation, which is located below the continental shelf border.

The $UAFP_{post}$ ratio between the analytical approach and the geological evidence is equal to 1.6, where at this point the analytical approach seems to be overconservative. However, the geological evidence is subjected to the dating method limitations and the shortage of samples tested at the shelf break to confirm this value. Therefore, at this point, the analytical approach and the geological evidence could be used as high and low estimates of the $UAFP_{post}$ respectively.

3.2 Probability of Debris Flow Impact on Seabed Structures

A failed submarine slope may evolve from a slide to a sediment gravity flow. Sediment gravity flows may travel large distances depending on the volume of released mass, slope geometry and other factors like interaction processes between the soil particles and the gravity flow fluid, as well as the sediment gravity flow and the environment fluid.

Fig. 12 shows the main types of submarine mass movements based on the disturbance of internal mass structure and travel distance of displaced sediments proposed by Middleton & Hampton in 1973 (Covault 2011).

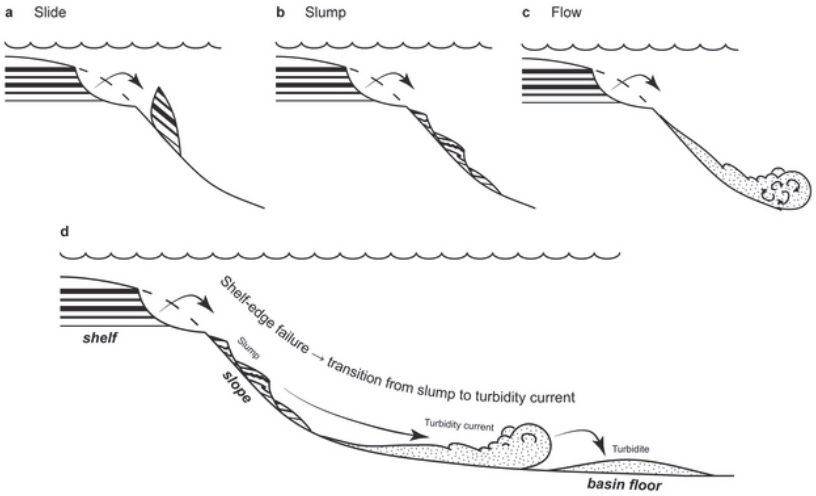

Figure 12. (a-c) Types of submarine mass movements based on the degree of internal structure disturbance. (d) Evolution of a failed submarine mass along the continental slope (after Covault 2011).

Journal paper no. 3 assesses the probability of debris flow impacting two manifolds that are required to develop a natural gas field in the south part of the Gulf of Mexico. The approach that was used to quantify the probability of impact on those offshore structures is based on runout distance numerical simulations that attempt to mimic the basic features of mudflows moving downwards by gravity in a water environment. This approach accounts for the uncertainties linked to the input parameters needed to run the numerical simulations by means of using the Monte Carlo method. The simulation results are used to develop probability distribution functions of the runout, which are in turn used to evaluate the probability of the mudflow reaching a given location.

3.2.1 Runout Numerical Simulations

Numerical modelling of submarine mass movements is often used to estimate gravity mass flow runout distances, velocities, and the final shape of the sediments in offshore geohazards studies. Since the pioneering work by Edgers and Karlsrud (1981), there have been important developments in this field.

In journal paper no. 3, the code BING developed by Imran et al. (2001a) was used to perform the runout numerical simulations. BING is a 1-D numerical model intended to simulate the downslope spreading of a finite-source subaqueous debris flow. The model considers three types of fluid rheology: Bingham, Herschel-Bulkley and Bilinear; and is able to compute runout distance, down-slope velocity and thickness of the deposit.

In this study, the Bilinear rheological model developed by Locat (1997) was used for the numerical simulations in BING, because it has shown to give acceptable results in previous studies (Jeong et al. 2010; Imran et al. 2001b; Locat 1997). Moreover, one additional advantage of the Bilinear model consists of requiring the solution of only one momentum equation in the numerical model because the flow is considered to consist of a single layer, as opposed to two separate layers (deforming and plug flow) in the popular Bingham and Herschel-Bulkley models (Imran et al. 2001b). This makes the Bilinear model relatively more stable than its predecessors do from the numerical point of view (Imran et al. 2001a).

The Bilinear model proposed by Locat (1997) has been adapted for numerical modelling by Imran et al. (2001a) as follows:

$$\frac{\tau}{\tau_{ya}} = 1 + \frac{\gamma}{\gamma_r} - \frac{1}{1+r\frac{\gamma}{\gamma_r}} \tag{2}$$

$$\gamma_r = \frac{\tau_{ya}}{\mu_{dh}} \tag{3}$$

$$r = \frac{\gamma_r}{\gamma_0} \tag{4}$$

where:

τ = shear stress (Pa)

γ = shear strain rate (s^{-1})

γ_r = reference strain rate (s^{-1})

r = ratio of strain rates

τ_{ya} = apparent yield strength (Pa)

μ_{dh} = viscosity at high shear strain rates (plastic viscosity) (Pa.s)

γ_0 = shear strain rate at the transition from a Newtonian to a Bingham behaviour (s^{-1})

Even though the BING code is a good option to perform debris flow numerical simulations, it has some limitations that are important to keep in mind during the interpretation of results. The main limitations of the model are listed below (Imran et al. 2001a):

a) Not suitable for too steep slope beds on which the flow will occur;

b) Lateral spreading of the debris flow is not considered;

c) Assumption of parabolic shape in the initial shape of the debris mass;

d) The assumption that the flow remains laminar during the entire simulation time;

e) The hydroplaning phenomenon observed by Mohrig et al. (1998) is not incorporated in the model;

f) The model does not incorporate the possibility of resistance generated at the interface between the moving debris and the ambient fluid above.

3.2.2 Accounting of Input Uncertainties using Monte Carlo Simulation

To account for the BING input parameters uncertainty on the runout distance, the Monte Carlo simulation method was used to obtain probability distribution functions of the runout distance.

The random variables used in the Monte Carlo simulations, together with their proposed probability distributions and probability moments or range of values are listed in Table 5.

Table 5. Random variables.

Variable	**Mean, Std or Range**	**Probability Function**
ρ_{mud} (kg/m^3)	1337, 29	Normal
τ_{ya} (Pa)	353, 100	Normal
γ_r (1/s)	1039, 52	Normal
r	6414, 1843	Normal
Initial Geometry	1 and 2	Discrete Uniform

The above input parameters are the mud density (ρ_{mud}), apparent yield strength (τ_{ya}), reference shear strain (γ_r), ratio of strain rates (r), and initial geometry configuration.

Since the water content in the flowing mass plays a key role in the dynamics of the mud flow, the range of values for the mud density as well as the parameters of the Bilinear rheological model (τ_{ya}, γ_r and r) were set based on the water content of the flowing mass and the empirical correlations developed by Locat (1997).

Regarding the random variable identified as Initial Geometry, this variable accounts for the initial geometry configuration of the failed sediments. BING assumes by default that the initial geometry of the debris mass has a parabolic shape. Thus, the input parameters are the initial length of mud deposit (base of the parabola), and the maximum thickness of mud deposit (height of the parabola).

Based on the seismic slope stability analyses for the site, it was estimated that the slide surface may occur at 8m beneath seafloor in the upper part of the composed slope model. Consequently the unit cross section volume along the failure surface is about 8m × 600m × 1m. To run the numerical simulations it was proposed to use two initial geometry configurations:

1. Configuration No.1 matches the initial length of the estimated slide surface with the initial length of mud deposit (i.e. base of the parabola = 600m), and a maximum thickness of mud deposit of 12m.

2. Configuration No.2 matches the initial thickness of the slide surface with the maximum thickness of the mud deposit (i.e. height of the parabola = 8m), and an initial length of mud deposit of 900m.

In the Monte Carlo simulations, 100 values for each random variable were generated using the specified ranges and probability distribution functions shown in Table 5. The stratified Latin Hyper Cube sampling technique proposed by McKay et al. (2000) was used to ensure a good representation of the distribution functions for all the random variables.

3.2.3 Probabilistic Runout Distance Estimation

Figure 13 shows the probability density functions generated in MATLAB (MathWorks 2012) to fit the numerically simulated runout distance data. It can be observed that the lognormal distribution fits the data well. The mean and standard deviation of the fitted distribution are 9.97 km and 2.83 km respectively. This probability distribution was used to estimate the probability of mud reaching specific locations once the slope under analysis has failed.

The offshore natural gas field in the South part of the Gulf of Mexico is planned to be developed by deploying a system of seven wells and two manifolds, called Manifold South and Manifold North (Fig. 14). The Manifold South will have four wells connected around it and the Manifold North will have three wells connected around it. The risk assessment study focused on the consequences of mudflow impact on the two manifolds that will be deployed to develop the natural gas field.

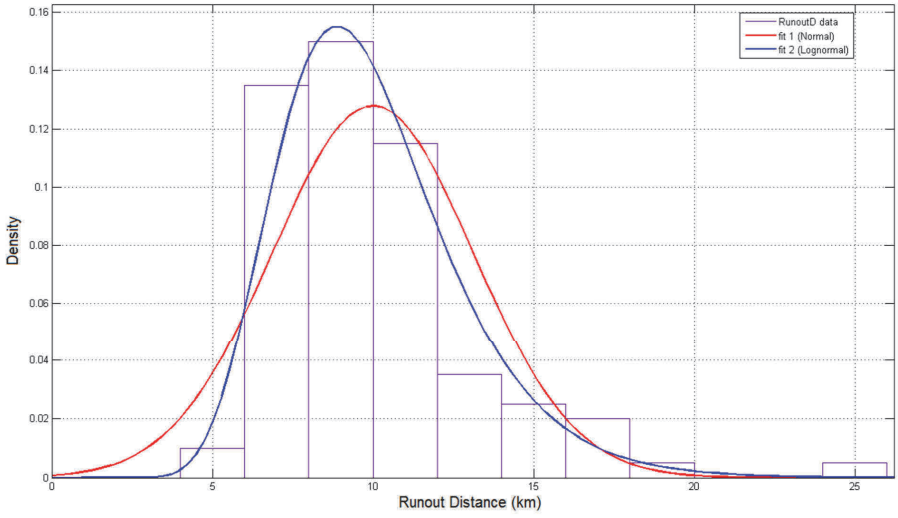

Figure 13. Runout distance probability density functions fitting the numerically simulation data.

Manifold South and Manifold North are located about 10.5 km and 14.0 km respectively from the crown of the slope under investigation (Fig. 14). The probability of these seabed structures been impacted by the mud flow, given that the slope has failed, was estimated using Eq. (5).

$$P_{impact} = P(Runout\ Distance \geq Manifold\ Location) \quad (5)$$

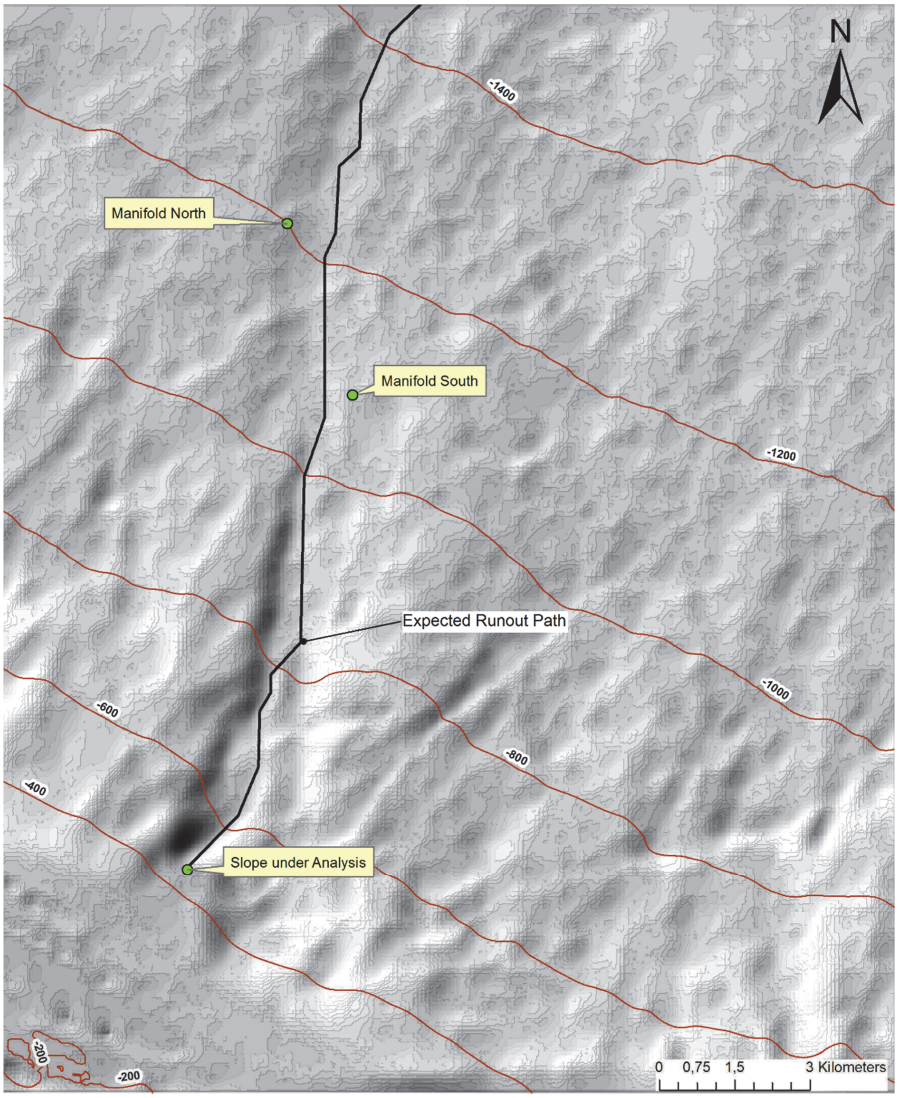

Figure 14. Expected runout path of the failed sediments, and location of source and exposed elements for the risk analysis.

The conditional impact probabilities (given that slope failure has occurred) for the Manifold South and Manifold North are $P_{impactMS}$ = 0.37 and $P_{impactMN}$ = 0.09 respectively. These probabilities are based on the lognormal probability distribution function that best fits the numerical runout distance data.

3.3 Consequences of Earthquake-Induced Slope Failure

In general, there are two categories of consequences: direct consequences and indirect consequences. There are methods and recommendations to quantify the direct consequences. However, quantification of indirect consequences is not trivial given their qualitative nature. The direct consequences are related primarily to the loss of human lives and economic losses.

In journal paper no. 3, the quantification of the direct consequences focused mainly on the cost of damage or total loss of the offshore equipment (i.e. production manifolds), rather than the economic losses due to production disruption and environmental impact. Although the economic losses due to production disruption and environmental impact may be more significant and important than the cost of the equipment, their estimation requires complex analytical scenarios that are beyond the scope of this research.

3.3.1 Vulnerability Curves for Manifolds

As mentioned earlier, in this analysis it was considered that the critical seabed installations exposed to mud flow impact hazard are the manifolds. A production manifold is a subsea structure containing valves and pipework designed to combine and direct produced fluids from multiple wells into one or more flowlines. It is assumed that the pipelines that transport the natural gas to onshore facilities for further distribution follow a safe route away from the mud flow impact critical zone. The same applies for the subsea umbilicals, which form the link between topside and subsea systems by a series of cables and pipes meant to provide power and control to the subsea systems.

To estimate the consequences, the vulnerability curves for each element at risk are required. The estimated vulnerability (fragility) curves for the manifolds were based on the lateral capacity of their foundation. The foundation solution of the manifolds are suction caissons with approximately 6 m diameter and about 17 m length.

The maximum lateral capacity of the suction pile that may resist the mud flow impact forces is about 650 kN, based on the foundation design carried out by Rahim (2014). It is noted that this capacity does not take into account the shear rate effect on soils that may increase the actual lateral capacity several times compared to the monotonic loading, as Mirdamadi (2014) showed experimentally on single piles subjected to lateral impacts.

The mud flow impact forces were estimated on the basis of the work done by Zakeri (2008) during his PhD studies. The fluid dynamics approach was adopted instead of the conventional, and strain-rate-dependent geotechnical approaches, because it represents better the basic features of the phenomenon.

Among the fluid dynamics approach methods, the Pfeiff and Hopfinger (1986) method was chosen, which is based on laboratory experiments with vertical cylinders moving through dense suspensions of polystyrene beads in water representing idealized mudflow. This formulation is based on the classic fluid dynamics approach regarding the force experienced by an object moving through a fluid at relatively large velocity (i.e. high Reynolds number,

Re >~1000). The drag coefficient is a function of the Reynolds number (Re = Inertial Forces/Viscous Forces) as well as the shape and surface rugosity of the object.

In this study it is assumed that the mud flow will impact the top part of the suction pile, at the interface between the suction pile and the manifold. Hence the impacted object was considered to have a cylinder shape with a smooth surface. The manifold itself is a very complex steel structure and it is difficult to estimate the drag coefficient based on its shape and surface rugosity.

Figure 15 shows the estimated vulnerability curves for the manifolds, which are a function of the velocity and the thickness of the mud flow.

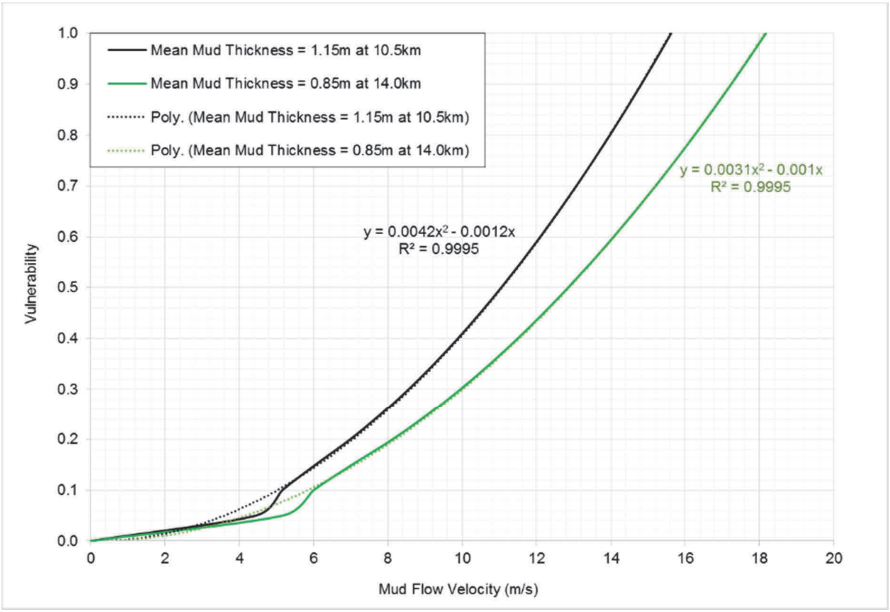

Figure 15. Vulnerability curves for exposed manifolds based on the velocity and mean thickness of the mud flow at 10.5 km and 14.0 km.

Table 6 shows the expected front velocity and thickness of the mud flow at 10.5 km (position of Manifold South) and 14.0 km (position of Manifold North) from the crown of the slope respectively. The values listed in Table 6 are based on probabilistic analyses of the simulation output data.

Table 6. Expected front velocity and thickness of mud flow.

Distance from the Crown of the Slope (km)	**Front Velocity (m/s)**	**Mud Thickness (m)**
10.5	23	1.15
14.0	21	0.85

3.4 Risk Quantification

To estimate the risk associated to earthquake-induced submarine slope failure for the future deepwater natural gas development in the Gulf of Mexico, the classical definition of Risk as shown in Eq. (6) was applied.

$$Risk = Hazard \times Consequences \tag{6}$$

In this context, *Hazard* can be defined as the probability of sediments impacting offshore structures given that a submarine slope has failed, and can be estimated with Eq. (7).

$$P[Sediments\ impacting\ seabed\ installation] = P[EQ\ induced\ slope\ failure] \times P[Sediments\ reaching\ seabed\ installation \mid Submarine\ slope\ has\ failed] \tag{7}$$

With respect to the *Consequences*, they can be estimated by the summation of the products of the element at risk, times its vulnerability as shown in Eq. (8).

$$Consequences = \sum_1^n Element\ at\ risk_1 \times Vulnerability_1 + \cdots Element\ at\ risk_n \times Vulnerability_n \tag{8}$$

In order to implement the contributions developed for the hazard analysis during this PhD programme into the risk analysis stage, the co-seismic and the post-seismic earthquake-induced slope failure risk analyses were estimated. Moreover, the estimation of the AFP based on the geological evidence approach was considered as the lower bound of the post-seismic annual failure probability, and the numerical approach as the upper bound of the post-seismic annual failure probability (i.e. $UAFP_{geological} = 7.3 \cdot 10^{-4}$ and $UAFP_{numerical} = 1.2 \cdot 10^{-3}$) during the risk assessment of the deepwater natural gas development in the Gulf of Mexico.

The main outcomes from the direct risk analysis are shown below. The detail calculations can be found in Journal paper no. 3.

To obtain the direct risk, the general formulation of Eq. (6) was used, together with the assumption that the cost of Manifold South and Manifold North are the same as follows:

Co-Seismic:

$$Direct\ Risk_{Co-Seismic} = \sum_1^2 2.58 \cdot 10^{-5}{}_{MS} \times Manifold\ South\ (\$)_{MS} + 6.27 \cdot 10^{-6}{}_{MN} \times Manifold\ North\ (\$)_{MN} = \boldsymbol{Manifold}(\$) \times \left(\mathbf{3.21 \cdot 10^{-5}}\right)$$

Post-Seismic:

$$Direct\ Risk_{Lower\ Bound} = \sum_1^2 2.70 \cdot 10^{-4}{}_{MS} \times Manifold\ South\ (\$)_{MS} + 6.57 \cdot 10^{-5}{}_{MN} \times Manifold\ North\ (\$)_{MN} = \boldsymbol{Manifold}(\$) \times \left(\mathbf{3.36 \cdot 10^{-4}}\right)$$

$$Direct\ Risk_{Upper\ Bound} = \sum_{1}^{2} 4.44{\cdot}10^{-4}{}_{MS} \times Manifold\ South\ (\$)_{MS} + 1.08{\cdot}10^{-4}{}_{MN} \times Manifold\ North\ (\$)_{MN} = \boldsymbol{Manifold}(\$) \times \left(\mathbf{5.52{\cdot}10^{-4}}\right)$$

Consequently, the lower bound post-seismic direct annual risk is 10 times greater than the co-seismic direct risk, and the upper bound post-seismic direct annual risk is 17 times greater than the co-seismic direct risk associated with the earthquake-induced submarine slope failure at the site under study.

Chapter 4

4. MAIN FINDINGS

The main findings of the PhD research, which are described in the peer-reviewed journal papers, are summarized below.

The aim of journal paper No. 1 was to quantify the influence of the presence of a weak layer on the stability of a clay submarine slope under seismic loading. This was done by considering the stability of the slope before (pre-seismic), during (co-seismic) and after the earthquake (post-seismic).

The study described methods to assess the evolution of the resistance forces of the slope, focusing mainly on the evolution of the undrained shear strength for the co-seismic and post-seismic phases.

The framework of the study is based on comparing two quasi-identical slopes: the reference case, called the Initial Slope Model, mimics the same characteristics as a submarine clay slope found in the Site 1 zone, Gulf of Mexico. The other case, identified as the Weak Layer Slope Model, is identical to the first model except for a weak layer located at 25m depth. The comparisons of the two slopes included static slope stability assessment using the limit equilibrium method and the finite element method, pseudo-static analyses using the limit equilibrium method, and 1-D and 2-D non-linear dynamic analyses using the finite element methods.

Given the complexity of the problem, the degradation of the soil strength during and after the earthquake loading was estimated through a decoupled approach based on the calculated shear strains and results of advanced laboratory tests.

The results of the study show quantitatively the important role of a weak layer in the initiation of a submarine landslide under a strong earthquake.

Journal paper No. 2 focused on estimating the probability of earthquake-induced submarine slope failure (hazard), which is an important input to quantitative risk assessment. A novel procedure called the Fragility Curve approach, which is based on probabilistic seismic hazard analyses, ground response analyses, and advanced laboratory tests, was developed and applied in the study. The Fragility Curve approach makes use of available geological, geophysical, geotechnical and seismological information, and accounts for their significant uncertainties in the estimation of the annual probability of slope failure.

Fragility curves for slope failure during the earthquake (co-seismic) and after the earthquake (post-seismic) were developed in the study. The probability of slope failure calculated for the latter situation compared well with the geological evidence. The example calculations showed that the Fragility Curve approach provides a clear and well organized procedure for estimating the Annual Failure Probability (AFP) of a submarine slope under earthquake loading.

Journal paper No. 3 presents a quantitative analysis of the risk associated with earthquake-induced slope failure for the future deepwater natural gas field development in the southern part of the Gulf of Mexico. The slope failure probability was estimated using the Fragility Curve approach described in journal paper No. 2. The main threat posed by a submarine slope failure on seabed installations at this site is the impact of mud flows on the manifolds on seabed.

The probability of a mud flow generated by slope failure impacting the manifolds required to develop the natural gas field was established by numerical simulations. The Monte Carlo simulation method was used to account for the input model parameter uncertainties. The consequences of mud flow impact were estimated based on the calculated vulnerability curves for the foundations of the manifolds.

The estimation of the direct risk was based on the cost of losing the manifolds by using the classic definition of risk (i.e. Risk = Hazard × Consequences).

The analyses implied that the direct risk after the earthquake event is about one order of magnitude greater than during the earthquake event. Therefore, the analysis of slope stability at different stages of the seismic event may provide valuable information in choosing the appropriate risk management option.

Chapter 5

5. CONCLUSIONS AND RECOMMENDATIONS FOR FUTURE WORK

The estimation of the risk associated to the failure of submarine slopes subjected to seismic loading involves the study of a wide spectrum of technical fields. In general, there are two main approaches to be followed, the deterministic approach, which provides the mechanics of the slope stability, sliding process and impact forces, and the probabilistic approach, which provides the frequency of events and accounts for the key uncertainties involved throughout the risk analysis. Together they help to estimate the risk associated to this natural process of mass transport in the marine environment.

The main conclusions of this research are categorized under the following themes: slope stability (deterministic), hazard analysis (probabilistic), and risk analysis (probabilistic):

Slope Stability

- The phenomenon of submarine landslides in passive margins with gentle slope angles is still under investigation by the international research community. The key to understand many of these events lies in better understanding of the preconditioning factors, rather than the external triggers.
- This research showed quantitatively the negative influence of geotechnical contrasting soil interfaces (i.e. weak layers, and NC soil layers overlaying OC soil layers) on the seismic stability of submarine slopes. Therefore, it is important to identify these interfaces / weak layers during the site investigation activities and characterize them based on their location, thickness and contrast in stiffness and strength relative to the neighbouring layers to assess their impact.
- The results regarding the influence of a hypothetical weak layer at 25m below seafloor, on the static stability of the slope before the earthquake showed that the presence of the weak layer may reduce the factor of safety by 42% (i.e. FS = 1.91 without weak layer vs. FS = 1.10 with weak layer).
- After accounting for the cyclic degradation of the shear strength of soil layers that developed large shear strains, a further decrease of 43% in the factor of safety of the Weak Layer Model was observed. According to the analyses, the Weak Layer Slope Model will fail during the earthquake, because the shear strength in the weak layers is degraded so much during the seismic loading that the slope is no longer able to support its own weight.
- After accounting for the undrained creep in the deformed layers of the Initial Slope Model, an additional 10% decrease of the factor of safety is shown due to strength degradation in the critical layer, reducing the safety factor from 1.47 during the earthquake to 1.33 after the earthquake.
- The current challenge is to predict the increment of the driving forces (i.e. triggers), as well as the decrease of the resisting forces (i.e. soil shear strength), in the time domain. This will help to forecast the state of equilibrium of the slope in all phases of

a seismic event to assist in the decision process to set offshore structures and installations.

Hazard Analysis

- This research developed a hazard analysis procedure called the Fragility Curve approach for estimating the submarine slope annual failure probability (AFP) parameter. This approach plays a key role for the assessment of the risk associated to the seismic submarine slope instability, and involves the determination of the co-seismic and post-seismic annual probabilities of slope failure.
- Thorough the hazard analysis, key uncertainties such as the geotechnical properties of the site, ground motion characterization, and dynamic response of the soil sediments are taking into account.
- The findings in this study suggest that the annual probability of earthquake-induced slope failure for the submarine slope located at the site under study, in the Gulf of Mexico, is about $7 \cdot 10^{-5}$ during the earthquake (co-seismic) and $1.2 \cdot 10^{-3}$ after the earthquake (post-seismic). This estimation seems representative for the conditions at the site, and is supported by the geological evidence with an AFP value of about $7 \cdot 10^{-4}$.
- The calculations show that, the shorter the return period of the earthquake, the greater the difference between the co-seismic and post-seismic conditional failure probabilities. This implies that the relative probability of slope failure by undrained creep increases in low magnitude earthquakes, which is consistent with the hypothesis of some researchers who suggest that undrained creep is the main factor for underwater slope failures.

Risk Analysis

- In this study, the quantification of the consequences focused mainly on the cost of the offshore equipment rather than the economic losses due to production disruption and environmental impact. It should be noted, however, that the economic losses due to production disruption and environment impact are likely to be greater than the cost of the equipment, but their estimation requires complex analytical scenarios that are beyond the scope of this study.
- Based on the location of the slope under analysis, it was estimated that once it has failed, the resulting mud flow will be transported along the existing natural channel. Thus the channel may increase the runout distance and flow velocity that BING model is not able to take into account. However, it is believed that the lack of implementing the channel effect in the numerical model may be compensated with the overconservative runout distances found in BING code, with the Bilinear rheological model, as Rodríguez-Ochoa et al. (2015) showed during runout back-analyses using BING.

- To estimate the direct risk associated to submarine slope failure for the future natural gas field development in the Gulf of Mexico, the manifolds located nearby the natural channel were considered as the main elements at risk. Vulnerability curves for the manifolds were developed based on the lateral capacity of their foundations (suction caissons), and debris flow drag forces estimated with the fluid dynamics approach. However, the lateral capacity of the foundations does not take into account the loading rate effect on the soils during the impact.
- The co-seismic and post-seismic direct risks were estimated based on the cost of the manifolds as shown in Table 7.

Table 7. Direct risk analysis.

Co-Seismic	**Post-Seismic**	
	Lower Bound (Geological Evidence)	**Upper Bound (Numerical Simulations)**
$(3.21 \cdot 10^{-5}) \times$ *Manifold* (\$)	$(3.36 \cdot 10^{-4}) \times$ *Manifold* (\$)	$(5.52 \cdot 10^{-4}) \times$ *Manifold* (\$)

Table 7 shows that the post-seismic direct risk is about one order of magnitude greater than the co-seismic direct risk. This suggests that analysing the slope stability at different stages of the earthquake event (i.e. during and after), may provide an opportunity to manage the risk more effectively and mitigate some of the potential consequences of the submarine slope failure.

Future Work

The present research provided insights for future work, which are summarized in the following recommendations:

- Perform sensitivity analyses to look at the critical change in strength, stiffness and thickness in contrasting soil layers that may induce seismic slope failure.
- Look for constitutive models to estimate excess pore pressure and strain softening in dynamic analyses without sacrificing practicality. The constitutive model that was used to mimic the dynamic response of the marine sediments in PLAXIS 2D was the Mohr-Coulomb (M-C) model, which is not the best model to simulate dynamic response because of its limitation to capture the cyclic strength degradation in the elastic range.
- Study the influence of thixotropy in soils as a factor that may counterbalance undrained creep after an earthquake event.
- Explore the influence of loading frequency rate on the mechanical behaviour of soils to improve the dynamic response predictions.

- Improve the available practical runout distance models to account for the evolution of the soil shear strength degradation as a function of the soil structure disturbance and increment of the water content in the soil mass.
- Develop a code to perform Monte Carlo probabilistic runout distance analyses using more advanced runout models than BING.
- Finally, this research met some limitations from the soil testing point of view, such as the lack of available soil samples consolidated under shear stress to represent the slope configuration; and the shortage of available soil samples from the shelf break to improve the geotechnical and dating characterization of the soils nearby the slope under investigation. It would be ideal to have PSHA data from the location of the slope under investigation instead of a nearby site.

REFERENCES

Andersen K, Lunne T, Kvalstad T, Forsberg C (2012) Deep Water Geotechnical Engineering (Ingeniería geotécnica en aguas profundas). vol Publication No. 208. Norwegian Geotechnical Institute, Publication No. 208, Oslo, Norway

Biscontin G, Pestana JM, Nadim F (2004) Seismic triggering of submarine slides in soft cohesive soil deposits. Mar Geol 203 (3–4):341-354. doi:http://dx.doi.org/10.1016/S0025-3227(03)00314-1

Brinkgreve RBJ (2011) PLAXIS 2D. 2011 edn. Delft University of Technology & PLAXIS bv, The Netherlands

Bryn P, Berg K, Forsberg CF, Solheim A, Kvalstad TJ (2005a) Explaining the Storegga Slide. Mar Pet Geol 22 (1–2):11-19. doi:http://dx.doi.org/10.1016/j.marpetgeo.2004.12.003

Bryn P, Berg K, Stoker MS, Haflidason H, Solheim A (2005b) Contourites and their relevance for mass wasting along the Mid-Norwegian Margin. Mar Pet Geol 22 (1–2):85-96. doi:http://dx.doi.org/10.1016/j.marpetgeo.2004.10.012

Camerlenghi A, Urgeles R, Ercilla G, Bruckmann W (2007) Scientific Ocean Drilling Behind the Assessment of Geo-Hazards from Submarine Slides. Workshop Reports. DOI:10.2204/iodp.sd.4.14.2007. doi:10.2204/iodp.sd.4.14.2007.

Cornell CA (1968) Engineering seismic risk analysis. Bulleting of the Seismological Society of America 58 (5):1583-1606

Consortium of Organizations for Strong-Motion Observation Systems (COSMOS) (1999) University of California, Berkeley. http://www.cosmos-eq.org/index.html. Accessed 05.02.2011

Covault J (2011) Submarine Fans and Canyon-Channel Systems: A Review of Processes, Products, and Models. Nature Education Knowledge 3 (10):4

Edgers L, Karlsrud K (1981) Viscous Analysis of Submarine Flows. Norwegian Geotechnical Institute, Norway

Fugro Chance de México SAdeCV (2009) Reporte Final, Investigación Geotécnica en Aguas Profundas, Golfo de México, México. Volumen I: Criterios para Diseño Geotécnico. vol Volumen I: Criterios para Diseño Geotécnico. FUGRO,

Fugro GeoConsulting I (2009) Investigación Geológica y Geotécnica Integrada, Sonda de Campeche, México. FUGRO, Sonda de Campeche, México

Geomatrix (2006) Evaluación de Peligrosidad Sísmica, Bahía de Campeche, México.

Gilbert RB, Lacasse S, Nadim F Advances in geotechnical risk and reliability for offshore applications. In, Hong Kong, 2014. 4th International Symposium on Geotechnical Safety and Risk, ISGSR 2013. pp 29-42

Hance JJ (2003) Development of a database and assessment of seafloor slope stability based on published literature. University of Texas at Austin,

Havel F (2004) Creep in soft soils. Norwegian University of Science and Technology, Trondheim, Norway

Imran J, Harff P, Parker G (2001a) A numerical model of submarine debris flow with graphical user interface. Computers & Geosciences 27 (6):717-729. doi:http://dx.doi.org/10.1016/S0098-3004(00)00124-2

Imran J, Parker G, Locat J, Lee H (2001b) 1D Numerical Model of Muddy Subaqueous and Subaerial Debris Flows. Journal of Hydraulic Engineering 127 (11):959-968

Jeong SW, Locat J, Leroueil S, Malet J-P (2010) Rheological properties of fine-grained sediment: the roles of texture and mineralogy. Canadian Geotechnical Journal 47 (10):1085-1100. doi:10.1139/T10-012

Kramer SL (1996) Geotechnical earthquake engineering. Prentice Hall, Upper Saddle River, N.J.

L'Heureux JS, Longva O, Steiner A, Hansen L, Vardy M, Vanneste M, Haflidason H, Brendryen J, Kvalstad T, Forsberg C, Chand S, Kopf A (2012) Identification of Weak Layers and Their Role for the Stability of Slopes at Finneidfjord, Northern Norway. In: Yamada Y, Kawamura K, Ikehara K et al. (eds) Submarine Mass Movements and Their Consequences, vol 31. Advances in Natural and Technological Hazards Research. Springer Netherlands, pp 321-330. doi:10.1007/978-94-007-2162-3_29

Locat J (1997) Normalized rheological behaviour of fine muds and their flow properties in a pseudoplastic regime. In: Chen C-l (ed) Debris-flow hazard mitigation: mechanics, prediction, and assessment. American Society of Civil Engineers, San Francisco, California, pp 260-269

Locat J, Lee H (2009) Submarine Mass Movements and Their Consequences: An Overview. In: Sassa Kyoji CP (ed) Landslides – Disaster Risk Reduction. Springer, pp 115-142

Locat J, Lee HJ (2002) Submarine landslides: advances and challenges. Canadian Geotechnical Journal 39 (1):193-212. doi:10.1139/t01-089

Locat J, Leroueil S, Locat A, Lee H (2013) Weak Layers: Their Definition and Classification from a Geotechnical Perspective. In: Krastel S, Behrmann J, Volker D et al. (eds) Submarine Mass Movements and Their Consequences 6th International Symposium, vol 37. Springer, Switzerland, pp 3-12

MathWorks (2012) MATLAB R2012b. 8 edn.,

McKay MD, Beckman RJ, Conover WJ (2000) A Comparison of Three Methods for Selecting Values of Input Variables in the Analysis of Output From a Computer Code. Technometrics 42 (1):55-61. doi:10.1080/00401706.2000.10485979

Meschyan SR (1995) Experimental rheology of clayey soils. Geotechnika (Book 13). CRC Press,

Mirdamadi A (2014) Deterministic and Probabilistic Simple Model for Single Pile Behavior under Lateral Truck Impact. Monograph, Texas A & M University,

Mohrig D, Ellis C, Parker G, Whipple KX, Hondzo M (1998) Hydroplaning of subaqueous debris flows. Geological Society of America Bulletin 110 (3):387-394. doi:10.1130/0016-7606(1998)110<0387:hosdf>2.3.co;2

Morgenstern NR (1967) Submarine slumping and the initiation of turbidity currents. Marine Geotechnique:189-210

Nadim F (1985) AMPLE a computer program for analysis of amplification of earthquakes. Oslo, Norway,

Nadim F (2012) Risk Assessment for Earthquake-Induced Submarine Slides. In: Yamada Y, Kawamura K, Ikehara K et al. (eds) Submarine Mass Movements and Their Consequences, vol 31. Springer, Dordrecht, pp 15-27. doi:10.1007/978-94-007-2162-3_2

Nadim F, Biscontin G, Kaynia AM Seismic Triggering of Submarine Slides. In: Offshore Technology Conference (OTC), Houston, Texas, USA, May 2007 2007. vol OTC 18911. pp 1-8

Nadim F, Krunic D, Jeanjean P Probabilistic Slope Stability Analyses of the Sigsbee Escarpment. In: Offshore Technology Conference, Houston, Texas, USA, 2003. vol OTC 15203.

Nadim F, Lacasse S, Jae CY, Hadley C (2014) Estimation of Temporal Probability in Offshore Geohazards Assessment. Paper presented at the Offshore Technology Conference, Houston, USA,

Nixon GT (1982) The relationship between Quaternary volcanism in central Mexico and the seismicity and structure of subducted ocean lithosphere. Geological Society of America Bulletin 93:514-523

Norwegian Geotechnical Institute (1997) Earthquake Hazard and Submarine Slide. Submarine slides - A literature survey. Norwegian Geotechnical Institute, Oslo, Norway

Parker EJ, Traverso C, Moore R, Evans T, Usher N Evaluation of Landslide Impact on Deepwater Submarine Pipelines. In: Offshore Technology Conference (OTC), Houston, Texas, USA, 2008. OTC, pp 1-12

Pfeiff C, Hopfinger E (1986) Drag on Cylinders Moving Through Suspensions With High Solid Concentration. PCH Physico Chemical Hydrodynamics 7 (2/3):101-109

Picarelli L, Comegna L, Tommasi P, Urciuoli G (2012) The detection of hidden shear zones in clay: A relevant issue in landslide hazard assessment. In: Quental-Coutinho R, Mayne PW (eds) The fourth international conference on site characterization, Pernambuco, Brazil, 2012. CRC Press, Taylor and Francis Group, p 1912

Rahim A (2014) Suction Pile Geotechnical Design. Lakach Manifold, Revision 3 edn. Norwegian Geotechnical Institute,

Rodríguez-Ochoa R, Nadim F, Cepeda JM Correction Factors for 1-D Runout Analyses of Selected Submarine Slides. In: 7th International Symposium on Submarine Mass Movements and Their Consequences, Wellington, New Zealand, 2015. vol (Accepted for publication). Springer,

Seismosoft_Ltd (2013) SeismoSignal. 5.1.0 edn., Italy

Selnes PB (1987) SHAKE (N) – Computer program for analysis of earthquake response in horizontally layered sites. Norwegian Geotechnical Institute, Oslo, Norway

Solheim A, Berg K, Forsberg CF, Bryn P (2005a) The Storegga Slide complex: Repetitive large scale sliding with similar cause and development. Mar Pet Geol 22 (1-2 SPEC. ISS.):97-107. doi:10.1016/j.marpetgeo.2004.10.013; 10.1016/j.marpetgeo.2004.10.009

Solheim A, Bryn P, Sejrup HP, Mienert J, Berg K (2005b) Ormen Lange - An integrated study for the safe development of a deep-water gas field within the Storegga Slide Complex, NE Atlantic continental margin; executive summary. Mar Pet Geol 22 (1-2 SPEC. ISS.):1-9. doi:10.1016/j.marpetgeo.2004.10.001

Suarez G, Singh SK (1986) Tectonic interpretation of the Trans-Mexican Volcanic Belt-Discussion. Tectonophysics 127:155-160

United States Geological Survey (2014) Mexico Seismicity Map - 1900 to 2012. Available from the Internet: http://earthquake.usgs.gov/earthquakes/world/mexico/seismicity.php (accessed 14.04.2014). http://earthquake.usgs.gov/earthquakes/world/mexico/seismicity.php. Accessed 14/04/2014 2014

PEER Ground Motion Database (2010) University of California, Berkeley. http://peer.berkeley.edu/peer_ground_motion_database. Accessed 05.02.2011

Urgeles R, Camerlenghi A, Ercilla G, Anselmetti F, Brückmann W, Canals M, Gràcia E, Locat J, Krastel S, Solheim A (2007) Scientific ocean drilling behind the assessment of geo-hazards from submarine slides, Barcelona, Spain, 25–27 October 2006. Eos,

Transactions American Geophysical Union 88 (17):192-192. DOI: 110.1029/2007EO170009. doi:10.1029/2007EO170009

Urlaub M (2013) The role of sedimentation rate on the stability of low gradient submarine continental slopes. University of Southampton,

Zakeri A (2008) Submarine Debris Flow Impact on Pipelines. Paper Based, University of Oslo Oslo, Norway

I

PAPER I

Influence of weak layers on seismic stability of submarine slopes

Rodríguez-Ochoa R, Nadim F, Hicks MA (2015)

Journal of Marine and Petroleum Geology

II

PAPER II

Hazard analysis of seismic submarine slope instability

Rodríguez-Ochoa R, Nadim F, Cepeda JM, Hicks MA, Liu Z (2015)

Georisk: Assessment and Management of Risk for Engineered Systems and Geohazards

III

PAPER III

Offshore risk: Earthquake-induced slope failure in the Gulf of Mexico

Rodríguez-Ochoa R, Nadim F, Cepeda JM

Canadian Geotechnical Journal (submitted for publication)

Appendix 1

Paper No.4 (Conference Paper no. 1)

Rodríguez-Ochoa R, Nadim F, Kaynia AM *Sensitivity Analyses for Submarine Slopes under Seismic Loading.* In: 15th World Conference on Earthquake Engineering, Lisbon, Portugal, 2012. International Association for Earthquake Engineering, p 10.

Sensitivity Analyses for Submarine Slopes under Seismic Loading

R. Rodríguez Ochoa
University of Oslo / International Centre for Geohazards

F. Nadim
Norwegian Geotechnical Institute / International Centre for Geohazards

A. M. Kaynia
Norwegian Geotechnical Institute

SUMMARY:
In a typical soil profile for offshore deep water, the clay layers extend beneath the seafloor for hundreds of meters beyond the geotechnical explorations, making it difficult to accurately establish their mechanical properties and locate the depth of the bedrock. To quantify the response of the soil mass accounting for the thickness of the soil mass, the stiffness at the base and the magnitude of submarine slope angles, a sensitivity analysis for a site in the Gulf of Mexico was carried out. The earthquake-induced shear strain within the soil deposit is a key parameter in the slope stability assessment, therefore the analyses focused on the maximum shear strain as the main outcome.
Based on these simulations one may conclude that the predicted response for the 100m soil profile is more sensitive to the stiffness of the bottom and the slope angles than that of the 200m soil profile.

Keywords: dynamic response analysis, offshore geohazards, submarine slopes, earthquake-induced shear strain, shear wave velocity

1. INTRODUCTION

The oil and gas industry remains the main source of energy all over the world despite the increasing attention to develop other sources of energy. Therefore vast effort is still focused on the quest for hydrocarbons, but many of the reservoirs are found in offshore sites with increasing water depths. Offshore structures are necessary for the development of oil and gas fields, many of them need to be placed in areas with potential submarine slide activity, for this reason it is important to take into account the stability of submarine slopes during the selection process of the sites.
In the south part of the Gulf of Mexico, in a region called Lakach, during the exploration activities the National Oil Company of Mexico (PEMEX) discovered a natural gas reservoir for development. The gas reservoir is located about 55 km from land with water depth about 1200m.
The geophysical survey was performed by Fugro GeoServices, Inc., from March 13th to April 24th in 2008, the geotechnical field investigation was carryout by Fugro Chance de Mexico, S.A. de C.V. from August 9th to November 23th in 2008 in a vessel called M/V Fugro Explorer, Fugro (2009, 2009a, 2009b).
Given the seismicity of the region, where the site is influenced by the subduction zone in the pacific coast, there is concern about submarine landslides trigger by earthquakes that could impact the marine environment and the natural gas production. Therefore it is important to estimate the dynamic behavior of the clay sediments at the site by means of numerical simulations to assess the stability of the submarine slopes under seismic activity.
To perform the ground response analysis, it is important to establish at what depth the control motion should be located to initiate the propagation of the shear waves throughout the soil. During the simulations the half-space is meant to be the boundary between the bedrock and the soil, but the geology of the offshore sites in deep waters normally makes it difficult to find the rock horizon clearly. In many offshore sites it is common to find layers of fine soil for hundreds of meters beneath seafloor, making it difficult to define reference bedrock on the basis of geotechnical and geophysical

explorations. An additional difficulty is to specify which shear wave velocity for the bedrock, there are different criteria depending on personal experience.
Taking into account the above issue, this paper explores the effect of the depth and stiffness of the bedrock in the response of the clay sediments, as well as the influence that the slope angle has on the dynamic response of the clay sediments. To achieve this, 1-D site response analysis for level ground was used as starting point to gain information about the response of the soil under earthquake loading conditions followed by simulations with sloping ground.
The sensitivity analyses were performed by means of using 2 computational programs for the simulations SHAKE(N) (Selnes, 1987) and AMPLE (Nadim, 1985), 2 soil profile thickness with different shear wave velocities at the half-space and 4 different slope angles. The initial shear wave velocities used for the half-space were based on the estimated geotechnical soil properties and the increasing velocities were assigned for sensitivity analyses.
The simulations illustrate in a quantitative manner the importance of the depth and stiffness of the half-space as well as the slope angle in the dynamic response of the soils. With SHAKE(N) the 100m soil profile shows more sensitivity to the increase in the shear wave velocity compared to the 200m soil profile, although the 200m soil profile produces larger shear strain values. Based on the simulations with AMPLE2, in general the sensitivity of both soil profiles is similar with respect to the shear wave velocity. Regarding the slope angle as changing variable, it can be seen the high impact that the slope angle has on the soil response, for example, when the slope angle increases from 0 degrees to 15 degrees the maximum shear strain increases about 20 times.

2. SITE CHARACTERIZATION

In order to characterize the site under investigation for stability analyses, it is necessary to divide the activities in two main stages, regional and site specific evaluations.
The objective of the regional survey is to get an overview of the relevant area and to give input for the site specific evaluations. The main sources of regional information are the geophysical surveys, including bathymetric mapping of the region and mapping of soil sediments. Location and estimation of slope angles, previous slide activities and possible unstable layers can be identified based on geophysical surveys.
The objective of the site specific evaluation is to determine the slope stability for critical slopes in the survey area and possible submarine slides that can damage the integrity of an offshore structure. Special laboratory testing has to be carried out to determine the soil response to a triggering mechanism such as earthquake loading.

2.1. Slope Geometry

In the Lakach area there were identified 9 potential unstable slopes ranging from 0.1 to 9.2 degrees during the high resolution shallow, 200m below seafloor, geophysical survey carried out by Fugro GeoServices, Inc., in the Lakach zone, Fugro (2009, 2009a).

2.2. Soil Geotechnical Properties

In situ and laboratory tests were carried out by Fugro (2009a, 2009b) to obtain the geotechnical parameters to establish the soil strength and soil deformation properties. In the area, 5 boreholes were completed until approximately 100m depth from the seafloor. In all boreholes, PCPT tests were carried out from the seafloor to 100m depth, also soil sampling at different intervals depending on the depth range. For advanced static and dynamic laboratory tests, 24 soil samples at different depths were obtained for each borehole by means of nickel Shelby type tubes.
Generally the sediments are cohesive materials classified as high plasticity clays (CH), calcareous soils with carbonate content between 11 to 23 %. The predominant clay mineral is montmorillonite followed by illite, according to the X-ray diffraction tests.
The undrained shear strength of the clay was estimated based on PCPT in situ tests, Triaxial UU, vane miniature (VM), torque-meter vane (TV) and pocket penetrometer (PP) tests.

Laboratory soil sensitivity varies from 3 to 5 until 20m depth and from 1.5 to 3 beneath 20m.
The stress history information was obtained by means of consolidation tests at constant rate (CRS); the pre-consolidation effective stresses $\sigma'_{v,m}$ were estimated using Casagrande and Becker methods as well as PCPT in situ tests using empirical correlations. The estimated OCR's indicate that the cohesive soils in general fluctuate from normally consolidated to slightly over consolidated.
The geotechnical properties of the sediments for this sensitivity study were obtained from the closest borehole, identified as AP-16, to the slope with the largest slope angle of 9.2 degrees, Fugro (2009, 2009a).
The undrained shear strength (s_u) soil profile for borehole AP-16 was obtained using the SHANSEP approach by Ladd and Foott (1974), see Fig. 2.1.

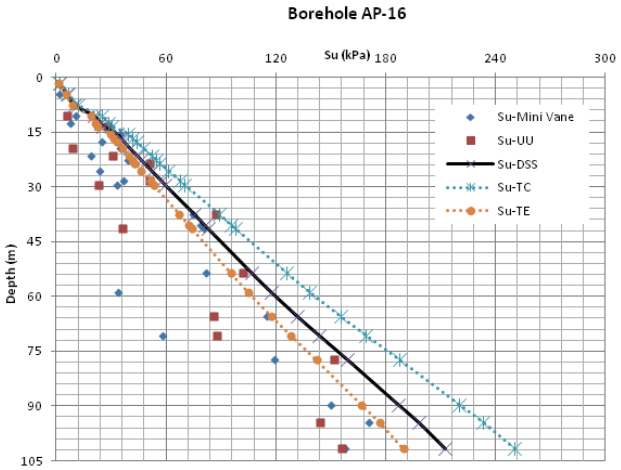

Figure 2.1. Undrained shear strength soil profile

3. SOIL DYNAMIC RESPONSE

In order to estimate the stability of a slope subjected to cyclic loading, like earthquake phenomena, it is important to understand the dynamic response of the sediments, to achieve this, ground response analyses were carried out using 2 computational programs SHAKE(N) (Selnes, 1987) and AMPLE (Nadim, 1985). Both computer programs use the simplified one-dimensional wave propagation through the soil medium. The former is based on the quasi-linear approach by means of transfer functions for horizontal soil layers and the latter is based on the non-linear approach which solves the one dimensional shear wave propagation problem in horizontal or sloping layered soil profile.

3.1. Shake(N)

Simulations were carried out using an improved version of the original program SHAKE (Schnabel, et. al., 1972) called SHAKE(N) (Selnes, 1987). This computer program for analysis of earthquake response in horizontally layered sites was used to estimate the dynamic response of the clay layers in the site. The program contains a wide range of options to facilitate site response studies such as computations of time-histories of acceleration, velocity, displacement, transfer functions, Fourier spectra, duration, Husid plot, response spectra and spectral ratios.

3.1.1. Input control motion
The control motion to perform the ground response analysis was the Denali earthquake, in Alaska USA. Magnitude 7.9 recorded at the UA station K2-06 in November 3rd, 2002, having a focal distance of 270 km. This motion was recommended by Geomatrix (2006) to perform the ground response

analysis in the region. The peak ground acceleration (PGA) was scaled to 0.098 g corresponding an earthquake with return period of 500 years, according to the Probability Seismic Hazard Analysis (PSHA) for the area done by Geomatrix (2006). For the simulations the recorded component 360 with duration of about 120 sec determined by means of 5-95 % total energy on Husid plot was used. The response spectrum for this motion is shown in Fig. 3.1.

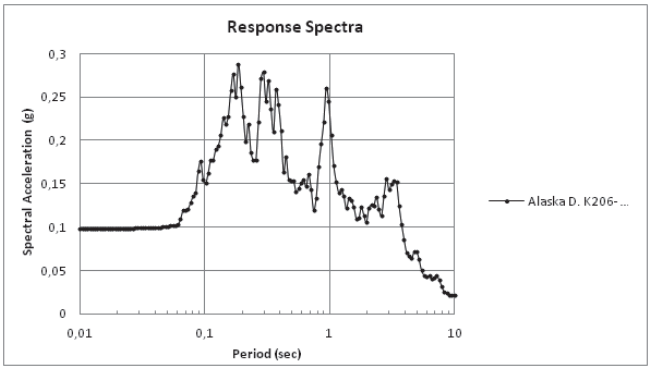

Figure 3.1. Response spectrum for Denali motion (damping ratio $\xi = 5\%$)

3.1.2. Soil profile models

To perform the sensitivity analyses, 2 soil models were established, the 100m soil profile thickness composed by 13 clay layers and the 200m soil profile thickness with 17 clay layers. The change in soil stiffness G and damping ratio ξ with respect to shear strain were obtained by means of resonant column tests until 10^{-1} γ (%), beyond this, cyclic DSS tests were run to estimate the G/G_{max}-γ (%) and ξ-γ (%) curves (Fugro, 2009b).

3.1.3. Stiffness at the base: Shear wave velocity (Vs) of half-space

To estimate the effect of stiffness at the base of the clay sediments, which is related with the propagation of shear waves in elastic media, 6 shear wave velocities (Vs) were used at the half-space for simulations using the 100m soil profile thickness: 300, 433, 500, 600, 750 and 1000m/s; and 5 shear wave velocities were used for the simulations with the 200m soil profile thickness: 433, 500, 600, 750 and 1000m/s. The base case initial shear wave velocities of respectively 300m/s and 433 m/s for the 100m and 200m deep profiles are based on the estimated geotechnical soil profile.

3.1.4. Dynamic response

In this study, the maximum shear strain was considered to be the main output because of its significance for the stability of slopes. The maximum shear strain is calculated at the middle of each layer. These simulations show an increase in the soil response as the shear wave velocity at the half-space increases having the largest response at the middle of layer 2 in all simulations, in addition the soil profile of 200m shows larger response than the 100m, see Fig. 3.2.

3.2 Ample

Non-linear dynamic response simulations were done using a modified version of AMPLE (AMPLE2), a computer program for nonlinear one-dimensional site response analysis (Nadim, 1985). AMPLE2 solves the one dimensional shear wave propagation in horizontally or sloping layered soil profile using infinite slope model. The soil profile is modeled as a nonlinear shear beam and the resulting nonlinear wave propagation problem is solved in the time domain by the explicit central difference method. AMPLE2 provides several choices for the constitutive law for soils, ranging from the linear elastic to the simple strain softening model. In this analysis the hyperbolic, failure-seeking model was used.

3.2.1. Input control motion

The control motion to perform the ground response analysis with AMPLE is called Imperial Valley-06 in California USA, magnitude 6.5 recorded at the Chihuahua, Mexico station in October 15th, 1979. The PGA was scaled to 0.098 g corresponding to an earthquake with return period T equal to 500 years, according to the Probability Seismic Hazard Analysis (PSHA) for the region prepared by Geomatrix (2006). The recorded component named 282 had duration of about 20 sec determined by means of 5-95 % total energy on Husid plot. The response spectrum for this motion is shown in Fig. 3.3.

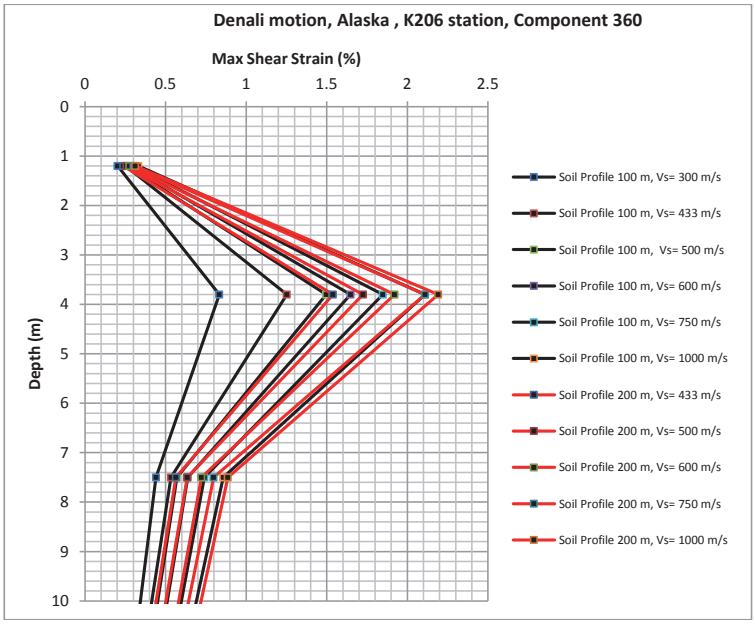

Figure 3.2. Maximum earthquake induced shear strains with SHAKE(N) simulations

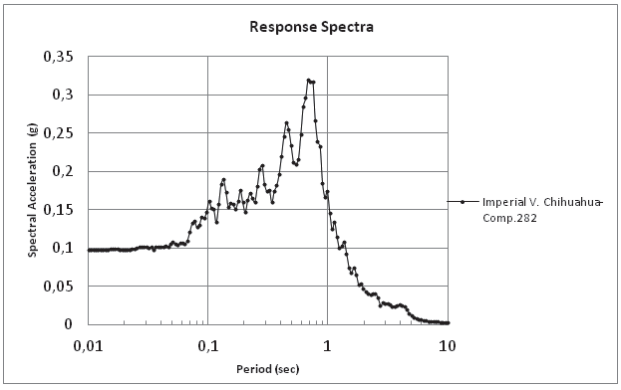

Figure 3.3. Response spectrum for Imperial Valley-06 motion (damping ratio $\xi = 5\%$)

3.2.2. Soil profile models

The same soil profiles were used as with SHAKE(N) but with a reduction in the thickness of the top clay layers to improve the performance of the computer program, resulting 22 clay layers for the 100m soil profile and 26 clay layers for the 200m soil profile.

To study the effects of the stiffness at the base on the dynamic response, the same shear wave velocities as in SHAKE(N) were used for this sensitivity analysis.

3.2.3. Slope angles

Taking into account the relationship between earthquake-induced shear strains in the soil mass and the stability of soil slopes, it is possible to evaluate the performance of clay slopes under seismic loading. To evaluate the influence of the slope angle in the response of the submarine slopes, 4 slope angles were used in the simulations: 0, 5, 10 and 15 degrees.

3.2.4. Dynamic response

The computed maximum shear strain in each layer was targeted as the main outcome given the close relationship with slope stability. These simulations show an increase in the soil response as the shear wave velocity at the half-space increases, having the largest response at the middle of layer 3 in all simulations. In addition, contrary to SHAKE(N), the soil profile of 100m depth shows larger response than the 200m soil profile depth. Moreover it can be seen throughout these simulations the important role of the slope angle in the dynamic response of the soil profile, the larger the slope angle the larger the response, see Fig. 3.4.

It should be noted, however, that the shear strains computed with AMPLE2 for a sloping soil profile are predominantly accumulated shear strains in the downslope direction, whereas the shear strains computed with SHAKE(N) are cyclic shear strains.

The color code in the Fig.3.4 is as follows: black for slope angles equal to 0 degrees, green for 5 degrees, yellow 10 degrees and red 15 degrees. The continuous lines correspond to soil profiles of 200m thickness and the dot lines correspond to soil profiles of 100m thickness.

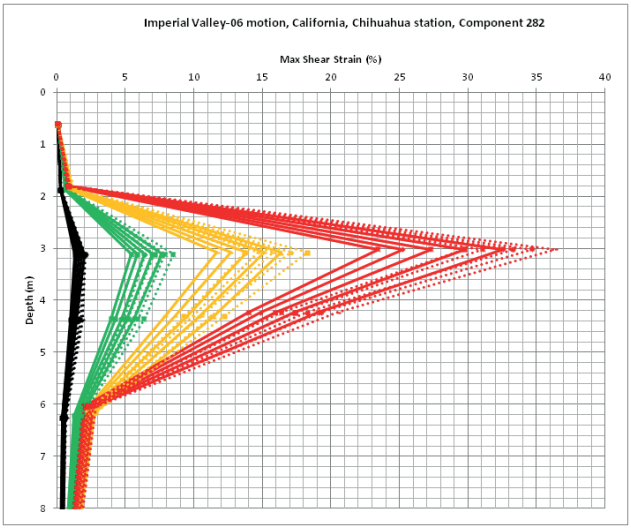

Figure 3.4. Maximum earthquake induced shear strains with AMPLE2 simulations

4. SENSITIVITY ANALYSES

The presentation of the results from the simulations using the computer program SHAKE(N) was set up in two main configuration. The first one was the soil profile thickness as changing variable with different shear wave velocities at the half-space; the second one was the shear wave velocity at half-space as changing variable for each soil profile. The maximum shear strain in the middle of layer number 2 at 3.75 m depth, which had the largest response in the simulations, was the main output.

The set up for the presentation of the results with AMPLE2 was basically the same as SHAKE(N), but with the slope angle as an additional changing variable. The main output was the maximum shear strain in the middle of layer 3 at 3.125 m for the horizontal layers.

4.1. Results of Sensitivity Analyses with Shake(N)

4.1.1. Changing variable: soil profile thickness

Based on the simulations, a larger response in the 200m soil profile than the 100m soil profile was observed. However as the value of the shear wave velocity increases the response in the 100m soil profile gets more intense than the 200m soil profile, see Fig. 4.1.

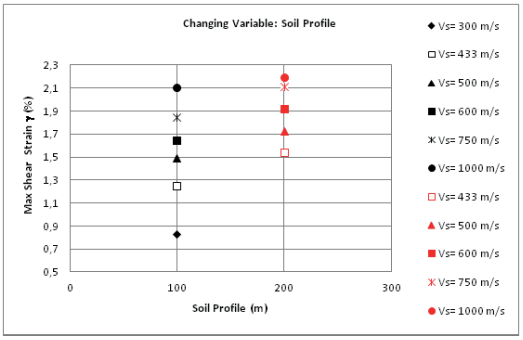

Figure 4.1. Sensitivity analysis based on soil profile thickness with SHAKE(N)

4.1.2. Changing variable: Vs at half-space

The simulations with SHAKE(N) show an increment of the normalized shear strain γ' with respect to the normalized shear wave velocity Vs', it shows that the response in the clay sediments with 100m thickness is more sensitive to the change in the shear wave velocities at the half-space than the 200m soil thickness. As an example, when the shear wave velocity increases 2 times the initial shear wave velocity the response in the 200m soil profile is 40% more than the initial one, and for the 100m soil profile there is an increment of 100%, see Fig. 4.2.

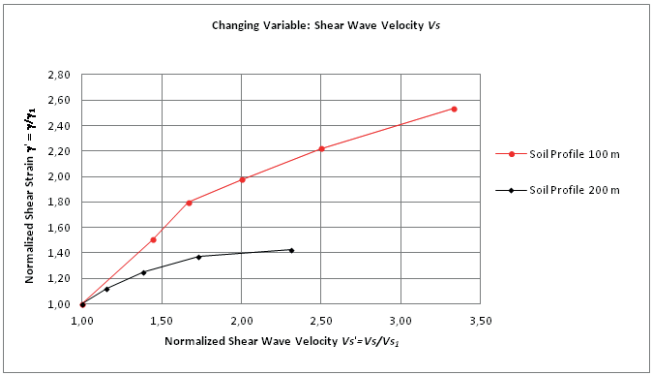

Figure 4.2. Sensitivity analysis based on shear wave velocity in half-space with SHAKE(N)

The normalized shear strain γ' comes from the ratio γ/γ_1 where γ_1 is the induced shear strain using the initial velocity Vs_1 at half-space in the simulations, therefore it is used as reference strain. The reference strain is γ_1= 0.83 (%) for the 100m soil profile and γ_1= 1.54 (%) for the 200m soil profile. Similarly the normalized shear wave velocity Vs' comes from the ratio Vs/Vs_1 where Vs_1 is the initial

shear wave velocity used in the half-space for the simulations. The reference velocities are Vs_1 = 300m/s for the 100m soil profile and 433m/s for the 200m soil profile.

4.2. Results of Sensitivity Analyses with Ample2

4.2.1. Changing variable: soil profile thickness

Contrary to SHAKE(N) simulations, in general, a larger response for the 100m soil profile than for the 200m soil profile was predicted by AMPLE2. One of the reasons for this relates to the change in control motion since the soil profiles are the same in both simulations. The spread of points indicates the sensitivity of the soil response with respect to the stiffness at the base. However, it is not easy to judge which soil profile is more sensitive to the stiffness at the base because the spread of data points looks similar, see Fig. 4.3.

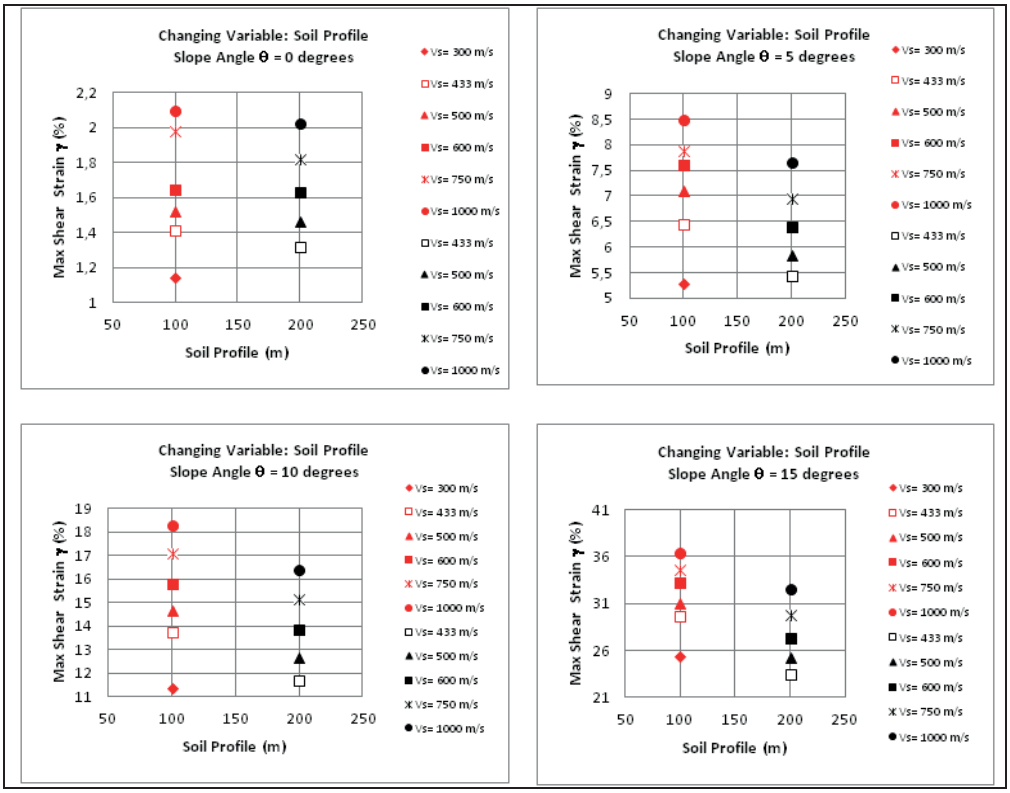

Figure 4.3. Sensitivity analysis based on soil profile thickness with AMPLE2

4.2.2. Changing variable: Vs at half-space

The simulations with AMPLE2 show also an increase in the normalized shear strain γ' with respect to the normalized shear wave velocity Vs'. However, the sensitivity of both soil profiles is very similar. In general the response of both soil profiles has an increment of 40 % when the shear wave velocity is 2 times the initial one.

It also can be seen that the lower the slope angle the larger the sensitivity in both cases. Even though the curves are similar for all the slope angles it can be seen that the sensitivity is slightly larger, for the 200m than the 100m with slope angles of 0 degrees and 15 degrees, and the opposite effect is observed for the slope angles of 5 and 10 degrees, see Fig. 4.4.

Again, it should be noted, that the shear strains computed with AMPLE2 for a sloping soil profile are predominantly accumulated shear strains in the downslope direction.

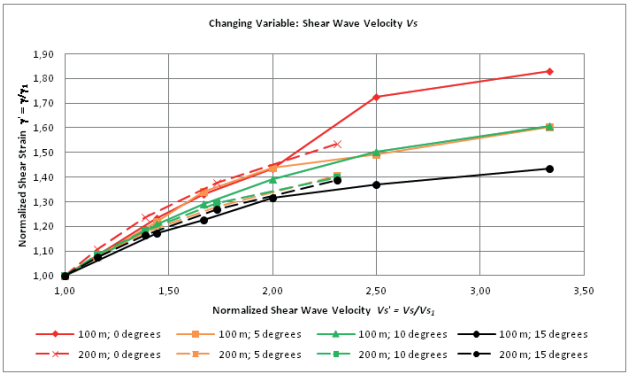

Figure 4.4. Sensitivity analysis based on shear wave velocity in half-space with AMPLE2

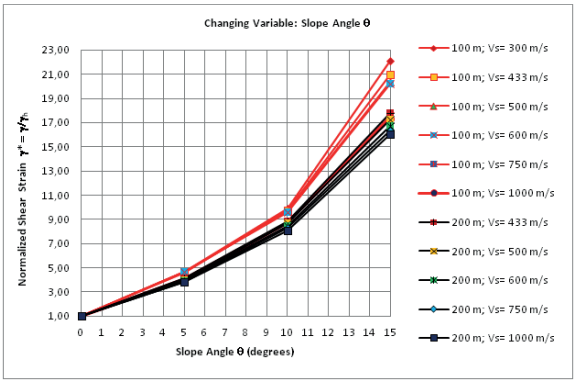

Figure 4.5. Sensitivity analysis based on slope angle with AMPLE2

The normalized shear strain γ^* in Fig. 4.5 comes from the ratio $\gamma^* = \gamma/\gamma_h$ where γ_h correspond to the induced shear strain with horizontal soil layers, slope angle $\theta = 0$ degrees.

5. CONCLUSIONS

This paper explores the influence in the dynamic response of clay sediments with respect to the thickness of soil media, the stiffness at the base of the sediments and the slope angle of submarine slopes. To quantify the effect of this variables in the response of the sediments, 2 computer programs were used SHAKE(N) and AMPLE2 with the following main observations for each software:

SHAKE(N): The 100m soil profile shows more sensitivity during the increase in stiffness at the base compare to the 200m soil profile, although the 200m soil profile exhibit larger shear strain values. As an example, when the shear wave velocity increases 100 % the initial velocity at the half-space, the shear strain increases 40 % for the 200m soil profile and 100 % for the 100m soil profile.

AMPLE2: Based on the simulations with AMPLE2 the sensitivity of both soil profiles with respect to the stiffness at the base show to be similar, although the 100m soil profile shows larger shear strains, both soil profiles exhibit and increment of 40% when the shear wave velocity at the half-space increases 100 %. It also can be seen that the lower the slope angle the larger the sensitivity in both soil profiles.

With respect to the slope angles as changing variable, in general, it can be seen the high impact that the slope angles have on the soil response, for example from 0 degrees to 5 degrees the maximum shear strain is about 4 times larger than the horizontal condition, with 10 degrees about 9 times, and with 15 degrees about 19 times larger than the horizontal condition. These results are not surprising because the shear strains computed with AMPLE2 for a sloping soil profile are predominantly accumulated shear strains in the downslope direction. The steeper slopes have a lower static safety factor and less resistance to inertial forces. Therefore they experience larger earthquake-induced shear strains through the mechanism described by Newmark (1965). Moreover these simulations show more sensitivity with 100m soil thickness with respect to the slope angle than the 200m soil thickness.
From these simulations one may conclude that the 100m soil profile is more sensitive to the stiffness of the bottom and steepness of the slope than the 200m soil profile. Therefore one may infer that the shorter the soil thickness the more sensitive the dynamic response of the soil mass relative to the stiffness at the base, and also relative to the slope angle and vice versa.

ACKNOWLEDGEMENT
This work was supported by the Mexican National Council for Science and Technology (CONACYT) by means of a PhD scholarship for the first author. The useful information to conduct this study was provided by the International Centre for Geohazards (ICG) and the Norwegian Geotechnical Institute (NGI). The data to do the analyses were provided by the Mexican Petroleum Institute (IMP).

REFERENCES

Biscontin, G., Pestana, J.M. and Nadim, F. (2004). Seismic triggering of submarine slides in soft cohesive soil deposits. *Marine Geology*, **203:3&4**, 341-354.

Fugro Chance de México, S.A. de C.V. (Fugro) (2009a). Reporte Final, Investigación Geotécnica en Aguas Profundas, Área de Lakach, Golfo de México, México. Volumen I: Criterios para Diseño Geotécnico, Reporte No. 0201-6420-100.

Fugro Chance de México, S.A. de C.V. (Fugro) (2009b). Reporte Final, Investigación Geotécnica en Aguas Profundas, Área de Lakach, Golfo de México, México. Volumen II: Criterios para Diseño Dinámico para Condiciones de Carga Sísmica, Reporte No. 0201-6420-100.

Fugro Geoconsulting, INC., (Fugro) (2009). Investigación Geológica y Geotécnica Integrada Polígono Lakach, Sonda de Campeche, México, Reporte No. 03.24083020-33.

Geomatrix (2006). Evaluación de Peligrosidad Sísmica, Bahía de Campeche, México. Project no. 12125.000.

Hance, J.J. (2003). Development of a database and assessment of seafloor slope stability based on published literature. M.S. Thesis, University of Texas at Austin.

Kramer, S.L. (1996). Geotechnical Earthquake Engineering. Prentice-Hall, U.K.

Kvalstad, T.J., Nadim, F., Kaynia, A.M., Mokkelbost, K.H. and Bryn, P. (2005). Soil conditions and slope stability in the Ormen Lange area. *Marine and Petroleum Geology* **22**, 299–310.

Ladd, C.C. and Foott, R. (1974). New design procedure for stability of soft clays. *Journal of the Geotechnical Engineering Division.* **100:GT7**, 763-786.

Nadim, F. (1985). AMPLE a computer program for analysis of amplification of earthquakes, NGI internal report.

Nadim, F., Biscontin G. and Kaynia, A.M. (2007). Seismic Triggering of Submarine Slides. *Offshore Technology Conference*. OTC **18911:** 1-8.

Newmark, M.N. (1965). Effects of earthquakes on dams and embankments. *Geotechnique*, **15:2**, pp 139- 160.

NGI Report (1997). Earthquake Hazard and Submarine Slide. Submarine slides – A literature survey. Project Manager: Nadim F.

NGI Report (2008). Slope Stability Evaluation and Laboratory Testing for Shah Deniz Full Field. Project Manager: Kaynia A.M.

Pestana, J. M. and Nadim, F. (2000). AMPLE2000: Nonlinear site response analysis of submerged slopes. Tech. Rep. UCB/GT/2000-04, Dept. of Civil and Environmental Engineering, University of California, Berkeley.

Schnabel, P.B., J. Lysmer and Seed H.B. (1972). SHAKE a computer program for earthquake response analysis of horizontally layered sites. University of California, Berkeley. College of Engineering. Earthquake Engineering Research Center. Report, EERC 72-12. 88 p.

Selnes, P.B. (1987). SHAKE (N) – Computer program for analysis of earthquake response in horizontally layered sites. NGI internal report.

Appendix 2

Paper No.5 (Symposium Paper no. 1)

Rodríguez-Ochoa R, Nadim F (2014) *Procedimientos de Vanguardia para la Estimación del Riesgo Asociado a la Falla de Taludes Submarinos en Aguas Profundas debido a Sismos.* Paper presented at the IV Simposio Becarios CONACyT en Europa, Strasburg, France, 5-7 November 2014.

Nombre y Apellido: Rafael Rodríguez Ochoa
Universidad actual: Universidad de Oslo
Grado académico en curso y área de investigación: Doctorado en Geociencias
Contacto: rafaro33@hotmail.com

Procedimientos de Vanguardia para la Estimación del Riesgo Asociado a la Falla de Taludes Submarinos en Aguas Profundas debido a Sismos

1. Introducción

Uno de los principales retos que enfrenta la industria petrolera para la extracción y transporte de hidrocarburos en aguas profundas está relacionado con geo-amenazas localizadas en el talud continental, las cuales representan un peligro para las estructuras e instalaciones que se encuentran sobre el suelo marino. Las amenazas naturales tales como sismos, fallas tectónicas, fallas de taludes, expulsión de gas, volcanes submarinos, diapirismo, hidratos de gas, etc., representan un peligro latente para el desarrollo de cualquier yacimiento petrolero en aguas profundas.

La investigación que se desarrolla en el presente programa de doctorado considera el estudio de la falla de taludes submarinos, la cual representa la principal geo-amenaza que afecta a las instalaciones submarinas (Hance). En especial, se investiga la falla de taludes submarinos en márgenes activos como es el caso de la zona sur del Golfo de México. En general se estudia, analiza y propone mejoras en los procedimientos y metodologías actuales para estimar el riesgo asociado a la falla de taludes submarinos. La investigación comprende los siguientes ejes temáticos:

Análisis Determinísticos: Mediante el uso del método de equilibrio límite y el método de elemento finito se realizan análisis estáticos y dinámicos para determinar la estabilidad de taludes submarinos antes, durante y después de un evento sísmico. Los métodos son alimentados en todo momento con información geológica, geofísica, geotécnica y sísmica del lugar en estudio.

Análisis Probabilísticos: Mediante el uso del método de Monte Carlo, FORM, y método Bayesiano en combinación con simulaciones de respuesta de sitio se estima la probabilidad condicional de falla de talud para diferentes periodos de retorno de los sismos. Lo anterior permite obtener la curva de fragilidad para la falla de taludes y se utiliza con la derivada de la curva de amenaza sísmica para determinar la probabilidad incondicional anual de falla del talud con base en el operador matemático esperanza matemática, que determina el promedio pesado de la probabilidad anual de falla.

Una vez que el talud submarino ha fallado, podría evolucionar en un movimiento masivo de sedimentos talud a bajo. La investigación también comprende el proceso de transporte de los sedimentos por gravedad, analizando y aplicando modelos matemáticos disponibles para estimar las distancias de recorrido y las velocidades que se podrían desarrollar al frente del material desplazado. Lo anterior permite determinar de manera razonable la probabilidad de impactar instalaciones talud abajo, así como la estimación del riesgo asociado a la falla de taludes submarinos una vez que se obtienen las curvas de vulnerabilidad de las estructuras afectadas.

2. Métodos para analizar la estabilidad de taludes submarinos ante carga sísmica

A continuación se presentan los procedimientos utilizados en esta investigación para estimar la estabilidad de taludes submarinos en márgenes activos.

a. Antes del Sismo

Antes del sismo se realiza un análisis de estabilidad utilizando el Método de Equilibrio Límite y/o Método de Elemento Finito. Un factor clave en la estabilidad de taludes submarinos en aguas profundas es la determinación de la resistencia del suelo marino, en este caso arcilla. La resistencia del suelo marino se simboliza utilizando el parámetro su y representa la resistencia estática al corte sin drenaje de las arcillas, su determinación implica tanto pruebas en campo como pruebas de laboratorio.

b. Durante el Sismo

El análisis de estabilidad durante el sismo se realiza siguiendo el procedimiento desarrollado por investigadores del Instituto Geotécnico Noruego. El procedimiento consiste en determinar la degradación de la resistencia del suelo por sismo con base en las deformaciones inducidas, numéricamente estimadas, así como pruebas de laboratorio.

Con este procedimiento se determina la reducción de la resistencia de las arcillas al final del sismo, obteniendo la resistencia cíclica de las arcillas $s_{u,cy}$. Una vez obtenida la resistencia cíclica de las arcillas $s_{u,cy}$ en los estratos de arcilla que desarrollaron significante deformación, dicha resistencia se utiliza como dato de entrada para determinar el factor de seguridad co-sísmico utilizando el método de equilibrio límite.

c. Después del Sismo

Una vez que la acción del sismo ha pasado, es posible que algunos taludes hayan desarrollado deformaciones importantes que los hacen entrar en una condición de fluencia "creep", es decir la masa de suelo se sigue deformando ante condiciones de carga constante. En las arcillas éste fenómeno se conoce como fluencia sin drenaje y perdura todo el tiempo que tarda en disiparse el exceso de la presión de poro inducida por el sismo. Dada la pequeña permeabilidad que tienen las arcillas en aguas profundas, el proceso de disipación del exceso de la presión de poro podría tardar meses o incluso años al igual que el proceso de fluencia. Lo anterior podría generar que los taludes fallen meses o años después de haber ocurrido el sismo.

El desarrollo de fluencia después del sismo implica una reducción adicional de la resistencia al corte de las arcillas. Para establecer la resistencia estática de las arcillas después del sismo, simbolizada como $s_{u\text{-}post}$, Andersen et al. recomienda incluir una reducción adicional del 25% al valor obtenido de la resistencia cíclica $s_{u,cy}$, es decir $s_{u\text{-}post} = 0.75 * s_{u,cy}$.

Una vez obtenida la resistencia estática después del sismo $s_{u\text{-}post}$, dicho valor se utiliza para determinar el factor de seguridad post-sísmico utilizando el método de equilibrio límite.

La Figura 1 muestra la evolución del factor de seguridad de un talud submarino sometido a carga sísmica en aguas profundas a lo largo del tiempo.

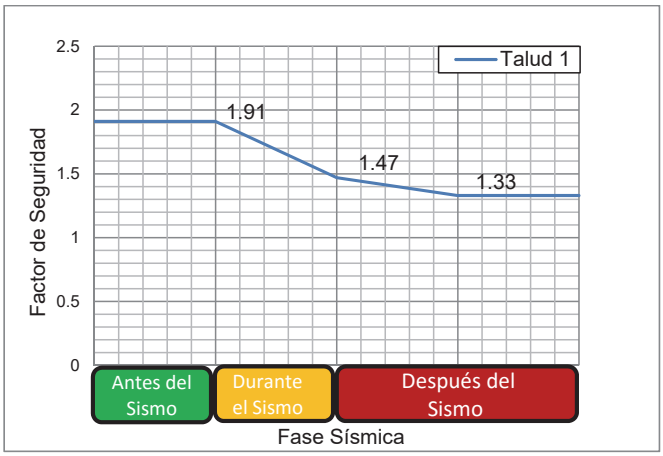

Figura 1. Curva de evolución del factor de seguridad. La curva muestra la cuantificación de los diferentes estados de estabilidad del talud submarino a través de las diferentes fases sísmicas: Antes (pre-sísmico), durante (co-sísmico) y después (post-sísmico).

3. Métodos para analizar la amenaza de falla de taludes submarinos por sismo

El objetivo principal de los análisis de amenaza de falla de talud por sismo es la estimación de la probabilidad incondicional anual de falla del talud por carga sísmica. Uno de los pocos procedimientos disponibles para estimar la amenaza de falla de talud debido a un evento sísmico es el desarrollado por (Nadim et al.) y regenerado por Rodríguez-Ochoa et al. (en revisión). El procedimiento tiene una plataforma probabilística, consta de 10 pasos lógicos y utiliza varios métodos matemáticos incluyendo Montecarlo, inferencia Bayesiana y First Order Reliability Method (FORM) (Hasofer and Lind).

La filosofía del procedimiento consiste en estimar la probabilidad incondicional anual de falla del talud con base en curvas de fragilidad, como las mostradas en la Figura 2. Las curvas de fragilidad de falla de talud se obtienen después de realizar análisis dinámicos para varios periodos de retornos de los sismos.

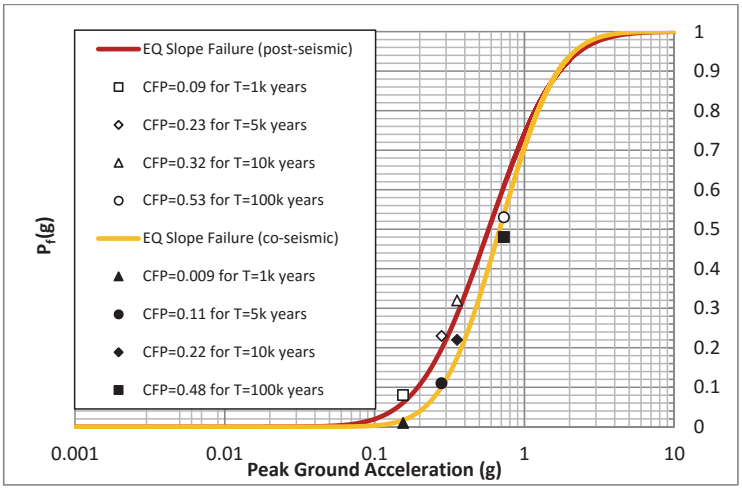

Figura 2. Curvas de fragilidad de falla de talud submarino obtenidas después de ajustar funciones probabilísticas lognormales a las probabilidades condicionales estimadas para sismos con periodos de retorno de 1000, 5000, 10,000 y 100,000 años; los puntos cerrados corresponden a las probabilidades condicionales durante el sismo y los puntos abiertos a las probabilidades condicionales después del sismo. La curva amarilla corresponde a la curva de fragilidad durante el sismo y la curva roja a la curva de fragilidad después del sismo.

Una vez que se determinan las curvas de fragilidad, se aplica el operador denominado esperanza matemática. La esperanza matemática o valor esperado de una variable aleatoria es la suma del

producto de la probabilidad de cada suceso por el valor de dicho suceso, en este caso la variable aleatoria es la probabilidad anual de falla (AFP).

La *formulación matemática de la propuesta para determinar la probabilidad incondicional de la falla anual por sismo se presenta en la ecuación 1.

$UAFP = f(Seismic\ Hazard\ Function, Fragility\ Slope\ Failure\ Function)$=

$$UAFP = E[AFP] = \int_0^\infty f_X(x) \cdot AFP_{f|x} \cdot dX \qquad (1)$$

donde:

UAFP= Unconditional Annual Failure Probability

AFP = Annual Failure Probability random variable

E [AFP] = Expected value of Annual Failure Probability (weighted average)

fX (x) = Probability density function fitting the seismic hazard curve

AFP f|x = Slope Failure Fragility function normalized with respect to return period T

X = Random variable representing the peak ground acceleration (PGA) in the bedrock

x = Values that take the random variable X

La Figura 3 muestra un ejemplo de los resultados obtenidos en un sitio en el Golfo de México después de aplicar la metodología propuesta para estimar la probabilidad incondicional anual de falla del talud por sismo. La curva azul representa la probabilidad de que ocurra un sismo de magnitud g que induzca una probabilidad condicional de falla dada (probabilidad del suceso), la curva verde representa el valor de dicha probabilidad condicional de falla y la curva amarilla representa la probabilidad condicional anual o probabilidad condicional normalizada con respecto al periodo de retorno T del sismo (valor del suceso). La curva roja es el producto de la función de probabilidad del suceso (curva azul) por la función del valor del suceso (curva amarilla), y la curva negra es la sumatoria de los productos. En el ejemplo que se muestra en la Figura 3, la sumatoria se realizó de 0 a 10g por considerarse el rango de aceleraciones que más aportan a la probabilidad de falla anual incondicional. En el presente análisis la probabilidad anual de falla se estimó en 6.97E-05 durante el evento sísmico y 1.20E-03 después del sismo considerando el efecto de fluencia sin drenaje en las arcillas que forman el talud submarino.

*La formulación matemática se presenta en la versión original desarrollada en ingles.

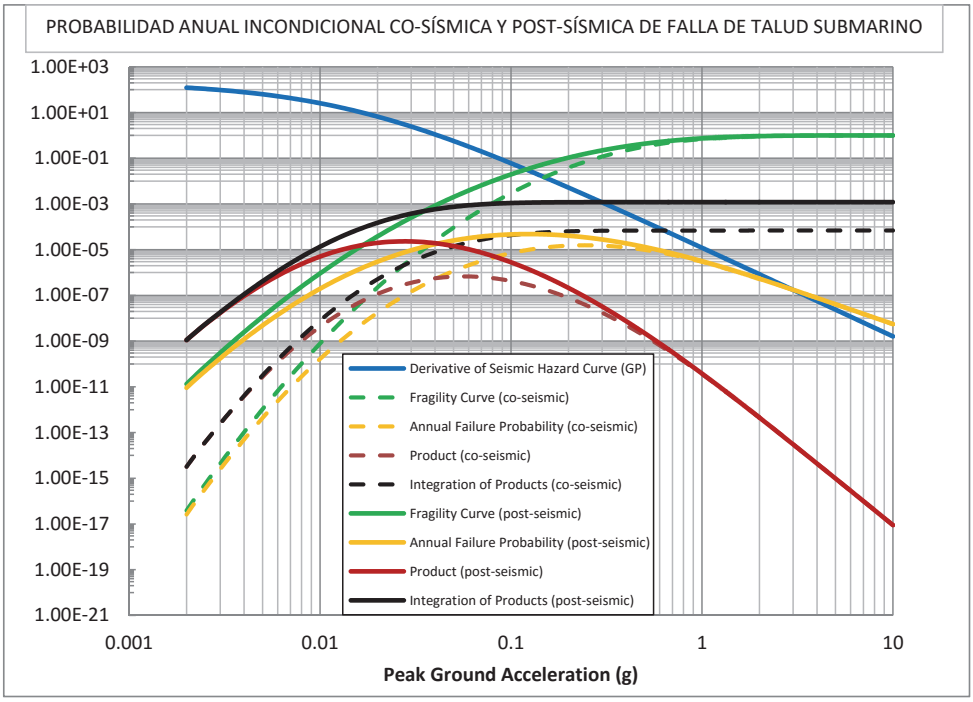

Figura 3. Representación grafica de la sumatoria de funciones para estimar la probabilidad de falla anual incondicional durante el sismo (líneas punteadas) y después del sismo (líneas continuas) con base en curvas de fragilidad y el operador esperanza matemática.

4. Métodos para analizar la amenaza de impacto a instalaciones submarinas

Una vez que se estima la probabilidad anual de falla de talud por sismo, el siguiente paso es determinar la probabilidad de ser impactadas las instalaciones submarinas por los sedimentos marinos transportados talud a bajo. La formulación probabilística se especifica en la ecuación 2:

$$P[\text{Impacto de sedimentos transportados a instalaciones submarinas}] = P[\text{Falla de talud por sismo}] \times P[\text{Impactar instalaciones submarinas I Talud falló por sismo}] \quad (2)$$

La Figura 4 muestra la representación esquemáticamente de la ecuación 2.

La probabilidad incondicional anual de falla de talud por sismo se estimó en la sección 3, la probabilidad condicional mostrada en la ecuación 2 se determina realizando un análisis probabilístico para estimar las distancias y velocidades que podrían recorrer los sedimentos desplazados.

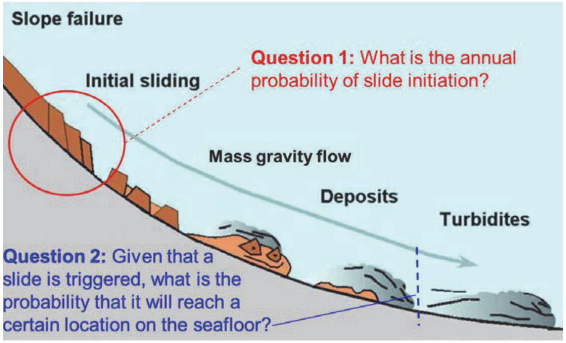

Figura 4. Representación esquemática de la probabilidad de impacto de sedimentos marinos, sobre instalaciones localizadas talud abajo, dado que el talud submarino falló por sismo (Nadim et al.).

La estimación de las distancias de recorrido y las velocidades que podrían desarrollar los sedimentos en movimiento se determinan utilizando un modelo analítico que simula los sedimentos transportados como si fuera un fluido viscoso desplazándose por gravedad talud a bajo. Un programa de computadora derivado de esa simplificación y ampliamente utilizado se denomina BING "debris flow model" (Imran, Harff and Parker), en la actualidad existen varias versiones del mismo. BING estima tanto las distancias de recorrido como las velocidades al frente de la masa del suelo en movimiento.

Una vez realizadas las simulaciones en BING, utilizando combinaciones derivadas del método de Monte Carlo, se obtienen funciones de probabilidad que se ajustan a los resultados de las distancias y velocidades estimados en las simulaciones analíticas. La probabilidad condicional de impacto se determina en base a dicha función probabilística, y su valor corresponde a la probabilidad de que los sedimentos se desplacen una distancia mayor a la distancia donde se encuentran las estructuras submarinas.

5. Métodos para analizar el riesgo por falla de taludes submarinos debido a sismos

El riesgo se define como el producto de la geo-amenaza (probabilidad de falla) multiplicado por las consecuencias, ecuación 3. Y las consecuencias se cuantifican como el número de elementos en riesgo multiplicado por su vulnerabilidad, ecuación 4.

$$Riesgo = Geo\text{-}amenaza \times Consecuencias \quad (3)$$

$$Consecuencias = Elementos\ en\ Riesgo \times Vulnerabilidad \quad (4)$$

Para estimar el riesgo inducido por falla de taludes submarinos debido a sismos, la geo-amenaza (probabilidad de falla) que se requiere en la ecuación 3 corresponde a la probabilidad anual de impacto de instalaciones submarinas por transporte de sedimentos presentada en la sección 4.

Referente a las consecuencias derivadas de la falla del talud se consideran dos grandes grupos, las consecuencias directas y las consecuencias indirectas. Existen métodos y recomendaciones para cuantificar las consecuencias directas, sin embargo la cuantificación de las consecuencias indirectas no es trivial dado su naturaleza cualitativa. Las consecuencias directas están relacionadas básicamente con la pérdida de vidas humanas y pérdidas económicas.

Las consecuencias directas se estiman utilizando las curvas de vulnerabilidad para los equipos submarinos e instalaciones que pudieran resultar dañados por el impacto de los sedimentos marinos. Algunos ejemplos de equipos e instalaciones son las tuberías para el trasporte del hidrocarburo ubicadas sobre el lecho marino, así como los equipos de extracción "Christmas trees" y "Manifolds" entre otros. La Figura 5 muestra los equipos que podrían estar expuestos en un desarrollo petrolero localizado en aguas profundas.

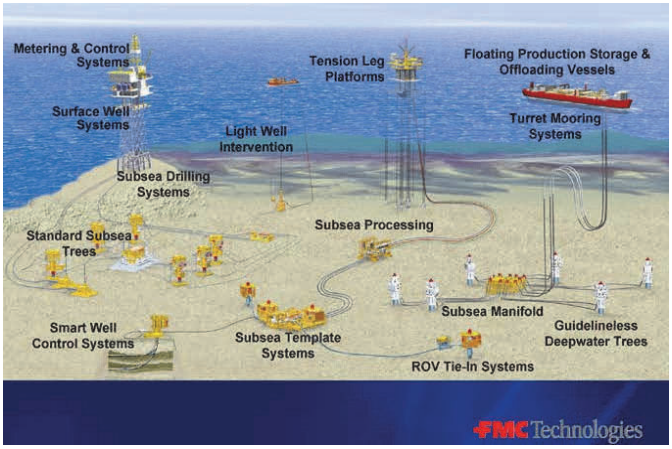

Figura 5. Equipos que podrían estar expuestos y tomados en cuenta en la estimación de las consecuencias directas.

Las curvas de vulnerabilidad relevantes para estos equipos e instalaciones son las que cuantifican el daño a la infraestructura en función de la velocidad y/o presión de impacto del suelo marino transportado. Los valores de las curvas de vulnerabilidad van de cero a uno, cero indica que no existe daño y uno significa daño total.

Finalmente la cuantificación del riesgo directo debido a la falla de un talud submarino por carga sísmica se obtiene al multiplicar la probabilidad anual de impacto por las consecuencias directas.

6. Discusión y Conclusiones

Los diferentes métodos presentados para estimar el riesgo asociado a la falla de taludes submarinos debido a sismos están continuamente mejorándose gracias a la aportación de geo-científicos y geo-ingenieros que están involucrados con el tema. Los métodos y procedimientos presentados en éste artículo se consideran a la fecha de vanguardia y se muestran de manera simplificada en la Figura 6.

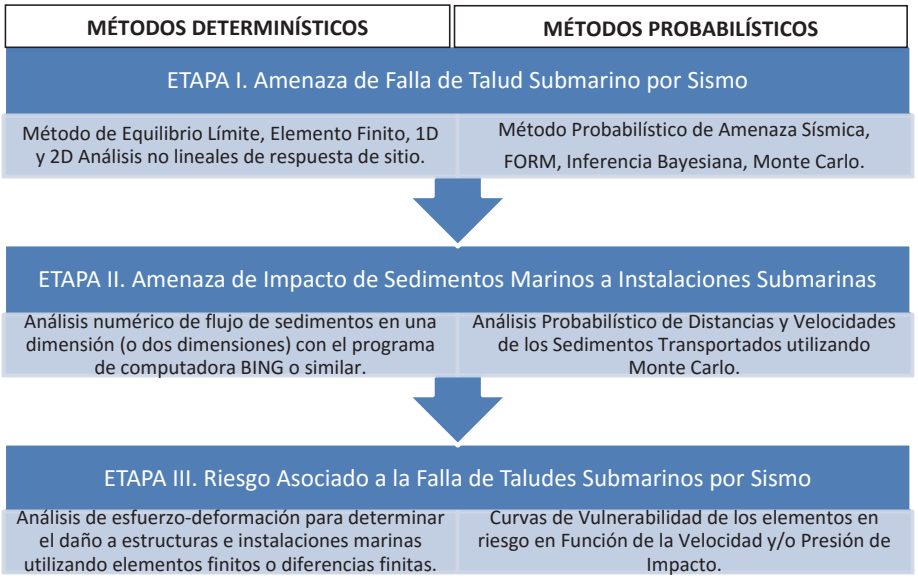

Figura 6. Procedimientos y modelos numéricos empleados, en las tres principales etapas del análisis, para la estimación del riesgo asociado a la falla de taludes submarinos por sismo.

Referencias:

Andersen, KH, et al. "Deep Water Geotechnical Engineering." Ed. NGI. Oslo, Norway: Norwegian Geotechnical Institute, Publication No. 208, 2012. Vol. Publication No. 208. Print.

Hance, James J. "Development of a Database and Assessment of Seafloor Slope Stability Based on Published Literature." University of Texas at Austin, 2003. Print.

Hasofer, A. M., and N. C. Lind. "An Exact and Invariant First Order Reliability Format." *J. Eng. Mech. Div., ASCE* 100.EM1 (1974): 111-21. Print.

Imran, Jasim, Peter Harff, and Gary Parker. "A Numerical Model of Submarine Debris Flow with Graphical User Interface." *Computers & Geosciences* 27.6 (2001): 717-29. Print.

Nadim, Farrokh, et al. "Estimation of Temporal Probability in Offshore Geohazards Assessment." *Offshore Technology Conference*. 2014. Print.

Appendix 3

Paper No.6 (Symposium Paper no. 2)

Rodríguez-Ochoa R, Nadim F, Cepeda JM *Risk analysis of earthquake-induced submarine slope failure*. In: 5th International Symposium on Geotechnical Safety and Risk (ISGSR), Rotterdam, The Netherlands, 13-16 October 2015. vol (Accepted for publication).

Risk Analysis of Earthquake-Induced Submarine Slope Failure

Rafael RODRÍGUEZ-OCHOA [a], Farrokh NADIM [b] and José M. CEPEDA [b]
[a] *Department of Geosciences, University of Oslo, Norway*
[b] *Norwegian Geotechnical Institute (NGI), Norway*

Abstract. This paper presents an offshore risk analysis in a systematic manner to assess the influence of earthquake-induced submarine slope failure on offshore structures. The risk analysis is carried out for the future development of a natural gas field in deep waters in the south part of the Gulf of Mexico. The study accounts for all the elements in the conventional risk formulation: *Risk = Hazard × Consequences*. The hazard analysis was performed in two steps: first estimating the probability of earthquake-induced slope failure by using the slope failure fragility curve approach; and second estimating the probability of failed sediments impacting offshore structures by running debris flow numerical simulations in a Monte Carlo method framework. The consequences were estimated focused solely on the damage to offshore structures, in monetary terms, and the development of vulnerability curves as function of the velocity and the thickness of the moving mud flow that may evolve from the failed sediments.

Keywords. offshore geohazards, earthquakes, submarine landslides, risk analysis

1. Introduction

The failure of submarine slopes on the continental shelf and/or continental slope poses a risk to offshore structures and facilities from diverse economic sectors. The oil and gas industry is especially concerned about this natural phenomenon due to its increasing interest in developing gas and oil fields in deep waters, which involves the deployment of seabed installations and equipment on the continental slope.

This paper presents an assessment risk analysis of earthquake-induced submarine slope failure for a future gas field development in deep waters in the south part of the Gulf of Mexico. The risk analysis is approached in a systematic manner, first accounting for the hazard by using the slope failure fragility curve approach developed by Rodríguez-Ochoa et al. (2015b), and then debris flow numerical simulations using the BING code (Imran, 2001a) in a Monte Carlo framework. The consequences were quantified by identifying the elements at risk and assessing their vulnerability curves.

The analysis focused on the direct consequences related to the damage of offshore structures.

2. Site Characterization

The submarine slope under study is located in the south of the Gulf of Mexico, in the transition zone of the continental shelf to the continental slope, with water depth of about 500 m (Figure 1).

This slope is one of the nine potential unstable slopes identified by Fugro (2009) during the geophysical explorations. The largest slope angle of all the nine identified slopes is about 9.2 degrees. This submarine slope was modelled as a composite slope, the first part has 10 degrees with 600m horizontal distance and the second part has 5 degrees with 400m horizontal distance.

The sediments are cohesive calcareous soils with carbonate content between 11 to 23% and are classified as high plasticity clays.

Laboratory soil sensitivity varies from 3 to 5 down to 20m depth and from 1.5 to 3 beneath 20m. The estimated overconsolidation ratios (OCR) indicate that the sediments are normally consolidated to slightly overconsolidated.

The seismicity of the region is of concern. The site is influenced by the subduction zone in the Pacific coast, nearby volcanos, and the transform zone in the Caribbean Sea. The main

risk posed to the marine environment and the planned natural gas production facilities on the seabed is considered to be due to submarine landslides trigger by earthquakes. For further information see Rodríguez-Ochoa et al. (2015c).

Figure 1. Location of the submarine slope under study.

3. Slope Failure Hazard Analysis

The main objective of the earthquake-induced slope failure hazard analysis is to estimate the annual probability of slope failure. One of the few methods available to estimate the slope failure hazard due to a seismic event was developed by Nadim (2012), and refined by Rodríguez-Ochoa et al. (2015b). The procedure follows a probabilistic framework comprising various mathematical methods including Monte Carlo simulation, Bayesian inference and First Order Reliability Method (FORM).

The philosophy of the updated method is to estimate the unconditional annual probability of slope failure based on fragility curves. The slope failure fragility curves are obtained by performing dynamic analyses to assess the seismic slope stability based on the induced shear strains in the clay layers. The input motions are obtained from a probabilistic seismic hazard analysis (PSHA) in the site to estimate the probable earthquakes that may strike the site. For this study four strong motions with return periods of 1000, 5000, 10,000 and 100,000 were recommended (Geomatrix, 2006).

Once the fragility curves are determined, the mathematical expectation operator is applied to the estimated seismic hazard function and the estimated fragility slope failure function, normalized with respect to the return period, to obtain the annual probability of slope failure; by summing the products of the probability of each event (Seismic Hazard Function) by the value of that event (Normalized Fragility Slope Failure Function).

After applying the proposed methodology, the unconditional annual probability of earthquake-induced slope failure was estimated to be $1.2 \cdot 10^{-3}$.

4. Mud Flow Impact Hazard Analysis

4.1. BING Computer Code

To estimate the probability of mud flow impacting downslope offshore installations once the slope has failed, the computer code BING (Imran et al. 2001a) was used. BING is a 1-D numerical model that simulates the downslope spreading of a submarine debris flow. BING is able to use three different rheological models: Bingham, Herschel-Bulkley, and Bilinear. The main outcomes of BING are the runout distance, front velocity, and the final shape of the failed sediments.

In this study, the Bilinear rheological model was used for the numerical simulations with BING. This model has shown to give acceptable results in previous studies (Locat 1997; Imran et al. 2001b; Jeong et al. 2010).

The bilinear model proposed by Locat (1997) has been adapted for numerical modelling by Imran et al. (2001a) as shown in Eqs. (1), (2) and (3).

$$\frac{\tau}{\tau_{ya}} = 1 + \frac{\gamma}{\gamma_r} - \frac{1}{1 + r\frac{\gamma}{\gamma_r}} \tag{1}$$

$$\gamma_r = \frac{\tau_{ya}}{\mu_{dh}} \tag{2}$$

$$r = \frac{\gamma_r}{\gamma_0} \tag{3}$$

where:

τ = shear stress (Pa);
γ = shear strain rate (s^{-1});
γ_r = reference strain rate (s^{-1});
r = ratio of strain rates;
τ_{ya} = apparent yield strength (Pa);

μ_{dh} = viscosity at high shear strain rates (plastic viscosity) (Pa.s);

γ_0 = shear strain rate at the transition from a Newtonian to a Bingham behaviour (s^{-1}).

4.2. Monte Carlo Simulation of Runout Scenarios

To quantify the effect of uncertainty in the BING input parameters on the runout distance, the Monte Carlo simulation method was used to obtain the probability distribution function of the runout distance.

The random variables used in the Monte Carlo simulations, with their range of values and proposed probability distributions are listed in Table 1. The means (μ) of the distribution functions were calculated by assuming symmetric normal distribution functions, and the standard deviations (σ) by using the following approximation: σ = (max-min)/6.

Table 1. Random variables

Variable	Mean, Std or Range	Probability Function
ρ_{mud} (kg/m^3)	1337, 29	Normal
τ_{ya} (Pa)	353, 100	Normal
γ_r (1/s)	1039, 52	Normal
r	6414, 1843	Normal
Initial Geometry	1 and 2	Discrete Uniform

The above input parameters are the mud density (ρ_{mud}), apparent yield strength (τ_{ya}), reference shear strain (γ_r), ratio of strain rates (r), and initial geometry configuration.

The range of values for the mud density as well as the parameters of the Bilinear rheological model (τ_{ya}, γ_r and r) were set based on the water content of the flowing mass and the empirical correlations developed by Locat (1997).

Regarding the random variable identified as Initial Geometry, this variable accounts for the initial geometry configuration of the failed sediments. BING assumes by default that the initial geometry of the debris mass has a parabolic shape.

To run the numerical simulations it was proposed to use two initial geometry configurations:

1. Configuration No.1 matches the initial length of the estimated slide surface with the initial length of mud deposit (i.e. base of the parabola = 600m), and a maximum thickness of mud deposit of 12m.
2. Configuration No.2 matches the initial thickness of the slide surface with the maximum thickness of the mud deposit (i.e. height of the parabola = 8m), and an initial length of mud deposit of 900m.

In the Monte Carlo simulations, 100 values for each random variable were generated using the specified ranges and probability distribution functions shown in Table 1. The stratified Latin Hyper Cube sampling technique proposed by McKay et al. (2000) was used to ensure a good representation of the distribution functions for all the random variables.

4.3. Runout Distance

Figure 2 shows the expected runout route down-slope of the failed sediments. This route goes along a natural channel that was formed due to previous slide activities and mass gravity flows which eroded the seafloor along the continental slope. Therefore, the topographic profile along the natural channel was used in BING to run the numerical simulations.

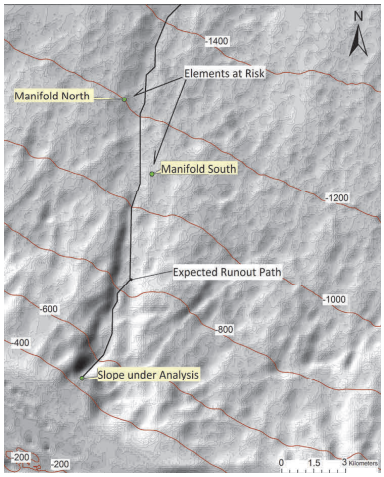

Figure 2. Expected runout path of the failed sediments, and location of source and exposed elements for the risk analysis.

Figure 3 shows the cumulative distribution functions generated to fit the numerically simulated runout distances. It can be observed that the lognormal distribution fits well the data. The mean and standard deviation of the fitted distribution were 9.97 km and 2.83 km respectively. This probability distribution was used to estimate the probability of a mud flow with potential to damage offshore structures reaching specific locations along the channel. The case study focused on two manifolds that will be deployed to develop the natural gas field, identified as Manifold South and Manifold North.

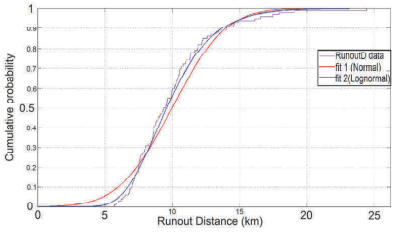

Figure 3. Runout distance cumulative distribution function along the natural channel.

Manifold South and Manifold North are located along the natural channel, respectively 10.5 km and 14.0 km from the crown of the slope under investigation (Figure 2). Therefore the probability of been impacted by the mud flow, given that the slope has failed, for the Manifold South and Manifold North are estimated using Eq. (4).

$$P_{impact} = P(\text{Runout Distance} \geq \text{Manifold Location}) \quad (4)$$

The conditional impact probabilities (given that slope failure has occurred) for the Manifold South and Manifold North are $P_{impactMS}$ = 0.37 and $P_{impactMN}$ = 0.09 respectively. These probabilities are based on the lognormal probability distribution function that best fits the numerical runout distance data.

5. Consequences

In this study the quantification of the direct consequences focused mainly on the cost of offshore equipment rather than the economic losses due to production disruption, and environment impact. It should be noted that the economic losses due to production disruption and environment impact are likely to be greater than the cost of the equipment, but their estimation requires complex analytical scenarios that are beyond the scope of this paper.

5.1. Elements at Risk

The offshore natural gas field is planned to be developed by deploying a system of seven wells and two manifolds (Figure 2). Manifold South will have four wells connected around it, and Manifold North will have three wells connected around it.

In this analysis it was considered that the critical offshore structures exposed to mud flow impact hazard are the manifolds. A production manifold is a subsea structure containing valves and pipework designed to combine and direct produced fluids from multiple wells into one or more flowlines. It is assumed that the pipelines that transport the produced natural gas to onshore facilities for further distribution follow a safe route away from the mud flow impact critical zone. The same applies for the subsea umbilicals, which are the link between topside and subsea systems by a series of cables and pipes that provide power and control to the subsea systems.

5.2. Vulnerability Curves

To estimate the consequences, the vulnerability curves for each element at risk are required. The estimated vulnerability (fragility) curves for the manifolds are based on the lateral capacity of their foundation. The foundation solution of the manifolds are suction caissons with nearly 6 m diameter and about 17 m length.

The maximum lateral capacity of the suction pile that may resist the mud flow impact forces is about 650 kN. The mud flow impact forces were examined through the work done by Zakeri (2008). The fluid dynamics approach proposed by Pfeiff and Hopfinger (1986) was applied.

This formulation is based on the classic fluid dynamics approach regarding the force experienced by an object moving through a fluid at relatively large velocity (i.e. high Reynolds

number, Re >~1000). The drag coefficient is a function of the Reynolds number (i.e. Re = Inertial Forces/Viscous Forces) as well as the shape and surface rugosity of the object.

In this study it is assumed that the mud flow will impact the top part of the suction pile, at the interface between the suction pile and the manifold. Hence the impacted object was considered to have a cylinder shape with a smooth surface. The manifold itself is a very complex steel structure and it is difficult to estimate the drag coefficient based on its shape and surface rugosity.

The estimated vulnerability curves for the manifolds shown in Figure 4 are functions of the velocity and thickness of the mud flow.

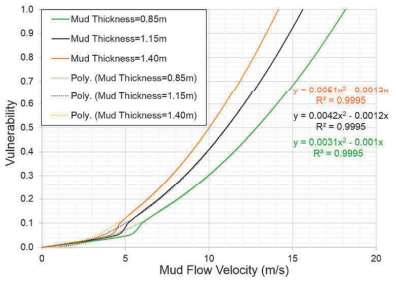

Figure 4. Vulnerability curves for exposed manifolds based on the velocity and thickness of the mud flow.

Table 2 shows the expected front velocity and thickness of the mud flow at 10.5 km (position of Manifold South) and 14.0 km (position of Manifold North) from the crown of the slope respectively. The values listed in Table 2 are based on probabilistic analyses of the simulation output data.

Table 2. Expected front velocity and thickness of mud flow

Distance from the Crown of the Slope (km)	Front Velocity (m/s)	Mud Thickness (m)
10.5	23	1.15
14.0	21	0.85

6. Risk Analysis

To estimate the risk associated to earthquake-induced submarine slope failure for the planned deep water natural gas development in the Gulf of Mexico, the classic definition of risk was applied (i.e. Risk= Hazard × Consequences).

In this context, *Hazard* can be defined as the annual probability of sediments impacting offshore structures given that a submarine slope failed, and can be estimated with Eq. (5).

$$P[\text{Sediments impacting seabed installation}] = P[\text{EQ induced slope failure}] \times P[\text{Sediments reaching seabed installation} \mid \text{Submarine slope has failed}] \quad (5)$$

Based on the information given in previous sections, the earthquake-induced slope failure risk analysis in the case study can be assessed by using the estimated unconditional annual probability of the earthquake-induced slope failure (i.e. UAFP = $1.2 \cdot 10^{-3}$) in section 3, and Eq. (5) as follows:

- Manifold South

  Using Eq. (5) to estimate the hazard:

  $P[\text{Sediments impacting Manifold South}] = [1.2 \cdot 10^{-3}] \times [0.37] = 4.4 \cdot 10^{-4}$

- Manifold North

  Using Eq. (5) to estimate the hazard:

  $P[\text{Sediments impacting Manifold North}] = [1.2 \cdot 10^{-3}] \times [0.09] = 1.1 \cdot 10^{-4}$

From the vulnerability curves shown in Figure 4 and Table 2, the estimated vulnerability for Manifold South and Manifold North is 1. Therefore the consequences can be estimated as follows:

Consequences = Manifold South ($) × 1= Manifold South ($).

Consequences = Manifold North ($) × 1= Manifold North ($).

It is noted that in this analysis the elements at risk have different hazard value given that they are located at different distances along the natural channel. The total risk for the elements at risk in this study can be estimated with Eq. (6).

$$Risk = \sum_{1}^{n} Hazard_n \times Consequences_n \quad (6)$$

Using Eq. (6) and assuming that the cost of Manifold South and Manifold North are the same, the total risk is $(4.4 + 1.1)\cdot10^{-4} \times Manifold(\$) = \mathbf{5.5\cdot10^{-4} \times Manifold(\$)}$.

In other words, the annual risk associated to the earthquake-induced submarine slope failure for the future deep water gas development in the Gulf of Mexico is equal to the cost of the Manifold multiplied by $5.5\cdot10^{-4}$.

7. Discussion and Conclusions

This paper presented an offshore risk analysis for the planned deep water natural gas development in the Gulf of Mexico. It is focused on the direct consequences rather than the indirect consequences, specifically the potential damage to two planned Manifolds for collecting and transporting the hydrocarbons onshore.

To simulate the dynamics of the mud flow downslope, the 1-D numerical model BING developed by Imran (2001a) was used. However, BING does not account for the transport of sediments along channel surface configurations, which usually induce larger runout distances and debris flow velocities due to the increase of inertial forces and thickness of the shear layer compared to non-channel surface configurations. On the other hand, the BING model does not account for the resistance generated at the interface between the moving debris and the ambient fluid above, which may result in overestimated runout distances and velocities of the debris flows, as Rodríguez-Ochoa et al. (2015a) showed. The latter limitation may counterbalance the absence of the channel effect during the debris flow numerical simulations.

This work presents all the required steps to carry out the risk analysis in a systematic manner, including:

1. Estimation of the annual probability of earthquake-induced slope failure;
2. Identification of the elements at risk;
3. Probability of impacting seabed installations (elements at risk) given that the submarine slope already failed;
4. Estimation of vulnerability curves for the elements at risk to assess the consequences; and
5. Evaluation of the risk.

To estimate the annual probability of earthquake-induced slope failure, the slope failure fragility curve approach proposed by Rodríguez-Ochoa et al. (2015b) was used. The probability of impacting a seabed installation given that the submarine slope already failed, was obtained by numerical simulation of debris flows in BING code (Imran 2001) and Monte Carlo method.

The annual risk associated to the failure of submarine slope was found to be about 0.0005 times the cost of the Manifold ($).

References

Fugro, GeoConsulting. (2009). *Investigación Geológica y Geotécnica Integrada, Sonda de Campeche, México.*

Geomatrix. 2006. *Evaluación de Peligrosidad Sísmica, Bahía de Campeche, México*.

Imran, J., Harff, P., Parker, G. (2001a). A numerical model of submarine debris flow with graphical user interface, *Computers & Geosciences* **27** (6), 717–729.

Imran, J., Parker, G., Locat, J., Lee, H. (2001b). 1D Numerical Model of Muddy Subaqueous and Subaerial Debris Flows, *Journal of Hydraulic Engineering* **127** (11), 959–968.

Jeong, S.W., Locat, J., Leroueil, S., Malet, JP. (2010). Rheological properties of fine-grained sediment: the roles of texture and mineralogy, *Canadian Geotechnical Journal* **47** (10), 1085–1100.

Locat, J. (1997). Normalized rheological behaviour of fine muds and their flow properties in a pseudoplastic regime, *Debris-flow hazard mitigation: mechanics, prediction, and assessment*. Chen et.al. (eds.), 260–269, San Francisco California, USA, 7-9 August 1997.

McKay, M.D., Beckman, RJ., Conover, WJ. (2000). A Comparison of Three Methods for Selecting Values of Input Variables in the Analysis of Output from a Computer Code, *Technometrics* **42**, 55–61.

Nadim, F. (2012). Risk Assessment for Earthquake-Induced Submarine Slides, *Submarine Mass Movements and Their Consequences*, Yamada et.al. (eds.), 15–27, Kyoto, Japan, 24-26 October 2011.

Pfeiff, C.F., Hopfinger, EJ. (1986). Drag on Cylinders Moving Through Suspensions With High Solid Concentration, *PCH PhysicoChemical Hydrodynamics,* **7** (2), 101–109.

Rodríguez-Ochoa, R., Nadim, F., Cepeda, JM. (2015a). Correction Factors for 1-D Runout Analyses of Selected Submarine Slides, *Submarine Mass Movements and Their Consequences*, (accepted), Wellington, New Zealand, 1-4 November 2015.

Rodríguez-Ochoa, R., Nadim, F., Cepeda, JM., Hicks, MA., Liu, Z. (2015b). Hazard analysis of seismic submarine slope instability, *Georisk* (accepted).

Rodríguez-Ochoa, R., Nadim, F., Hicks, MA. (2015c). Influence of Weak Layers on Seismic Stability of

Appendix 4

Paper No.7 (Symposium Paper no. 3)

Rodríguez-Ochoa R, Nadim F, Cepeda JM *Correction Factors for 1-D Runout Analyses of Selected Submarine Slides*. In: 7th International Symposium on Submarine Mass Movements and Their Consequences, Wellington, New Zealand, 2015. vol (Accepted for publication). Springer.

Appendix 5

Conference Abstract

Rodríguez-Ochoa R, Nadim F (2014) *Recurrence Periods of Earthquake-Induced Submarine Landslides.* Abstract presented at the American Geophysical Union (AGU) Fall Meeting, San Francisco, USA, 15-19 December 2014.

26 October, 2014

Rafael Rodríguez-Ochoa
University of Oslo
Oslo, 0806, Norway

REF: 2014 AGU Fall Meeting
Abstract ID: 6391
Abstract Title: Recurrence Periods of Earthquake-Induced Submarine Landslides

Dear Rafael Rodríguez-Ochoa,

Thank you for submitting an abstract for consideration for the 2014 AGU Fall Meeting that will be held 15-19 December in San Francisco, California, USA. Letters of notification will be distributed in early-October 2014 regarding the status of your abstract submission.

This letter serves as an invitation for you to attend the 2014 AGU Fall Meeting. The Fall Meeting is open to all those with related interests in the Earth and space sciences. Participation in the meeting includes attending sessions in your areas of interests and an opportunity to communicate with others working in the field of geophysical sciences.

This is an invitation to participate in the meeting, but not a personal sponsorship of your stay in San Francisco. You will need to secure your own funding for travel, registration, and housing expenses as needed. Please refer to the AGU website for information at: http://fallmeeting.agu.org.

We look forward to your attendance at the 2014 AGU Fall Meeting.

Sincerely yours,

Jennifer Tomb
Assistant Director, Meetings Operations
American Geophysical Union

Recurrence Periods of Earthquake-Induced Submarine Landslides

Submarine landslides represent a constant threat to offshore installations deployed along the continental slope, therefore the estimation of the recurrence period of slope failures is a key parameter to assess the risk associated with potential massive transport of soil sediments. The initiation of submarine slope failures may be due to long-term triggers like the formation of weak layers, sedimentation rates and fault displacements, as well as short-term triggers like earthquakes and storm waves, or a combination of both of them.

The recurrence period of submarine slope failures can be linked to the recurrence period of their triggers. When the main trigger of slope failure is an earthquake, it is possible to estimate numerically the probability density of the return period for slope failure by using the seismic hazard curve and a mechanical model for earthquake-triggered slope instability.

This paper presents a procedure to calculate the conditional probability of slope failure with the maximum probability density (peak) to obtain the return period of the earthquake event with the largest probability of inducing a slope failure. The conditional probability corresponding to the maximum probability density is estimated after obtaining several conditional cumulative probability points for different earthquake return periods, and matching a cumulative distribution function (CDF) to those points; finally, the maximum probability density of the corresponding probability density function (PDF) is obtained.

The suggested analytical procedure is applied and compared with available geological evidence in a site located in the Gulf of Mexico.

Appendix 6

Report No.1

Rodríguez-Ochoa R (2010) *Seismic Stability Assessment of Submarine Slopes*, University of Oslo (UiO) Technical Report, Supervisor: Farrokh Nadim.

UiO

REPORT GEO9101SP

Seismic Stability Assessment of Submarine Slopes

Responsible Teacher: Dr. Farrokh Nadim

Prepared by ***Rafael Rodríguez Ochoa***

CONTENTS

INTRODUCTION

This report presents a summary of the best practices to evaluate the stability of submarine slopes under earthquake loading in deepwater sites by means of deterministic analyses. Information of ground response techniques is presented with focus on identifying the advantages and limitations of the current available techniques to reproduce the actual behavior of soils under cyclic loading. Particular attention is given to earthquake-induced potential landslide scenarios and based on laboratory tests and a simplified constitutive model SIMPLE DSS developed for the one-dimensional wave propagation analysis three scenarios are illustrated. Throughout this analysis the cyclic-induced deformations and excess pore pressures are shown as a key element in the degradation of static and cyclic shear strength of fine-grained soils ($\tau_{cy,}$ $S_{u,fin}$) during and after earthquake motion, which can lead to slope instability. Theoretical background is also given concerning available soil constitutive models intended to reproduce the dynamic behavior of soils in the slope, such as permanent deformations and excess pore pressures during the earthquake phenomenon. The information presented in this report is guided by the chronological order of the events: Pre-earthquake static stability, Dynamic (earthquake) stability and Post-earthquake static stability.

1. GROUND RESPONSE ANALYSIS

1.1 BACKGROUND

Since the complex nature of the mechanism of fault as well as the complex mechanism of energy transmission between the source and the site, ground response analyses are mainly focused on determining the response of the soil deposit to the motion of the bedrock immediately beneath it. Despite the fact that seismic waves may travel through tens of kilometers of rock and often less than 100 m of soil, the soil plays a very important role in determining the characteristics of the ground surface motion.

In the course of the years, a number of techniques have been developed for ground response analysis. These techniques are often grouped according to the dimensionality of the problems they can address, many of the two and three dimensional techniques are relatively straightforward extensions of corresponding one-dimensional techniques (Kramer 1996).

1.2 ONE DIMENSIONAL GROUND RESPONSE ANALYSIS

One-dimensional ground response analyses hold the assumption that all boundaries are horizontal and that the response of a soil deposit is predominantly caused by SH-waves propagating vertically from the underlying bedrock. One-dimensional ground response analysis also assumes that the soil and bedrock surface extend infinitely in the horizontal direction.

- Linear Approach

The linear approach is based on transfer functions, which can be used to express various response parameters, such as displacement, velocity, acceleration, shear stress and shear strain, having an input motion parameter such as bedrock acceleration. Because the linear approach relies on the principle of superposition, this approach is limited to the analysis of linear systems. However nonlinear behavior can be approximated using an iterative procedure with equivalent linear soil properties.

Although the calculations involve manipulation of complex numbers, the approach itself is simple. In general a known time history of bedrock (input) motion is represented as a Fourier series in the frequency domain, usually using the Fast Fourier Transformation FFT. Where each term in the Fourier series of the bedrock (input) motion is then multiplied by the transfer function to produce the Fourier series of the ground surface (output) motion. The ground surface (output) motion can then be expressed in the time domain using the inverse FFT. Thus the transfer function determines how each frequency in the bedrock (input) motion is amplified, or de-amplified by the soil deposit.
Currently there are available transfer functions ranging from very simple to more realistic and complicated geotechnical conditions, including:
Uniform Undamped Soil on Rigid Rock
Uniform, Damped Soil on Rigid Rock
Uniform, Damped Soil on Elastic Rock
Layered, Damped Soil on Elastic Rock

- Equivalent Linear Approximation of Nonlinear Response

As the nonlinearity of soil behavior is well known, the linear approach must be modified to provide reasonable estimates of ground response for practical problems of interest. It is important to point out that linear approach requires that G and ξ be constant for each soil layer, the problem becomes one of determining the values that are consistent with the level of strain induced in each layer.
Taking into account that the computed strain level depends on the values of the equivalent linear properties, an iterative procedure is required to ensure that the properties used in the analysis are compatible with the computed strain levels in all layers.
Even though the process of iteration toward strain-compatible soil properties allows nonlinear soil behavior to be approximated, it is important to remember that the complex response method is still a linear method of analysis. The strain-compatible soil properties are constant throughout the duration of the earthquake, regardless of whether the strains at a particular time are small or large. The method is incapable of representing the changes in soil stiffness that actually occurs during the earthquake. The equivalent linear approach to one-dimensional ground response analysis of layered sites has been coded into a widely used computer program called SHAKE (Schnabel et al., 1972), Kramer 1996.

- Nonlinear Approach

An alternative approach is to analyze the actual nonlinear response of a soil deposit using direct numerical integration in the time domain. As a result of integrating the equation of motion in small time steps, any linear or nonlinear stress-strain model, or advanced constitutive model can be used. Through this method, a nonlinear inelastic stress-strain relationship can be followed in a set of small incrementally linear steps.
Available nonlinear one-dimensional ground response analysis computer programs characterize stress-strain behavior of the soil by cyclic stress-strain models like the hyperbolic model and the modified hyperbolic model. Alternative computer programs have been based on advanced constitutive models such as the nested yield surface model. A number of techniques can be used to integrate the equations of motion such as the explicit finite-difference and the implicit finite-difference, however most existing computer programs for nonlinear ground response analysis use the explicit formulation (Kramer 1996).

1.3 COMPARISON OF ONE-DIMENSIONAL GROUND RESPONSE ANALYSES

- Equivalent linear analyses can be much more efficient than nonlinear analyses, particularly when the input motion can be characterized with acceptable accuracy by a small number of terms in a Fourier series.
- Nonlinear methods can be formulated in terms of effective stresses to allow modeling of the generation, redistribution, and eventual dissipation of excess pore pressure during and after earthquake shaking. Equivalent linear methods do not have this capability.
- Nonlinear methods require a reliable stress-strain or constitutive model. The parameters that describe such models are not as well established as those of the equivalent linear model. A substantial field and laboratory testing program may be required to evaluate nonlinear model parameters.
- Differences between the results of equivalent linear and nonlinear analyses depend on the degree of nonlinearity in the actual soil response.

1.4 TWO-DIMENSIONAL DYNAMIC RESPONSE ANALYSIS

When some conditions such as sloping or irregular ground surfaces, heavy or stiff embedded structures, or walls and tunnels are present in the analysis, it is necessary two-dimensional or even three dimensional approaches. Problems in which one dimension is considerably greater than others can often be treated as two-dimensional plane strains.

Techniques for the solution of such problems have been developed using both frequency-domain (complex response) methods and time domain (direct integration) methods. Normally two and three dimensional dynamic response and soil-structure interaction problems are most commonly solved using dynamic finite-element analyses:

- Equivalent Linear Approach.

The two-dimensional equivalent linear approach is very similar to the one-dimensional approach, but in this case the system is represented by a two-dimensional finite-element model. The input motion is represented by a Fourier series and the equations of motion are solved for each frequency of the series with the results summed to obtain the total response.

- Nonlinear Approach.

Two-dimensional nonlinear analyses can be used to estimate permanent displacement of slopes, retaining structures, and other constructed facilities. Two-dimensional nonlinear dynamic response analyses are performed by writing the global equations of motion from a finite-element idealization in incremental form and then integrating them in the time domain. Such analyses can be divided into two main groups according to the manner in which the soil behavior is represented: Cyclic Nonlinear Stress-Strain Models and Advanced Constitutive Models.

- Other Approaches to Two-Dimensional Dynamic Response Problems.

These approaches typically involve simplifying assumptions that allow two-dimensional problems to be solved by one-dimensional analyses:

1. Shear Beam Approach (Mononobe et al. 1936). The shear beam approach is based on the assumption that the dam deforms in simple shear, thereby producing only horizontal displacements.
2. The Layered Inelastic Shear Beam (Stara-Gazetas, 1986). Combines the shear beam approach with a one-dimensional nonlinear response analysis.

1.5 IMPORTANT FACTORS INFLUENCING SOIL STRENGTH UNDER CYCLIC LOADING

Based on laboratory tests, Nadim et al. (2007) made a compilation of the main aspects of a typical soil element within a submarine slope to address the strength behavior of clays in submarine slopes under earthquake loading. The following factors were investigated:

- Rapid Rate of Loading

It was confirmed that the undrained shear strength increases as the rate of loading increases.

- Permanent (static) Shear Stress

It was observed that the effect of a consolidation shear stress τ_c (i.e., a slope) increases the strength of the soil when shearing downhill, but reduces the available shear strength for the slope by decreasing the difference between the permanent shear stress τ_c and the soil shear strength s_u.

- Post-earthquake static shear strength and creep deformations after the earthquake.

It was shown that the cyclic shear strains induced by the earthquake tend to reduce the shear strength. If the earthquake-induced cyclic shear strains are large, the slope could undergo further creep displacements after the earthquake and experience a significant reduction of static shear strength.

2. STABILITY OF SUBMARINE SLOPES

2.1 BACKGROUND

The oil and gas industry remains the main source of energy all over the world, despite the increasing attention to develop other sources of energy. For that reason vast effort is still destined to the quest of hydrocarbons, where many of the reservoirs are found in offshore sites with increasing water depths. Offshore structures are necessary for the development of oil and gas fields, many of them need to be placed in areas with potential of submarine slide activity, for this reason is important to take into account the stability of submarine slopes in the selection of sites.

In order to characterize the site under investigation for stability analyses, it is necessary to divide the activities in two main stages, regional and site specific evaluations.

2.1.1 Regional Evaluation

The objective of the regional survey is to get an overview of the relevant area and to give input to site specific evaluations. The main tool to get regional information comes from geophysical surveys including bathymetric mapping of the region and mapping of soil sediments. Location of slope angles, previous slide activities and possible unstable layers can be identified based on geophysical surveys (NGI Report, 1997).

2.1.2 Site Specific Evaluation

The objective of the site specific evaluation is to determine the slope stability for critical slopes in the survey area and possible submarine slides that can damage the integrity of a structure. To achieve a detailed evaluation of seabed stability the following background data and information has to be available: seabed topography, soil layering to bedrock, previous slide activity, trigger mechanisms for submarine slides and soil properties. Special laboratory testing has to be carried out to determine the soil response to a triggering mechanism.

2.2 PRE-EARTHQUAKE STATIC STABILITY

The analyses for evaluation of static stability of slopes are based on the limit equilibrium theory, which calculate the factor of safety of critical slip surfaces by the method of slices. Currently there are several computer slope stability programs to calculate the factor of safety of critical failure surfaces, like SLOPE/W (Geo-Slope Inc), Slide (Rocscience) and BEAST (Clausen, 1990) among others. It is common to choose the method of Morgenstern and Price (1965) or a variation of it for equilibrium of the slides.

These programs can be used to evaluate the stability in the short term using undrained shear strengths, and in the long term using friction angles. Laboratory tests such as triaxial compression and direct simple shear tests, and correlations between tip resistance of CPT tests and laboratory tests are the main sources of information regarding shear strength.

The input data for the slope stability programs are the geometry of the slope, stratigraphy, submerged unit weight, static shear strength and in some cases shear strength anisotropy. Laboratory tests like triaxial extension S_u^E, and direct simple shear test under consolidation shear stress S_u^{DSS} are used to evaluate strength anisotropy, obtaining anisotropy factors by means of relationships such as S_u^{DSS}/S_u^C and S_u^E/ S_u^C where S_u^C is the untrained shear strength in triaxial compression.

2.3 DURING-EARTHQUAKE DYNAMIC STABILITY

2.3.1 EFFECT OF EARTHQUAKE LOADING ON SLOPES

Regarding the main effects of submarine slopes under earthquake loading, Biscontin et al. (2004) described three scenarios for earthquake-induced submarine slide. The findings were based on a simplified constitutive model called SIMPLE DSS developed for the one-dimensional wave propagation analysis of submerged clay slopes under seismic loading. The model assumes a soil element within the slope subjected to direct simple shear stress state, similar to earthquake induced shear stresses in level ground, with shear stress direction parallel to the dip of the slope. This analogy can be assumed given the geometry of the slopes under study, which usually have a large longitudinal distance with constant slope angle. The model was calibrated using normally consolidated Boston Blue Clay under monotonic and cyclic direct simple shear DSS test, where some specimens were consolidated under normal effective stress and shear stress (τ_c) to reproduce the slope effect. SIMPLE DSS model is able to simulate excess pore pressures during cyclic loading; this allows determining effective stress paths.

To perform the seismic site response analysis for sloping ground the SIMPLE DSS constitutive model was implemented in the finite element program AMPLE2000. Nadim et al. (2007) summarized the three scenarios described by Biscontin et al. (2004) as follows:

Scenario 1 – Failure occurs during the earthquake. The soil would need to have strong strain-softening characteristics and high sensitivity. The strains and pore pressures generated by the cyclic stresses degrade the shear strength so much that the slope is not able to carry the static shear stresses. It should be noted that even if the earthquake does not cause a complete failure of the slope, it might still induce large down-displacements (slumping). The earthquake-induced permanent displacement may be from a few centimeters to several meters.

Scenario 2 – Post-earthquake failure due to increase in excess pore pressure caused by upward seepage from deeper layers. This scenario requires a layer near the sea floor (5 –

10m depth) with much lower permeability and lower consolidation coefficient (2 orders of magnitude or more) than the rest of the soil deposit. This scenario could occur over a time span of decades or even centuries in deep marine clay deposits.

Scenario 3 – Post-earthquake failure due to creep and/or significant reduction of static shear strength. This scenario requires that large cyclic shear strains occur during the earthquake shaking. The effective stress paths for a typical soil element on a potential slip surface for these scenarios are illustrated on Figure 1.

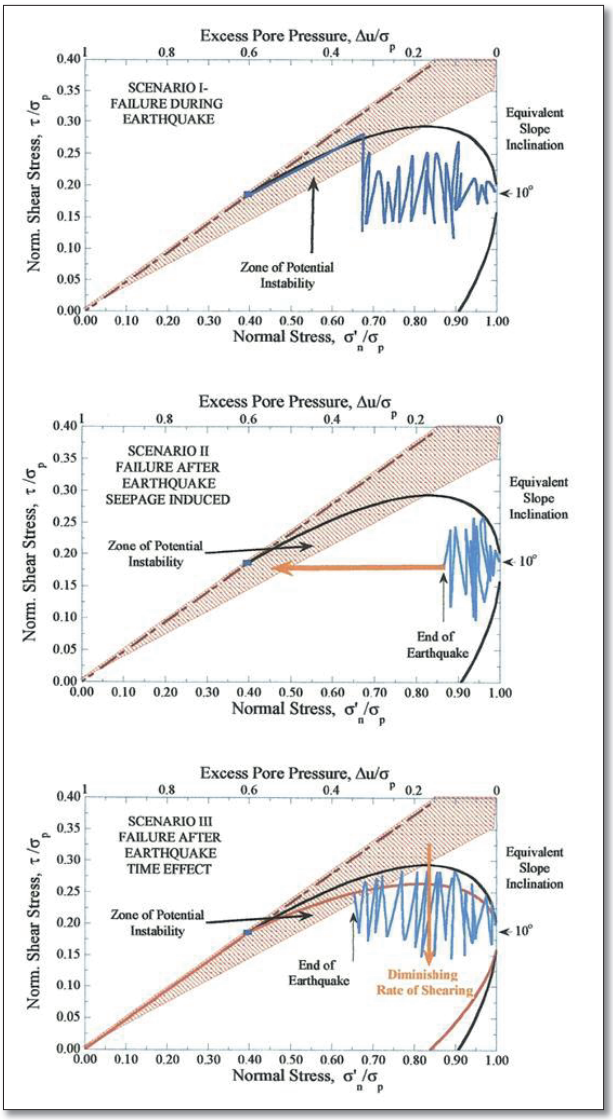

Figure 1. Effective stress path for a soil element on the critical slip surface.

2.3.2 PSEUDO-STATIC ANALYSES

A pseudo-static analysis is carried out by applying a horizontal static load equal to the mass times the maximum ground acceleration to simulate the inertial force. The cut-off acceleration is computed by increasing the acceleration gradually until a condition of SF=1 is obtained under simultaneous actions of the own slope weight and the pseudo-static horizontal earthquake force. This type of analysis can also be carry out by slope computer programs such as Slide and BEAST.

However, failure conditions last only for fractions of seconds during the most intense earthquake shaking and may generate a gradual accumulation of strains and displacements, but after the earthquake the slope is again subjected solely to gravity forces. Therefore, this approach may present factors of safety below one even when the slope remains stable. Hence, it is the degradation of soil strength by earthquake induced strain and the associated increase in pore pressure that governs stability under and after earthquake loading (Kvalstad et al. 2005). Because this approach is not able to estimate deformations, ground response analyses are required to address this issue.

2.3.3 GEOTECHNICAL PARAMETERS

Important soil parameters to perform ground response analyses can be obtained as follow:

- Cyclic Soil Strength Parameters

Cyclic undrained shear strength (τ_{cy}) to be used as input in ground response analysis is obtained mainly from Cyclic Direct Simple Shear Tests and Cyclic Triaxial Tests for an equivalent number of cycles N.

- Dynamic Soil Parameters

Maximum Shear Modulus G_{max} is obtained from bender element and resonant column tests. G/G_{max} and damping ratio ξ curves are obtained from resonant column tests.

2.3.4 ESTIMATING DEFORMATIONS

Due to the difficulty to simulate excess pore water pressure during cyclic loading with available methods, in practice it is recommended to perform 1D non-linear earthquake response analysis using AMPLE (Nadim, 1991), or similar, to calculate earthquake induced shear strains and displacements. It has been shown that shear strains give a good estimation of strength degradation in soils.

AMPLE models a layered soil profile as one-dimensional, non-linear shear beam. The non-linearity is due to the non-linear soil stress-strain characteristics. The resulting wave propagation equations are solved numerically in the time domain using the explicit central difference method. The base rock acceleration time history is scaled to the relevant peak ground acceleration (PGA) design criteria and the response of a 1D soil column from base rock to seabed is calculated. A hyperbolic soil model is used to assume a stress-strain response with initial stiffness of G_{max} and limiting strength of s_u. The failure-seeking rule (Cundall, 1979) is used to model the unloading-reloading response, which also takes the effect of the inclined seabed (infinite slope) into account.

Subsequently, 1D response at relevant depth is used as input to more comprehensive 2D dynamic finite element earthquake analyses to be performed with the program PLAXIS. Elastoplastic soil models can be applied to calculate accumulation of displacements and shear strains caused by earthquake loading to let comparisons with previous 1D analysis.

Static stability is also considered using PLAXIS to compare safety factors with results from limit equilibrium analyses. Phi-c reduction procedure can be used as loading parameter.

2.3.5 CONSTITUTIVE MODELS

Ground response analyses require soil constitutive models that imitate key features of the cyclic soil behavior in order to simulate the response of sediments under earthquake loadings.

In general, there are three broad classes of soil models: Equivalent Linear Models, Cyclic Nonlinear Models and Advanced Constitutive Models. Equivalent linear models are the simplest and most commonly used but have a limited ability to represent many aspects of soil behavior under cyclic loading conditions. At the other end of the spectrum, advanced constitutive models can represent many details of dynamic soil behavior, but their complexity and difficulty of calibration currently make them impractical for many common geotechnical earthquake engineering problems (Kramer 1996).

- Equivalent Linear Model

The parameters G_{sec} and ξ are often referred to as equivalent linear material parameters. For certain types of ground response analyses, they are used directly to describe the soil behavior; other types of analyses require the actual path of the hysteresis loop as described by a cyclic nonlinear or advanced constitutive model.

The equivalent linear model cannot be used directly for problems involving permanent deformation or failure; they also imply that the strain will always return to zero after cyclic loading, and since a linear material has no limiting strength, failure cannot occur. However, the assumption of linearity allows a very efficient class of computational models to be used for ground response analyses. For that reason it is commonly employed, giving considerable attention to the characterization of G_{sec} and ξ for different soils (Kramer 1996).

- Cyclic Nonlinear Models

The nonlinear stress-strain behavior of soils can be represented more accurately by cyclic nonlinear models that follow the actual stress-strain path during cyclic loading. Such models are able to represent the shear strength of the soil, and with an appropriate pore pressure generation model, also changes in effective stress during undrained cyclic loading can be predicted. The cyclic nonlinear models are characterized by two key elements:

1. Backbone curve.
2. Series of rules that govern unloading-reloading behavior, stiffness degradation, and other effects. Models that follow just two rules describe Masing behavior (Masing, 1926), models that have two more complementary rules are called extended Masing models.

The ability to represent the development of permanent strains is one of the most important advantages of cyclic nonlinear models over equivalent linear models. When incorporated into computational models for ground response analysis, cyclic nonlinear models allow prediction of the generation, redistribution, and eventual dissipation of pore pressures during and after earthquake shaking (Kramer 1996), but that is not an easy task.

- Advanced Constitutive Models

The most accurate and general methods for representing of soils behavior are advanced constitutive models, which use basic principles of mechanics to describe observed soil behavior for: (a) general initial stress conditions, (b) a wide variety of stress paths, (c)

rotation of principal stress axes, (d) cyclic or monotonic loading, (e) high or low strain rates, and (f) drained or undrained conditions.

Advanced constitutive models hold three main characteristics:

1. *Yield surface* that describes the limiting stress conditions for which elastic behavior is observed.
2. *Hardening law* that describes changes in the size and shape of the yield surface as plastic deformation occurs, and
3. *Flow rule* that relates increments of plastic strain to increments of stress.

The Cam-Clay (Roscoe and Schofield, 1963) and modified Cam-Clay (Roscoe and Burland, 1968) models were among the first of this type.
Even though advanced constitutive models allow considerable flexibility and generality in modeling the response of soils to cyclic loading, their description usually requires many more parameters than equivalent linear models or cyclic nonlinear models. Evaluation of these parameters can be difficult, and the parameters obtained from one type of test can be different from those obtained from another (Kramer 1996).
During the selection of the constitutive model process it is important to keep in mind that models range considerably in complexity and accuracy, this means a model that is appropriate for one type of problem may not be appropriate for another. No single stress-strain model is appropriate for all problems. Selection of a stress-strain model requires careful consideration of the problem to which it is to be applied, recognition of the assumptions and limitations of the models, and a good understanding of how the model is used in all required analyses (Kramer 1996).

2.4 POST-EARTHQUAKE STATIC STABILITY

Once the accumulated strains are computed, post-cyclic static strength $S_{u,fin}$ from direct simple shear and triaxial compression tests are used to determine the degradation of shear strength after cyclic loading, and the associated reduction of the factor of safety in static stability conditions.

CASE HISTORIES

Seismic activity is known as the main trigger of submarine landsides (NGI Report 1997, Hance 2003). Hance (2003) developed a database on published literature which includes 534 submarine slide events where 14 different triggering mechanisms were identified; information on the triggering mechanism(s) causing the slope failure is available for 366 of the 534 landslides. Although in most of the landslides where reported multiple triggers because the specific trigger was uncertain, over 40 percent were attributed to earthquake and faulting mechanisms, which cover 225 of the slope failures, Figure 2.

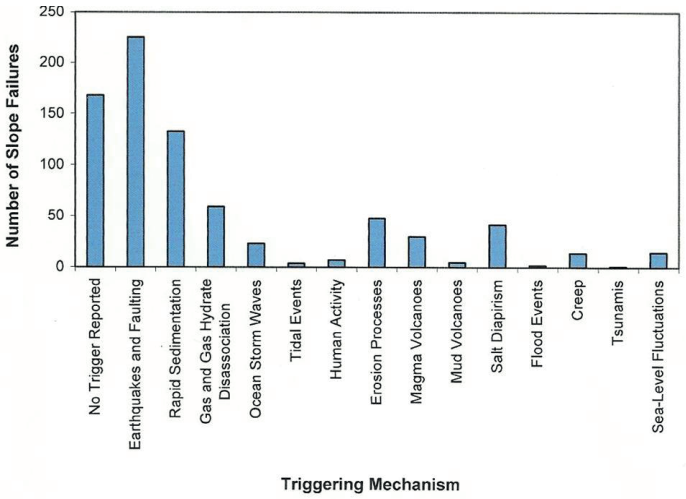

Figure 2. Distribution of triggering mechanisms.

The occurrence of submarine slides are common in marine sediments, however it is not easy to identify them given the intrinsic nature of the phenomenon. According to Hance (2003), the majority of the slope failures are located in the northern and western hemispheres of the world, however these locations are probably just an indicative where offshore exploration activity has occurred and data have been published. Therefore, these locations are probably not indicative of the occurrence of submarine landslides worldwide.

Further information from Hance's database relates to water depths of submarine landslides, where in order to identify the affected area by the landslide the shallowest and deepest water depths were recorded for each landslide. About 80% of the 534 slide events have water depths information, where means for the shallowest and deepest water depths were about 1125 m and 1868 m, respectively, which is a difference of about 750 m. Assuming an average slope of 10 degrees it can be estimated a run-out distance about 4,250 m for a change in elevation of 750 m. In consequence, the water depths for the slope failures suggest that failed materials travel long distances, at least 4 km considering that the inclination of the seafloor is typically less than 10 degrees (Hance 2003).

Concerning the type of soil, the majority of the slides where information on soil type was available involved fine-grained material, i.e. clays and silts. In the continental shelf fine-grained soil is common to find given the large distance from the main sediment sources (rivers), having also low deposition rates (Biscontin et al. 2004).

Another important parameter for slope stability analyses is the slope angle, it is known that many of the submarine landslides have been developed in gentle planes; the average angle of the slope at failure was recorded for 399 of the 534 seafloor slope failures in Hance's database. The 3 to 4 degree slope angle interval has the highest frequency of slope failures. The median slope angle for the 399 slides is 4.0 degrees, and the mean is 5.8 degrees, this agrees with Biscontin et al. (2004.)

DISCUSSION

Currently the evaluation of submarine slope stability under earthquake loading can be addressed by means of quantifying the deformation in the slope couple with extensive laboratory testing to characterize the shear strength degradation of soils under study. However, it is important to keep on working in developing or improving approaches that simulate effective stress paths under cyclic loading to unveil the real behavior of submarine slopes.

Another source of information could be the field instrumentation of submarine slopes with identified low factors of safety to measure creep deformations, and hopefully provide information on changes in pore pressure during a slide event.

REFERENCES

- Biscontin, G., J. M. Pestana and F. Nadim (2004) "Seismic triggering of submarine slides in soft cohesive soil deposits", *Marine Geology*, Vol. 203 (3 & 4), 341-354.
- Hance, J.J. (2003). "Development of a database and assessment of seafloor slope stability based on published literature." M.S. Thesis, University of Texas at Austin.
- Kramer**,** Steven L. (1996)**.** Geotechnical Earthquake Engineering. Prentice-Hall, 653 pp.
- Kvalstad, T.J., Nadim, F., Kaynia, A.M., Mokkelbost, K.H. and Bryn, P. (2005). "Soil conditions and slope stability in the Ormen Lange area" Marine and Petroleum Geology 22, 299–310.
- Nadim, F., G. Biscontin, A. M. Kaynia (2007) "Seismic Triggering of Submarine Slides", *Offshore Technology Conference*, OTC 18911 May, pp. 1-8.
- NGI Report (1997), Earthquake Hazard and Submarine Slide. Submarine slides – A literature survey. Project Manager: Farrokh Nadim
- NGI Report (2008), Slope Stability Evaluation and Laboratory Testing for Shah Deniz Full Field. Project Manager: Amir M. Kaynia.
- Pestana, J. M. and Nadim, F. (2000). "AMPLE2000: A computer program for non-linear site response analysis of infinite slopes."